

Preparation and characterization of dual functional antimicrobial (bio)degradable polymers

Dissertation

zur Erlangung des akademischen Grades eines Doktors der
Naturwissenschaften (Dr. rer. nat.) an der Bayreuther
Graduiertenschule für Mathematik und Naturwissenschaften der
Universität Bayreuth

Vorgelegt von

Hui Wang

Geboren in Peking

Bayreuth 2016

Die vorliegende Arbeit wurde in der Zeit vom Mai 2012 bis Juli 2012 in Marburg am Lehrstuhl Makromolekulare Chemie, Philipps-Universität Marburg und von August 2012 bis Februar 2016 in Bayreuth am Lehrstuhl Makromolekulare Chemie II unter Betreuung von Frau Professor Dr. Seema Agarwal angefertigt.

Vollständiger Abdruck der von der Bayreuther Graduiertenschule für Mathematik und Naturwissenschaften (BayNAT) der Universität Bayreuth genehmigten Dissertation zur Erlangung des akademischen Grades eines Doktors der Naturwissenschaften (Dr. rer. Nat.).

Dissertation eingereicht am: 10. 02. 2016

Zulassung durch die Promotionskommission: 01. 03. 2016

Wissenschaftliches Kolloquium: 29. 06. 2016

Amtierender Direktor: Prof. Dr. Stephan Kümmel

Prüfungsausschuss:

Prof. Dr. Seema Agarwal (Erstgutachterin)

Prof. Dr. Ruth Freitag (Zweitgutachterin)

Prof. Dr. Birgit Weber (Vorsitz)

Prof. Dr. Peter Strohrriegl

Table of contents

Zusammenfassung	1
Summary	3
List of symbols and abbreviations.....	5
1 Introduction	7
1.1 Motivation and aim.....	8
1.2 Overview of (bio)degradable polymers	9
1.2.1 (Bio)degradable polyesters.....	9
1.2.2 Synthesis of (bio)degradable polyesters.....	11
1.2.3 Application of (bio)degradable polyesters	15
1.2.4 Degradation of polyesters.....	17
1.2.5 Biodegradation test methods	19
1.3 Antibacterial materials.....	22
1.3.1 Cationic antibacterial compounds	22
1.3.2 Polyguanidine based antibacterial materials	25
1.3.3 Antibacterial test methods	27
1.4 (bio)degradable polymers with antimicrobial activity.....	29
1.5 References	34
2. Cumulative part of dissertation	41
2.1 Oligomeric dual functional antibacterial polycaprolactone	42
2.2 Biodegradable aliphatic-aromatic polyester with antibacterial property	47
2.3 Antibacterial 45S5 Bioglass [®] -based scaffolds reinforced with genipin cross-linked gelatin for bone tissue engineering.....	53
3. Oligomeric dual functional antibacterial polycaprolactone	59
4. Biodegradable aliphatic-aromatic polyester with antibacterial property	81
5. Antibacterial 45S5 Bioglass [®] -based scaffolds reinforced with genipin cross-linked gelatin for bone tissue engineering	103
List of Publications.....	139
Acknowledgements	140

Zusammenfassung

Die vorliegende Doktorarbeit behandelt die Herstellung von (bio)abbaubaren Materialien mit antibakteriellen Eigenschaften zur Verwendung in unterschiedlichen Bereichen, wie z.B. Verpackungsmaterialien, Komposttüten, Hygieneprodukten, oder auch Bioglass[®]-Gerüsten für das ‚Tissue Engineering‘.

Die verschiedenen Wege zur biologischen Abbaubarkeit und antimikrobiellen Eigenschaften zu kombinieren sind in den drei Teilen dieser Arbeit dargelegt. In allen Teilen der Arbeit wurde ein Polyguanidinsalz als antibakterieller Wirkstoff eingesetzt, da Polyguanidine für ihre antimikrobielle Wirkung gegen Gram-positive und Gram-negative Bakterien, Pilze und Viren bekannt sind. Die Synthese von Oligoguanidin mit niedrigem Molekulargewicht erfolgte über Polykondensation. Die antibakterielle Aktivität von wasserlöslichem Oligoguanidin wurde mit Hilfe von Tests zur Bestimmung der minimalen Hemmkonzentration (MHK) und der minimalen bakteriziden Konzentration (MBK) nachgewiesen. Als biologisch abbaubare Materialien wurden aliphatische Polyester und 45S5 Bioglass[®] eingesetzt. In der gesamten Arbeit wurden die Techniken Polymersynthese, Extrusion und Beschichtung für die Produktion von neuen antimikrobiellen und bioabbaubaren Materialien verwendet.

Eine große Herausforderung dieser Arbeit ist die Herstellung von neuen Materialien mit antibakterieller Aktivität ohne Verlust der Bioabbaubarkeit. Um dieses Ziel zu erreichen, wurde im ersten Teil ein Polyguanidinsalz, als antimikrobielles Material, in Polycaprolacton, als abbaubarem Matrix Material, immobilisiert. Wegen der Aminendgruppe (-NH₂) konnte Oligoguanidin hydrochlorid als Initiator genutzt werden, um das Lacton zu öffnen. Die Struktur der gebildeten Blockcopolymer wurde mittels 2D-NMR und MALDI-ToF-MS Analyse nachgewiesen. Das auf diese Weise hergestellte Copolymer besitzt eine starke antibakterielle Aktivität. Das Copolymer zeigt außerdem enzymatische Abbaubarkeit. Der Polycaprolacton-Block wurde nach kurzer Inkubationszeit komplett abgebaut. Kombiniert mit der niedrigen Zytotoxizität sind viele Anwendungen für das Material denkbar: Als Additiv für Lebensmittelverpackungen, für Tissue Engineering oder Gentransfektion.

Der zweite Teil beschäftigt sich mit der Extrusion des bioabbaubaren Polymers Poly(butylenglycol-co-terephthalat) (PBAT) mit dem antibakteriellen Additiv Polyhexamethylen guanidinhydrochlorid (PHMG). PBAT ist ein bioabbaubarer aliphatisch-aromatischer Polyester

Zusammenfassung

mit guten mechanischen Eigenschaften, weshalb es häufig als Matrixmaterial benutzt wird, um es mit anderen Polymeren zu mischen. In dieser Arbeit wurde PBAT durch Beimischen von PHMG eine antimikrobielle Wirkung hinzugefügt. Das Highlight der Arbeit ist die Balance zwischen antibakteriellen Eigenschaften und biologischer Abbaubarkeit. Nach der Schmelzextrusion mit einer wässrigen Lösung des antibakteriellen Zusatzes, wurden die mechanischen Eigenschaften gegenüber dem reinen Matrixmaterial sogar verbessert. Der Blend PBAT/PHMG zeigt biologische Abbaubarkeit im Kompost und zudem langanhaltende antibakterielle Aktivität. Wegen der verbesserten mechanischen Eigenschaften kann das Material direkt als Verpackungsmaterial und für Komposttüten verwendet werden.

Im dritten Teil dieser Arbeit wurde das antibakterielle Polymer Poly-*p*-xylylguanidinhydrochlorid (PPXG) als Beschichtungsmaterialien auf Oberflächen von Bioglasgerüsten für Knochen eingesetzt. PPXG ist ein neues Polyguanidinsalz, das durch Polykondensation von Guanidinhydrochlorid und *p*-Xylylendiamin synthetisiert wurde. Das neu hergestellte PPXG mit aromatischen Gruppen zeigt höhere Thermostabilitäten als aliphatische Polyguanidinsalze und auch einen höheren Glasübergang. Allerdings schränkt der unflexible Benzolring die Wechselwirkung mit der Bakterienmembran ein, sodass eine schwächere antibakterielle Aktivität gegenüber den flexibleren Alkylketten beobachtet wurde. Die antibakterielle Aktivität von PPXG wurde mittels MHK und MBK Tests bestimmt. Außerdem wurde die antibakterielle Wirkung von beschichteten Bioglassgerüsten mit Kirby-Bauer- und zeitabhängigen Tests quantifiziert. Mit 10 mg mL⁻¹ antibakteriellem Polymer inkorporiertes Bioglass[®] zeigte eine stark antibakterielle Aktivität gegen die Gram-positiven Bakterien *B. subtilis* und einen hemmenden Effekt gegen die Gram-negativen Bakterien *E. coli*. Wegen der niedrigen Zytotoxizität der antimikrobiellen Beschichtungen zeigt das Bioglass[®] Bioaktivität und *in vitro* Biokompatibilität bei MG-63 Zellen.

Summary

Summary

The present thesis covers the preparation of (bio)degradable materials with antimicrobial properties, which has a broad range of applications, e.g. packaging materials, compost bags, hygienic products or Bioglass[®] scaffolds for tissue engineering.

Selected routes to combine (bio)degradability and antimicrobial properties are comprised in the three parts of this work. In all parts of this work polyguanidine salts are used as antimicrobial materials, which are well-known antimicrobial agents against Gram-positive and Gram-negative bacteria, fungi and viruses. Polyguanidine hydrochloride is synthesized by step-growth reaction to produce low molecular weight polymers. The antibacterial activity of water-soluble polyguanidine is determined by minimum inhibition concentration (MIC) and minimum bactericidal concentration (MBC) tests. As (bio)degradable materials aliphatic polyesters and 45S5 Bioglass[®] were chosen. Throughout the work, polymer synthesis, extrusion or coating techniques were employed to produce new antimicrobial and (bio)degradable materials.

A major challenge of this work was the production of new materials with antibacterial activity without sacrificing (bio)degradability. In the first part, polyguanidine salts as antibacterial material were immobilized in (bio)degradable polycaprolactone (PCL) to achieve this goal. Due to the amine end group (-NH₂), polyguanidine hydrochloride (PHMG) can be used as an initiator to open the caprolactone ring for the synthesis of block copolymers of PHMG and polycaprolactone. The structure of the block copolymer has been confirmed by 2D-NMR and MALDI-ToF MS analysis. The copolymer has high antibacterial activity and a fast antibacterial action. Reduction of bacterial cells was higher than 3 log levels in a short period of time. The copolymer also showed enzymatic degradability. The polycaprolactone block completely degraded within hours. Because of its low cytotoxicity, the new material has many potential applications, e.g. additive for food packaging, tissue engineering or gene transfection.

The second part deals with the formation of antibacterial (bio)degradable polymers by melt blending of PHMG and poly(butylene adipate-co-terephthalate) (PBAT). PBAT is a (bio)degradable aliphatic-aromatic polyester with good mechanical properties, which is often utilized as the matrix material for blending with other functional polymers, to create multifunctional materials. In this work, the antimicrobial additive was added by physical blending of an aqueous solution into molten PBAT. The highlight of this part is the achieved

Summary

balance between antibacterial properties and (bio)degradability. After melt extrusion with an aqueous solution of the antibacterial additive, the mechanical properties of the new material were even improved. The PBAT/PHMG blends showed (bio)degradability in compost and permanent antibacterial activity. Due to the enhanced mechanical properties, the material can be directly applied as packaging material or in compost bags.

In the third part of this thesis the antibacterial polymer poly(*p*-xylylene guanidine) hydrochloride (PPXG) as additive is coated on the surface of bioactive glass scaffolds for bone tissue engineering. PPXG is a new polyguanidine salt, which was synthesized by polycondensation of guanidine hydrochloride and *p*-xylylene diamine. The new PPXG with aromatic group shows higher thermal stability than the aliphatic counterpart and it exhibits a higher glass transition temperature. However, the inflexible benzene ring limits the interaction between polymer chain and bacterial membrane, hence leading to weaker antibacterial activity compared to PHMG. The antibacterial activity of PPXG was determined by MIC and MBC tests. The antibacterial activity of Bioglass[®] was determined by Kirby-Bauer and time-dependent tests. Bioglass[®] loaded with 10 mg mL⁻¹ antibacterial polymer shows strong antibacterial activity against Gram-positive bacteria *B. subtilis* and an inhibiting effect against Gram-negative bacteria *E. coli*. Because of the low cytotoxicity of the antimicrobial polymer, coated Bioglass[®] scaffolds still showed bioactivity, i.e. *in vitro* biocompatibility in MG-63 cells.

List of Symbols and Abbreviations

List of symbols and abbreviations

°C	degree Celsius
APCI	atmospheric pressure chemical ionization
ATR-IR	attenuated total reflectance spectroscopy
<i>B. subtilis</i>	<i>bacillus subtilis</i>
C	concentration
CFU	colony-forming unit
DMSO	dimethyl sulfoxide
DSC	differential scanning calorimetry
<i>E. coli</i>	<i>Escherichia coli</i>
EDX	energy-dispersive X-ray spectroscopy
g	gram
GCG	genipin cross-linked gelatin
GPC	gel permeation chromatography
H	hour
H ₂ O	water
HSQC	heteronuclear single quantum coherence spectroscopy
kg	kilogram
kV	kilovolt
M	meter
MALDI	matrix-assisted laser desorption/ionization
MBC	minimal bactericidal concentration
MeOD	methanol-d ₄
MeOH	methanol
MG-63	Osteoblast-like cells
MIC	minimal inhibitory concentration
min	minute
mL	milliliter
M _n	number average molar mass
MPa	mega pascal
M _w	weight average molar mass

List of Symbols and Abbreviations

n	degree of polymerization
NMR	nuclear magnetic resonance
PBAT	poly(butylene adipate-co-terephthalate)
PBH	poly(hydroxybutyrate)
PCL	polycaprolactone
PDI	polydispersity index
PEI	polyetherimide
PET	poly(ethylene terephthalate)
PG	polyguanidine hydrochloride
PHMG	poly(hexamethylene guanidine) hydrochloride
PLA	poly(lactic acid)
PLLA	poly(L-lactide)
PPXG	poly(<i>p</i>-xylylene guanidine) hydrochloride
PU	polyurethane
PVA	poly(vinyl alcohol)
ROP	ring-opening polymerization
s	second
SEM	scanning electron microscopy
T	temperature
T_{5%}	temperature at which 5% weight loss took place
T_d	decomposition temperature
T_g	glass transition temperature
TGA	thermogravimetric analysis
TPS	thermoplastic starch
WST	water soluble tetrasodium
wt%	weight percent
ε-CL	ε-Caprolactone
μm	micrometer
ρ	density

1 Introduction

The present thesis deals with the investigation of new materials combining (bio)degradability with antibacterial properties. These new materials could be of interest for pharmacological and food-related products, like bioscaffolds and food packaging.

The work involves synthesis of new materials and their characterization in terms of structure, mechanical properties, thermal stability, (bio)degradability and antibacterial properties. In chapter 3 a polyguanidine (PG) was used as macroinitiator to synthesize a polycaprolactone-*b*-polyguanidine block copolymer (PCL-*b*-PHMG) by ring-opening polymerization (ROP). PHMG is one of the very intensively investigated antimicrobial polycations, which was used as antimicrobial material in this work. Due to the low molecular weight, the copolymer PCL-*b*-PHMG did not show good mechanical properties. In chapter 4 the typical (bio)degradable aliphatic-aromatic polyester PBAT, which has relatively high molecular weight and advantageous mechanical properties, was blended as matrix material with the antimicrobial additive PHMG. Furthermore, chapter 5 presents a new application of biocidal PG, which was incorporated into 45S5 bioactive glass scaffolds as antimicrobial coating.

Introduction

1.1 Motivation and aim

Every year global production of synthetic polymers reaches approximately 140 million tonnes.¹ Since their extreme stability, the degradation cycles of synthetic materials are limited. Plastic pollution has been recognized as a major problem. Therefore, (bio)degradable materials have been highly investigated in the past decades. They are used for various applications such as food packaging materials,^{2,3} compost bags,⁴ medical sutures, drug delivery vehicles or scaffolds for tissue engineering⁵. Meanwhile, the contamination with microorganisms in food and water or bacterial infections by medical devices are always a huge risk in our daily life. The aim of this work is to combine antibacterial property with (bio)degradability in one, generating dual functional polymers.

The challenge of this work was the synthesis and processing of (bio)degradable materials with a high antibacterial activity. (Bio)degradation takes place through the action of enzymes or chemical decomposition associated with living organisms like bacteria fungi, etc.⁶ However, the guanidine based cationic polymers present excellent growth inhibition against bacteria, fungi and virus.⁷⁻⁹ Therefore, the focus was to find a balance between antibacterial activity and (bio)degradability, which can keep the antimicrobial activity, while controlling the rate of (bio)degradation.

Introduction

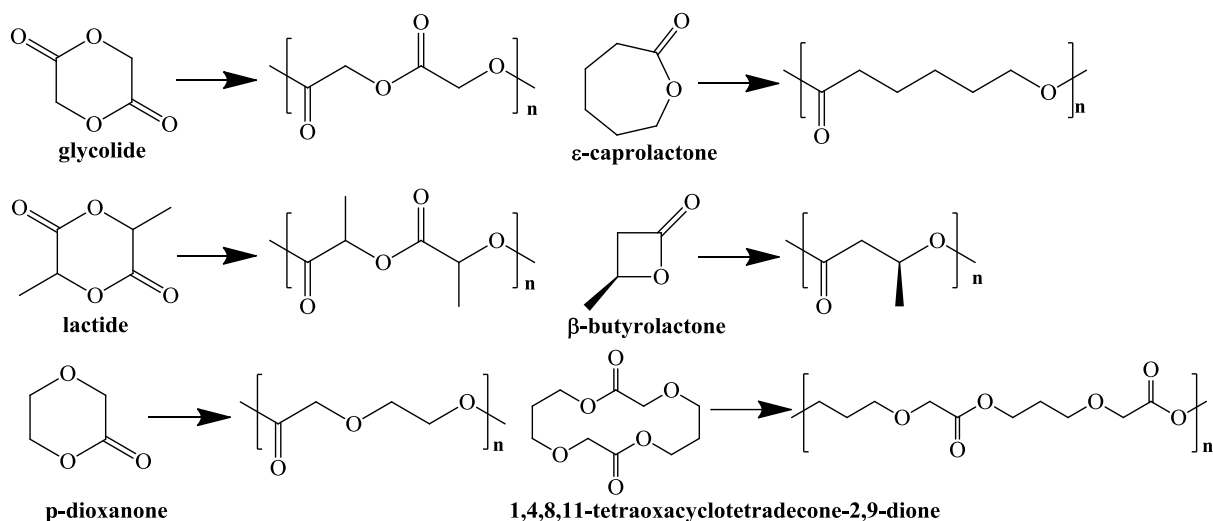
1.2 Overview of (bio)degradable polymers

1.2.1 (Bio)degradable polyesters

(Bio)degradable polymers have a long history because of their wide range of applications. They can be divided into two groups, synthetic and natural polymers. Polysaccharides and proteins are typical natural (bio)degradable polymers obtained from renewable sources,¹⁰ while aliphatic polyesters, polyphosphoesters (PPE), aliphatic polycarbonates and poly(amino acids) are typical synthetic (bio)degradable polymers.¹¹ Compared to the natural (bio)degradable polymers, the synthetic polymers exhibit more potential of improvement, because for biologically derived (bio)degradable polymers a chemical modification is usually difficult or is likely causing the alteration of the bulk properties. For designed synthetic (bio)degradable polymers a variety of properties can be obtained and further modifications are possible without altering the bulk properties. In the past decades, the properties of (bio)degradable polymers could be successfully adapted to the requirement of their application through variation of the synthetic methods.¹

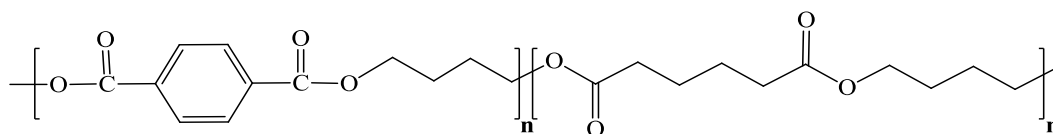
Among synthetic biodegradable polymeric materials, polyesters represent one of the most promising families due to interesting applications as biomedical and degradable packaging materials. This thesis deals with the synthesis of biodegradable aliphatic polyesters with antibacterial function and blends of biodegradable aliphatic polyesters with antibacterial additives. In the 1960s biodegradable poly(L-lactide) (PLLA) was identified as a biocompatible and bioresorbable material.¹² PLLA and polyglycolide were chosen to form the basis of many medical applications, like body implants, surgical sutures and drug delivery devices.^{13–15} However, those polyesters initially were developed with low molecular weight and poor mechanical properties. In recent years, due to a number of requirements for marketing (bio)degradable polyesters, alternatives to commodity plastics have been investigated.^{16,17} The synthetic methods and techniques were renewed. ROP of lactones, lactides and cyclic diesters have yielded polyesters with very high molecular weight and good mechanical properties (Scheme 1-1).^{18–20} In order to modify or improve the properties, various polymer architectures and blends have also been intensively studied.^{21,22}

Introduction



Scheme 1-1. Monomers for the preparation of polyester derivatives.

In addition to (bio)degradable aliphatic polyesters, (bio)degradable aliphatic-aromatic polyesters have also been investigated extensively. PBAT is a typical (bio)degradable aliphatic-aromatic polyester (Scheme 1-2), which is prepared by polycondensation of 1,4-butanediol and a mixture of adipic and terephthalic acid. PBAT has been produced on an industrial scale by BASF (Germany), Eastman chemical (USA).²³ BASF's Ecoflex[®] has a long-chain branched structure, while Easter Bio[®] from Eastman chemical is highly linear in structure. In this work Ecoflex[®] blends were studied. Ecoflex[®] as matrix polymer has also been blended with other bio-based polymers, like starch or poly(lactic acid) (PLA). These new polymer blends exhibited interesting property profiles, like improved mechanical toughness or faster degradability.²³ It has a broad range of applications, like organic waste bags, shopping bags, agricultural foils, household films, coated paper board and stiff foamed packaging.²⁴



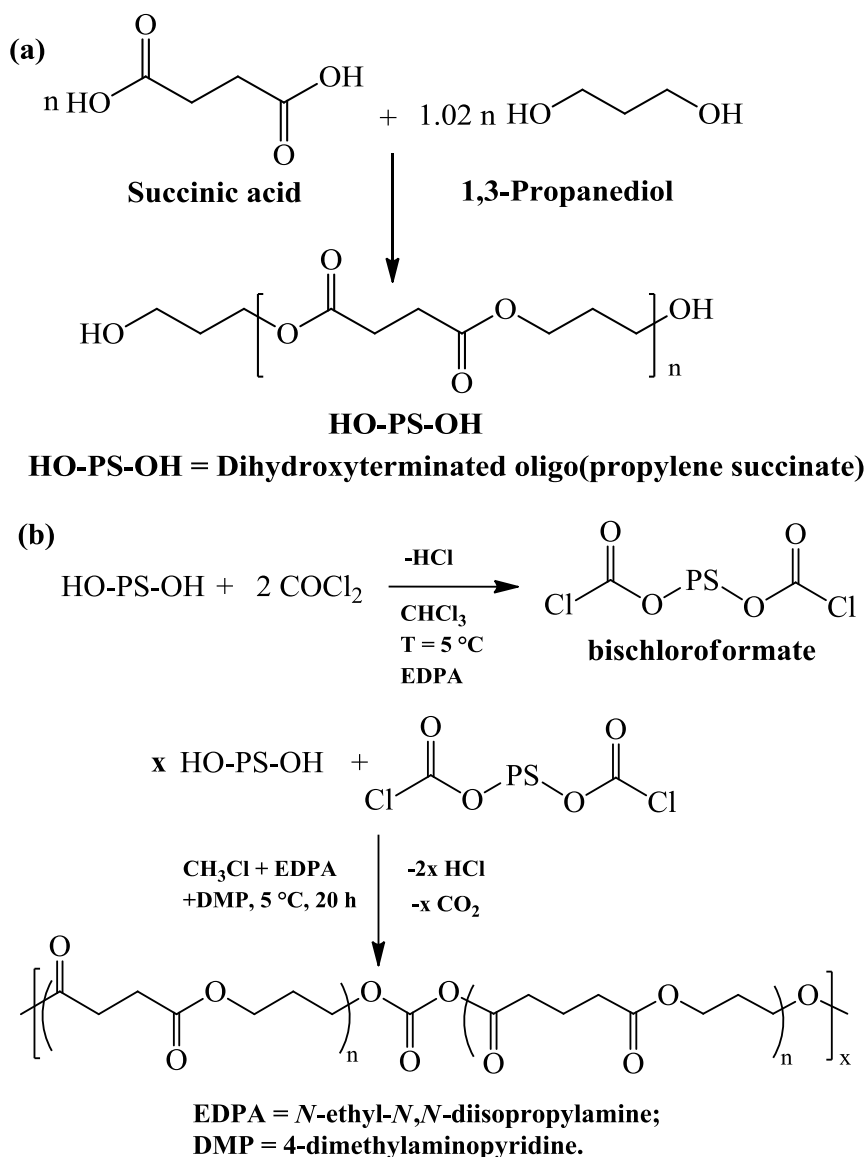
Scheme 1-2. Chemical structure of poly(butylene adipate-co-terephthalate).

Introduction

1.2.2 Synthesis of (bio)degradable polyesters

The traditional synthetic method for polyesters is the polycondensation using diacids or acid derivatives and diols. Each growth step of the polycondensation involves elimination of small molecules, like H₂O, HCl, MeOH etc. The reaction temperature of polymerization in bulk, i.e. without solvent, depends on the melting temperature of monomers and mostly the reactions need high temperature and long reaction times. A polycondensation with high conversion is very difficult to achieve because of side-reactions and the volatilization of monomers causing a stoichiometric imbalance of reactants. The stoichiometric imbalance between reactive acid and hydroxy groups is the main reason for causing low molecular weight of synthetic polyesters. However, for good mechanical properties a high molecular weight is required. The volatilization of reactants can be compensated by a slight excess of one monomer, to precisely control the stoichiometric balance of the reactants in the mixture. In addition chain extension agents are usually used to produce the desired molecular weight by polycondensation. In 2000, Ranucci *et al.* reported high molecular weight poly(ester carbonate)s. Firstly an dihydroxyterminated oligo(propylene succinate) was obtained by traditional synthesis with a molar ratio of 1,3-propanediol to succinic acid of 1.02 (Scheme 1-3a).²⁵ A high molecular weight poly(ester-carbonate) was synthesized by polycondensation with the chain extension agent bischloroformate, resulting in a final M_n of 30,000 and M_w of 48,000 (Scheme 1-3b).

Introduction

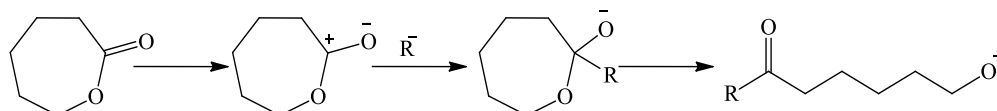


Scheme 1-3. (a) Polycondensation of dihydroxyterminated oligomeric propyl succinate. (b) Chain extension reaction by the dichloroformate route.²⁵

The ROP as a renewed synthetic method to obtain high molecular weight polyesters, was intensively studied in the last 50 years. Compared to polycondensation, the ROP of lactones is an advantageous choice for the synthesis of biocompatible and (bio)degradable polyesters, because they usually have a higher molecular weight and a lower polydispersity. In the first part of this thesis the new antibacterial polycaprolactone was synthesized by ROP. The antibacterial PHMG was used as a macroinitiator for the ROP of polycaprolactone. The mechanism has been reported by Oledzka *et al.* in 2011, whereas the guanidine and *p*-amino functional groups in amino acids have been used as initiators for L-lactide and caprolactone polymerizations. This reaction mechanism can be classified as anionic ROP.^{26,27}

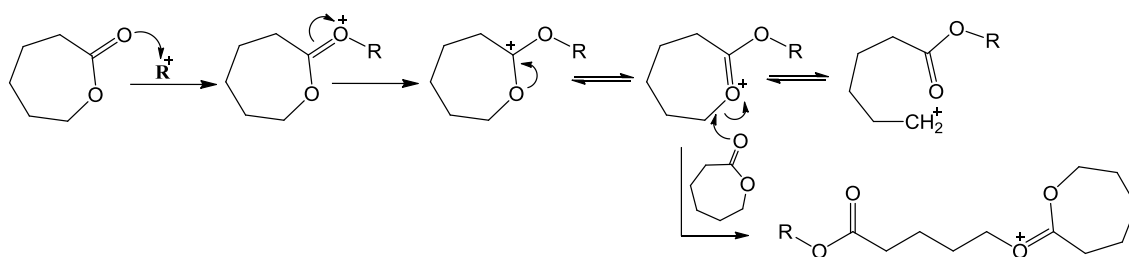
Introduction

The mechanism of ROP of lactones depends on the catalyst, which may lead to anionic, cationic, monomer-activated or coordination-insertion ROP. Anionic ROP starts with an attack of the ionic species at the carbonyl carbon of the monomer ring and subsequently the ring is opened giving an ion at the chain end.²⁸ The drawback of the anionic ROP is that the intramolecular transesterification, i.e. back-biting, which only yields low molecular weight polymers. Scheme 1-4 shows the mechanism of the initiation step of anionic ROP.



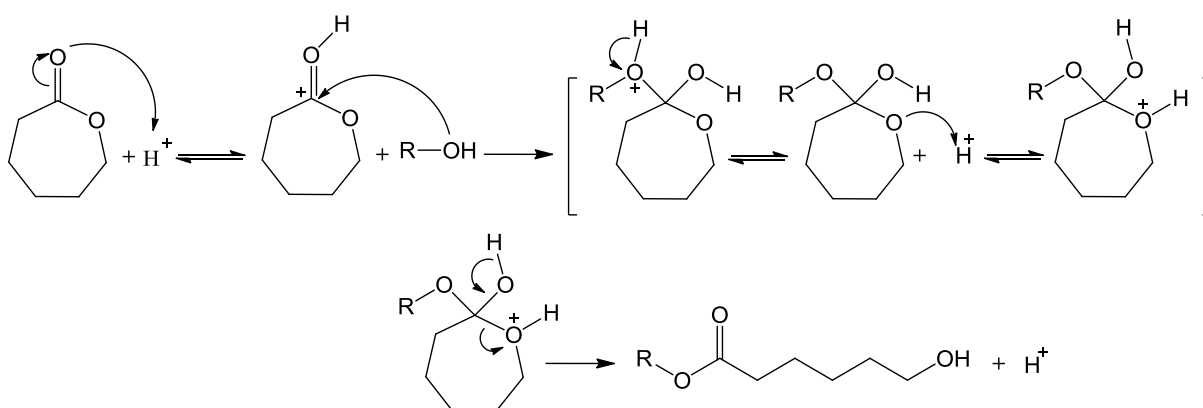
Scheme 1-4. Mechanism of initiation step of anionic ROP.²⁹

The formation of a cationic ROP (Scheme 1-5) happen via a bimolecular nucleophilic substitution (S_N2) reaction, which involves the addition of cationic center to a monomer molecule.²⁰



Scheme 1-5. Mechanism of initiation step of cationic ROP.²⁹

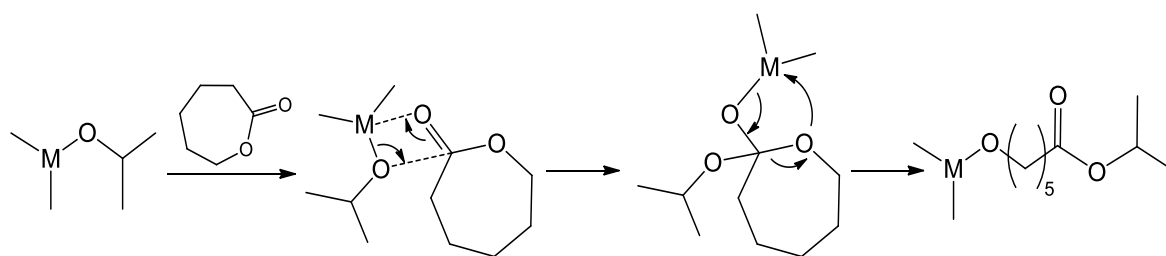
Scheme 1-6 shows the mechanism of the initiation step for monomer-activated ROP. The monomer is activated by a catalyst and subsequently added onto the polymer chain end.



Scheme 1-6. Mechanism of the initiation step of the monomer-activated ROP.^{30,31}

The coordination-insertion is a pseudo-anionic ROP (Scheme 1-7). The reaction starts with the coordination of the monomer to the catalyst and the monomer inserts into a metal-oxygen bond of the catalyst. The growing chain is connected to the metal center through an alkoxide bond.^{29,28}

Introduction



Scheme 1-7. Mechanism of the initiation step for coordination–insertion ROP.²⁹

In addition to this, radical ROP is also often used for synthesis of (bio)degradable polyesters. During radical ROP a constant volume is maintained, which is interesting for application such as tooth fillings, coatings and accurate molding of electrical and electronic components.³⁰ There exist several vinyl substituted cyclic monomers undergoing radical ring-opening polymerization, e.g. ketene acetals³² and phenyl vinyl oxiranes.^{33–35}

Introduction

1.2.3 Application of (bio)degradable polyesters

In order to overcome the environmental problems associated with synthetic plastic waste, the requirement of (bio)degradable plastics is ever growing in the last decades. Table 1-1 shows an overview of applications and volumes for the whole (bio)degradable polymer market in 2007 and 2015.

Table 1-1. Application and volumes of (bio)degradable polymers.²³

Application	Volume 2007 (kt)	Volume 2015 (kt)	Comment
Organic waste bags and shopping/carrier bags	16	131	Most established segment
Packaging including foam	42	248	Food and non-food packaging
Mulch film and horticulture	7	21	-
Sum	65	400	-

Among the commercialized (bio)degradable polymeric materials, PCL is a very useful biomedical polyester, which is used in tissue engineering, drug delivery and release systems³⁶ and the production of surgical sutures.²⁷ In addition, PCL has been promoted as a soil degradable container material,^{37,38} which can be used as a thin-wall tree seedling container.¹² Through the copolymerization with other cyclic monomers, like glycolide,³⁹ L-lactide,⁴⁰ dioxepan-2-one⁴¹ etc. its physical properties and degradability has been modified for different applications. Regarding property modifications, many PCL blends were studied, too. PCL with starch and its derivatives can be used in shopping bags.⁴² PCL/polypropylene and PCL/polyethylene blends spun into fibers show higher tenacity and are dyeable with dispersed dye formulation.⁴³ The here presented copolymers of PCL a linear polyguanidine, which have high antibacterial activity, are suitable as additive of food packaging or hygienic applications.

In general, polymers can undergo degradation either by surface erosion or by bulk erosion.⁴⁴ In the next chapter 1.2.4 the two different (bio)degradable mechanisms will be explained in detail. PCL is reported to undergo surface erosion.⁴⁵ When used as implant for in-vivo application, it will erode from the surface only and become smaller while keeping its original geometric shape. The predictability of the erosion process in drug delivery is also an advantage of surface eroding polymers.⁴⁶

Introduction

Compared to aliphatic polyesters, the (bio)degradable copolymers consisting of aliphatic and aromatic units show better physical and mechanical properties. In this thesis a (bio)degradable aliphatic and aromatic polyester “Ecoflex”, which has been used on an industrial scale, was studied as matrix polymer in blends with antibacterial additive. Ecoflex[®] and its blends from BASF are used as short-lived plastic films like organic waste bags, cling films or in paperboard coatings for completely compostable paper cups.²³ Ecoflex[®]/PLA and Ecoflex[®]/starch blends are the two commercially most important Ecoflex[®]/biopolymer blends. The blend of Ecoflex[®] with starch compounds is used to enhance the mechanical and thermal properties as well as hydrophobicity of compounded materials. The temperature resistance of Ecoflex[®]/starch blends is improved by more than 60 °C, which delivers the optical stability of organic waste bags during storage and biowaste collection. Ecoflex[®] is a soft (bio)degradable material, which is an ideal material to efficiently reduce the stiffness of brittle (bio)degradable materials like PLA. The stiffness of PLA is reduced by 25 %, with an addition of 20 % Ecoflex[®]. BASF sells compostable and bio/based Ecoflex[®]/PLA blends under the trade name Ecovio[®], which can be used as plant pots, seed/fertilizer tape and binding materials, foams and nets. From degradation tests in compost (discussed in chapter 4) Ecoflex[®] shows the (bio)degradable mechanism “bulk erosion”. The advantage is that the size of the polymer will remain constant for a considerable portion of time during its application.

Introduction

1.2.4 Degradation of polyesters

A (bio)degradable plastic is defined by the ASTM (American Society for Testing and Materials) as “A plastic designed to undergo a significant change in its chemical structure under specific environmental conditions resulting in a change of properties that may vary as measured by standard test methods appropriate to the plastic and the application in a period of time, that determines its classification, in which the degradation results from the action of microorganisms occurring naturally such as bacteria, fungi, and algae.”⁴⁷ However, this definition is only suitable for biotically driven degradation of (bio)degradable plastics. If the abiotic molar mass reduction occurs by hydrolysis of linear polyesters or the oxidation, degradation of polyolefins prior to the bioassimilation, these mechanisms are not included in the definition. Therefore hydro-biodegradation and oxo-biodegradation are two major parallel classes of (bio)degradable plastics, which are defined as “biodegradation in which polymer chain cleavage is primarily due to hydrolysis or oxidation which may be mediated by abiotic chemistry, microorganisms or a combination of both.”⁴⁸ Figure 1-1 shows the general features of hydro- and oxo-(bio)degradable polymeric materials. The mechanisms of biodegradation depend on the nature of the polymer and the environment.^{49,50} The nature of polymer defines the surface and bulk conditions like surface area, hydrophilic and hydrophobic properties, chemical structure, molecular weight and molecular weight distribution, glass transition temperature, melting temperature, modulus of elasticity, crystallinity and crystal structure *etc.*⁵¹

There exist two different erosion mechanisms for (bio)degradable polymers depending on the above mentioned characteristics. The first can be described as a bulk degradation process, if water diffuses into the polymer matrix faster than the polymer is degraded. The hydrolysable bonds of the whole polymer matrix are divided homogeneously, leading to a homogenous decrease of the average molecular weight of the polymer. The other mechanism is surface erosion, which is present, when water diffuses slower into the polymer matrix than the degradation rate of the polymer. The degradation occurs only at the surface layer. Thus a molecular weight change of the bulk sample is not observed. Surface erosion is a heterogeneous process, which has a strong dependency on surface condition of the sample.⁵²

Introduction

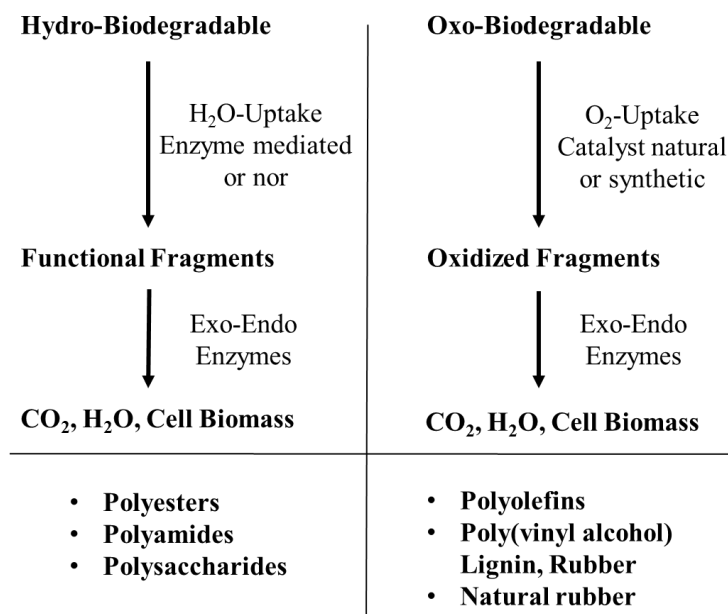
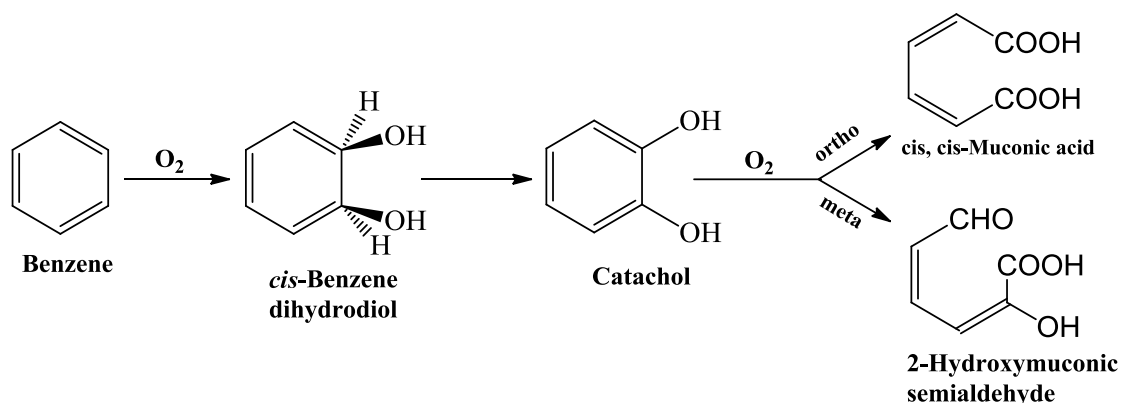


Figure 1-1. General features of hydro- and oxo-(bio)degradable polymeric materials⁵³.

The biodegradation behavior of aromatic/aliphatic polymers has been very well studied. PBAT is a completely degradable aromatic/aliphatic polyester and used as compost bags, agricultural films and packaging materials. Many studies show, that aromatic compounds degrade under nitrate-reducing, iron-reducing, sulfate-reducing, and methanogenic conditions.⁵⁴ However the information of biodegradation behavior of aromatic compounds under anaerobic conditions is very limited.⁵⁵ Scheme 1-8 shows the mechanism of aerobic biodegradation process of benzene, which involves the oxidation by molecular oxygen. By oxidation intermediates are produced, which enter central metabolic pathways including the Krebs Cycle and β -oxidation.⁵⁶⁻⁵⁸ The benzene ring is hydroxylated by microorganisms using oxygen, which leads to the subsequent fission of the ring. The major step of degradation is the elimination of the double bond of the ring between two hydroxylated carbon atoms (*ortho* pathway), or adjacent to a hydroxylated carbon atom (*meta* pathway), or in an indole ring.⁵⁴



Scheme 1-8. Aerobic benzene biodegradation.

Introduction

1.2.5 Biodegradation test methods

(bio)degradable polymers, as environmentally friendly materials, claim to be degraded by attack of microorganisms. Therefore, the biodegradation behavior must be proved by using scientifically based and generally accepted methods.

The biodegradation testing of chemicals has been carried out for over 30 years. Generally the tests can be subdivided in principle into three categories: field tests, simulation tests and laboratory tests, as shown in Figure 1-2.⁵⁹

Laboratory - tests			Simulation - tests	Field - tests	
Enzyme - test	Clear-zone Test	Sturm-Test	Laboratory reactor: water soil compost material from landfill	In nature: water soil compost landfill	
enzymes	individual-cultures	mixed-cultures			
→	synthetic environment		→	complex environment	
→	defined conditions		→	defined conditions	
				→	variable conditions

Figure 1-2. Schematic overview of biodegradation tests for polymeric materials.⁵⁹

The biodegradation behavior of polymers depends not only on the properties of the materials but also on the environmental conditions such as temperature, pH-value or humidity. Field tests represent the ideal practical environmental conditions, by burying polymers in soil and compost or placing it in a lake or river. However, field tests have also some disadvantages. For example, the test conditions of the environment are not controllable and the analytical methods are very limited. In most cases it is only possible to evaluate visible changes or to measure weight loss on the polymer specimen. Therefore, instead field tests various simulation tests have been used to measure the (bio)degradability of polymers. In simulation tests, the biodegradation takes place in compost, soil or lake-, river-, sea-water in a controllable environment within a laboratory. During testing more analytical methods are available than for the field tests. Examples of such qualitative and quantitative analyses of residues and intermediates are the determination of CO₂ evolution or O₂ consumption. Another advantage of simulation tests is,

Introduction

that the testing time can be reduced by changing the testing parameter, e.g. increasing microbial activity, temperature or humidity etc. in order to accelerate degradation.

Composting tests are common simulation tests, particularly for (bio)degradable packaging materials. Table 1-2 shows the norms of composting tests of polymers from ASTM, ISO (International organization for standardization); EN (European Norm) and Japanese Greenpla.⁶⁰ All these standards define basic requirements for packaging and packaging materials to be identified as (bio)degradable and compostable in industrial composting facilities. European Norm EN 13432, the American ASTM D 6400-04 and the Japanese GreenPla are the most important standards, while the international standard ISO 17088, is analogous to ASTM D 6400-04 standard, based on ISO 14855-1:2005 and ISO 14855-1:2007, which became effective in 2008.⁶⁰ It can be used worldwide. According to ISO 14855 the controlled composting test is the most important proof of ultimate aerobic (bio)degradability. It is also the central part of every standard named above for (bio)degradable polymers.²³

Table 1-2. Norms for composting test of (bio)degradable polymers.

EN 134329 (European)	Requirements for packaging recoverable through composting and biodegradation. Test scheme and evaluation criteria for the final acceptance of packaging.
ASTM D 6400-04 (American)	Standard Specification for Compostable Plastics.
GreenPla. (Japanese)	The generic term for (bio)degradable plastics, raw materials and products that contain (bio)degradable plastics.
ISO 17088	Specifications for compostable plastics.
ISO 14855-1:2005	Determination of the ultimate aerobic biodegradability of plastic materials under controlled composting conditions—method by analysis of evolved carbon dioxide-part 1: general method.
ISO 14855-2:2007	Determination of the ultimate aerobic biodegradability of plastic materials under controlled composting conditions—method by analysis of evolved carbon dioxide-part 2: gravimetric measurement of carbon dioxide evolved in a laboratory-scale test.

The laboratory biodegradation tests are the most reproducible tests. In most cases, synthetic media and inoculated media with either a mixed microbial population or individual microbial strains are used, which are especially optimized for polymers. Because of those reasons, in laboratory tests, polymers often show a much higher degradation rate than within field tests. It is only possible to derive limited conclusions on the absolute degradation rate of materials in nature.⁵⁹ However these tests are always widely used for many systematic investigations of polymeric (bio)degradability.

Enzymatic biodegradation tests are typical laboratory biodegradation tests, which are very useful in examining the kinetics of depolymerization, oligomer and monomer release from a

Introduction

polymer chain under different conditions or types of purified enzymes, respectively. Enzymatic test methods have been widely used for studying the hydrolysis of aliphatic polyesters,⁶¹⁻⁶³ starch plastics or packaging materials containing cellulose.⁶⁴⁻⁶⁷ For example, the commercially available lipase from *Pseudomonas cepacia* is often chosen to quantify the degradation behavior.^{62,68,69}

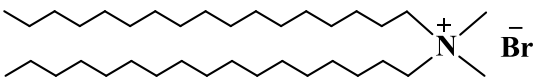
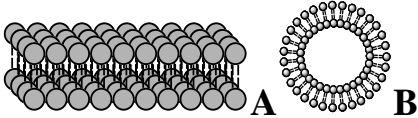
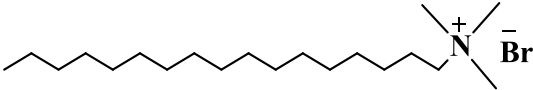
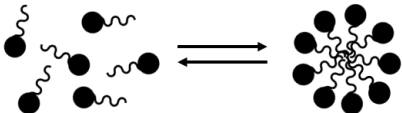
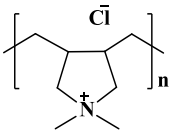
Introduction

1.3 Antibacterial materials

1.3.1 Cationic antibacterial compounds

Cationic compounds are the most promising candidates of all antimicrobial materials. For example, cationic surfactants, lipids, peptides and natural or synthetic polymers have been intensively studied as antimicrobial agents. Table 1-3 shows structure of some cationic surfactants, lipids, polymers and their assemblies.⁷⁰ Those compounds display antimicrobial properties by either themselves or in combinations with inert materials such as natural polymers. Due to the high antimicrobial activity and low toxicity, they fulfill a major requirement for biomedical applications as well as for food packing, preservation and antifouling applications.⁷

Table 1-3. Antimicrobial cationic compounds and assemblies.

Cationic molecule or assembly	Name
	Dioctadecyldimethylammonium bromide (DODAB)
	Cationic bilayer fragment (A) Large cationic vesicle (B)
	Hexadecyltrimethylammonium bromide (CTAB)
	CTAB micelle
	Poly (diallyldimethyl) ammonium chloride (PDDA)

A high number of interesting antibacterial cationic polymers have been synthesized in the recent years.^{71,72} The antimicrobial activity of cationic polymers depends on the nature of polymer such as molecular weight, molar mass, polydispersity, water solubility and the amphiphilic balance of polymer chains.⁷³ The target of antibacterial cationic polymers is to destroy the membrane of Gram-positive and Gram-negative bacteria cells. Mostly the same cationic polymer shows higher antibacterial activity for Gram-positive bacteria than Gram-negative bacteria. This can be explained by different features of bacterial cell walls. Gram-positive cell walls have one single phospholipid bilayer surrounded by a murein sacculus, whereas Gram-

Introduction

negative cell walls have a unique outer membrane, which develops a barrier function, shown in Figure 1-3.

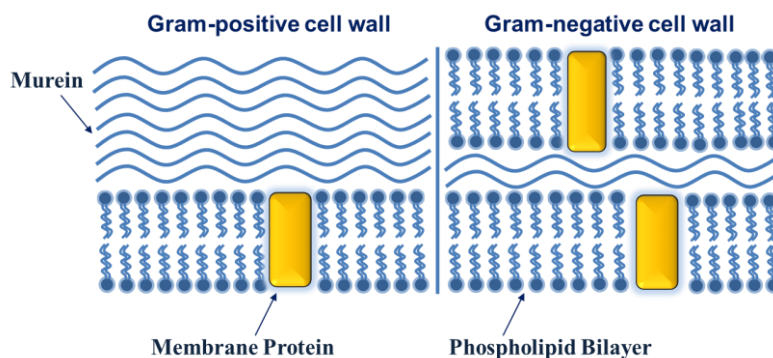


Figure 1-3. Simplified illustration of Gram-positive and Gram-negative bacterial cell walls.

PG exhibits excellent antimicrobial activity against Gram-positive and Gram-negative bacteria,⁷ fungus,⁹ and virus⁸, which is a typical antimicrobial cationic polymer.⁷⁴ Table 1-4 shows some chemical structures of polyguanidine hydrochlorides. Compared to aliphatic PG, the aromatic groups in the polymer chains of PPXG limit the dispartment into the lipid membrane and lead to a weaker adsorption compared to flexible alkyl polymer chains.⁷⁵ However the limited antimicrobial activity led to a low cytotoxicity, which is an advantage for application of tissue engineering material. In Chapter 5 PPXG is used as an antimicrobial coating on Bioglass[®] scaffolds, which showed antibacterial activity and biocompatibility with low cytotoxicity. Increased hydrophobicity of the polymer chains from C₄ to C₈ leads to better dispartment in the hydrophobic parts of phospholipids of bacterial cell membrane. Furthermore, it causes stronger adsorption on the membrane surface, which improves the antibacterial properties. After adsorption, the phospholipids were rearranged causing the disorganization of cell membrane. The hydrophobic parts of polymer insert into the membrane core that lead to the aggregation of phospholipids around the polymer chain. The membrane destabilizes, while a hole is formed. As a result, the intracellular content is discharged and the bacteria cell dies.^{76,77}

Introduction

Table 1-4. Polyguanidine hydrochloride derivatives.⁷⁸⁻⁸⁰

Name	Structure of Polymer
polyhexamethylene guanidine hydrochloride (PHMG)	
Polytetramethylene guanidine hydrochloride (PTMG)	
Polyoctamethylene guanidine hydrochloride (POMG)	
poly(<i>m</i> -xylyleneguanidine) hydrochloride (PMXG)	
poly(<i>p</i> -xylyleneguanidine) hydrochloride (PPXG)	
Poly(cyclohexane guanidine) hydrochloride (PCHG)	
Poly(tetraethylenepentamine guanidine) hydrochloride (PTEPAG)	

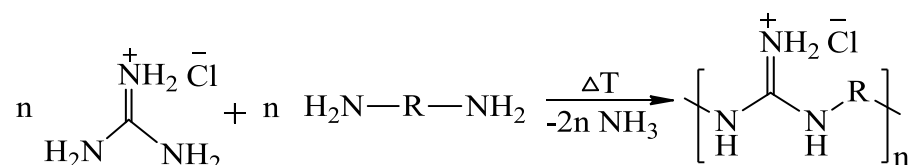
Of all PGs, PHMG has been the most extensively studied. It was used for many years as an antiseptic in medicine and in recent years it also found application in swimming pool sanitization, treatment for cooling systems to prevent infection,⁸¹ as solid surface cleaner in food industry, the treatment of heating eggs to prevent salmonella infection,^{82,83} impregnation of gauze wound-dressing to avoid the *Pseudomonas* infection⁸⁴ and as a durable anti-odor material in textiles.⁸⁵ Polyguanidine hydrochloride is synthesized by melt polycondensation with equimolar amounts of diamine and guanidine hydrochloride.⁸⁶ since the low molecular weight, PHMG has been also considered as a promising antimicrobial additive blending with other matrix materials, which have good mechanical properties.^{4,87} In Chapter 4 the new antimicrobial Ecoflex[®] is described, which was obtained by melt extrusion with an aqueous PHMG solution.

Introduction

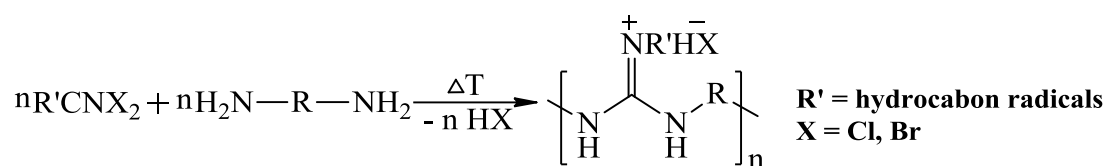
1.3.2 Polyguanidine based antibacterial materials

PG can be easily prepared by step-growth reaction. The first patent about oligoguanidine compounds as antibacterial agents was filed in the 1940s.⁸⁸ PG was synthesized either by polycondensation⁸⁹ or polyaddition,⁹⁰ respectively. The starting materials can either consist of monomeric guanidines, isocyanide dihalides, guanido acid esters, cyanogen halides or dicyanamides, respectively.⁸⁸ The respective reactions are represented by the following examples in (a)-(e) (R may be aliphatic or aromatic):

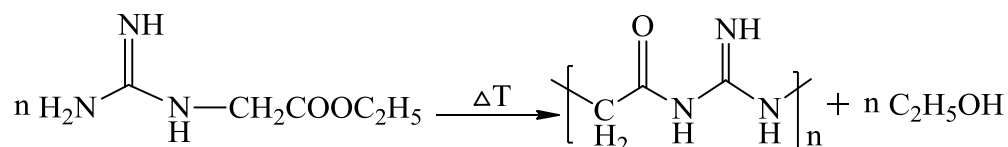
Polycondensation:



- (a) A mixture of a diamine and a guanidine in equivalent proportions is heated for 2 to 12 h at temperatures ranging from 130 °C to 180 °C. The polycondensation reaction begins with the evolution of ammonia.



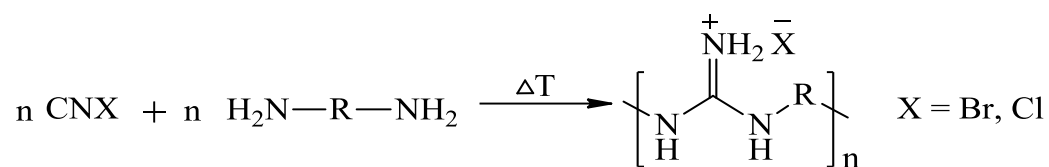
- (b) Polycondensation of an isocyanide dihalide and a diamine started in dry benzene or other inert solvents in the presence of an equivalent amount of potassium carbonate at 45 °C. Subsequently, the reagents are separated from the solvent and further polymerized under nitrogen for 9 h at 180 °C.



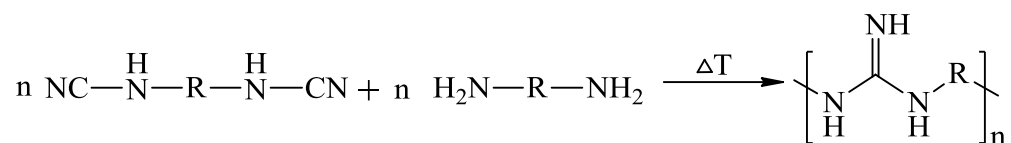
- (c) The self-condensation of a guanido ester produces a polyacyl guanidine. The polymerization is allowed to take place under the same conditions as in (a). The reaction begins with the evolution of alcohol. The amount of alcohol evolved is as a measure of the extent of polymerization.

Introduction

Polyaddition:



(d) To a cyanogen halide dissolved in absolute ethanol is added an equimolar quantity of diamine dissolved in an anhydrous alcoholic solution. After 1 h of heating the solution is concentrated under reduced pressure and the residue is further polymerized at 175 °C.



(e) An *N, N'*-dicyanamide and a diamine are allowed to react under the same condition as in (a) without small molecule elimination.

Introduction

1.3.3 Antibacterial test methods

In this thesis, standard methods, which are described and classified by the German Institute for Standardization (DIN) (Deutsches Institut für Normung) and American Type Culture Collection (ATCC) norms, were used to evaluate the antibacterial activity of polymeric materials by Gram-positive bacteria *B. subtilis* (ATCC 11774) and Gram-negative bacteria *E. coli* (ATCC 11229).

Usually, the first quantitative test to identify the antibacterial activity of water soluble polymers or polymer suspensions are MIC and MBC tests, which are carried out according to the DIN 58940-6 and DIN 58940-7 norms. MIC describes the minimal amount of inhibition of the visible bacteria growth and MBC corresponds to the amount that is required to kill more than 99.9 % bacteria. The test methods are described below and the schematic illustration is shown in Figure 1-4. Firstly, a serial dilution of polymer is added in a 24-wells plate from high concentration, for example $2000 \mu\text{m mL}^{-1}$, to zero, as blank sample. Then a bacterial suspension with 10^6 - 10^7 cfu/mL is added in every well. After 24 h at 37°C incubation the wells are visually evaluated for turbidity. The lowest concentration of the well that is transparent is defined as MIC. For determining the MBC, 100 μL last three transparent suspensions are chosen to be spread on new agar plates. After another 24 h incubation at 37°C colony formation shows up and the lowest concentration with biocidal activity is taken as MBC.

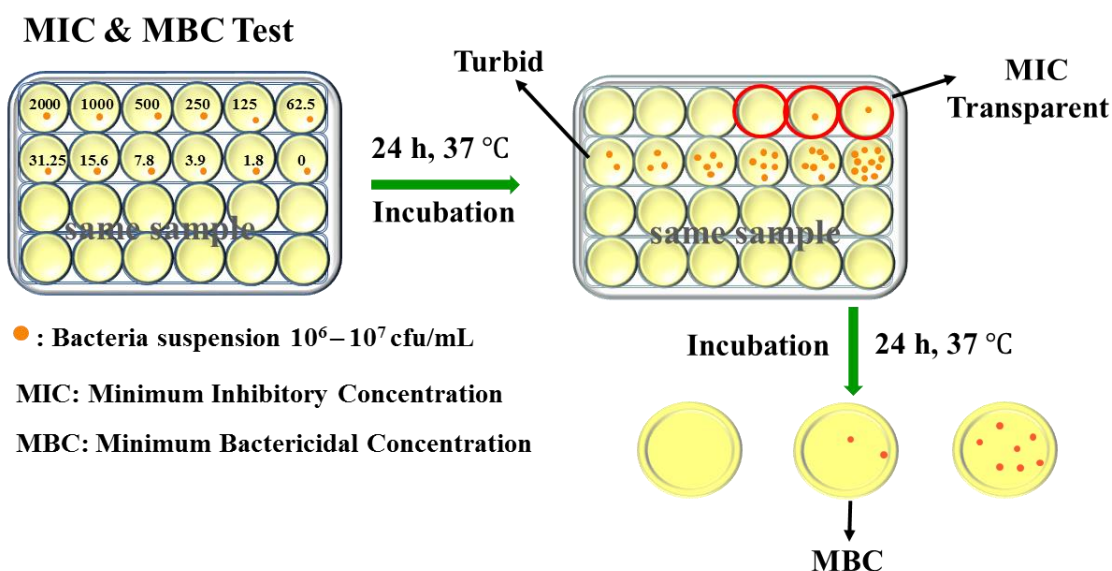


Figure 1-4. Schematic illustration of MIC and MBC tests of antibacterial polymers.

The next important method is the shaking flask test, which is used to evaluate the rate of bacterial reduction by the polymers, e.g. antibacterial polymers with release mechanism. It is a

Introduction

so-called time-dependent test. Of course, the method is also adaptable to a polymer solution and suspension with different concentration or a water insoluble material. The process of the shaking flask test is shown in Figure 1-5. Firstly, the sample is added in a sterilized centrifugal tube with 1.5 mL bacterial suspension (10^6 - 10^7 cfu/mL) and incubated for a defined time interval. Then a tenfold dilution series of specimens from 10^0 to 10^{-3} out of the bacterial suspension is spread on new agar plates. After 24 hours at 37 °C incubation, the number of colonies is counted. With a relative cell density of inoculum the percentage or logarithmic stages reduction of bacterial cells is calculated. The formula for calculation is shown below.

$$\text{Bacteria reduction [\%]} = \frac{A - B}{A} \times 100 \%$$

$$\text{Bacteria reduction [log stages]} = -\log\left(\frac{B}{A}\right)$$

$A = \text{colony count}_{\text{blank}}$; $B = \text{colony count}_{\text{sample}}$

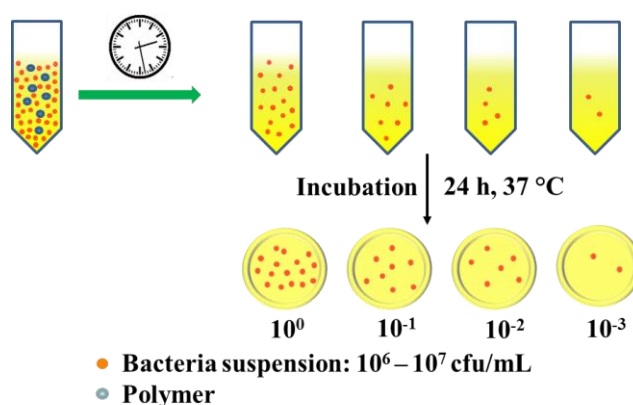


Figure 1-5. Schematic illustration of the shaking flask test.

The Kirby-Bauer test is another standard method to determine the antibacterial activity of surface and leaching behavior. The Kirby-Bauer test process is illustrated schematically in Figure 1-6. Firstly, 100 μ L of a bacterial suspension with concentrations between 10^6 - 10^7 cfu/mL is spread on an agar plate, on which the specimen and a blank sample are placed. If the sample shows leaching effect, after overnight incubation, a “zone of inhibition” is formed, in which bacteria colony formation is absent. After removing the sample with a swab, the sample is transferred to a new agar plate. If after 24 hours of incubation no bacterial colony has grown on the agar plate, all bacteria under the sample were killed due to surface contact. In contrast, with the blank sample after incubation the colonies should grow.

Introduction

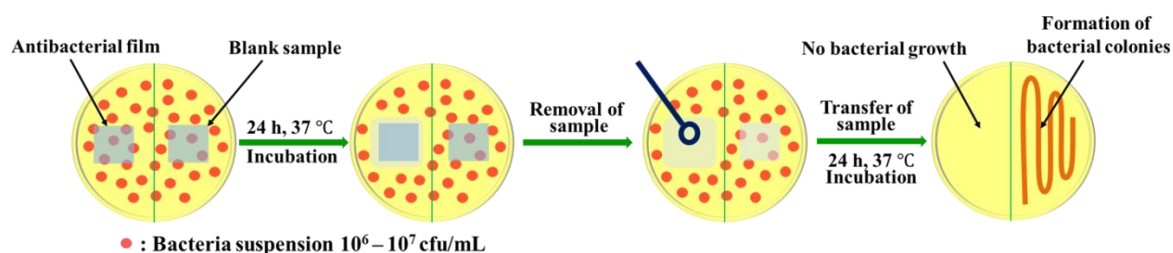


Figure 1-6. Schematic illustration of the Kirby-Bauer test.

1.4 (bio)degradable polymers with antimicrobial activity

Materials of food packaging or medical applications have a significant risk of contamination with bacteria coming from the material itself or the surrounding environment. To reduce the risk, it is possible to combine the antimicrobial activity and (bio)degradability in one material. The formation of antimicrobial (bio)degradable polymers can be achieved by several methods:

- 1) Use of (bio)degradable polymers with inherently antimicrobial properties.
- 2) Coating or adsorbing antimicrobial materials onto polymer surface.
- 3) Immobilization of antimicrobial agents onto (bio)degradable polymers by ion or covalent bonds.
- 4) Incorporation of leaching or non-leaching antimicrobial agents directly into polymer matrix.

The simplest method is to directly use a polymer, which possesses both properties, e.g. poly-L-lysine³ and chitosan.⁹¹ Chitosan is a polymer, which is the deacetylated form of chitin with repeating units of disaccharides having amino group, (1,4)-2-amino-2-deoxy- β -D-glucan.^{92,93} Chitosan is commercially available as packaging material for food and medical applications.^{92,94,95} Zheng and Zhu studied the relationship between molecular weight and antimicrobial activity of chitosan. In their report chitosan with molecular weight below 305 kDa was investigated. For Gram-positive bacteria *S. aureus* the antimicrobial effect was enhanced with increasing molecular weight, whereas for Gram-negative bacteria *E. coli* the antibacterial activity decreased with increasing molecular weight. The reason may be, that the relative short polymer chains can easily enter the microbial cell and better interact with the metabolism of the cell.⁹³ Makarios-Laham and Lee reported that chitosan-based antimicrobial films as packaging materials containing 10% chitosan are degraded and broken down in the soil environment.⁹² Berkeley reported that chitosan-hydrolyzing enzymes (chitosanases) are produced by many

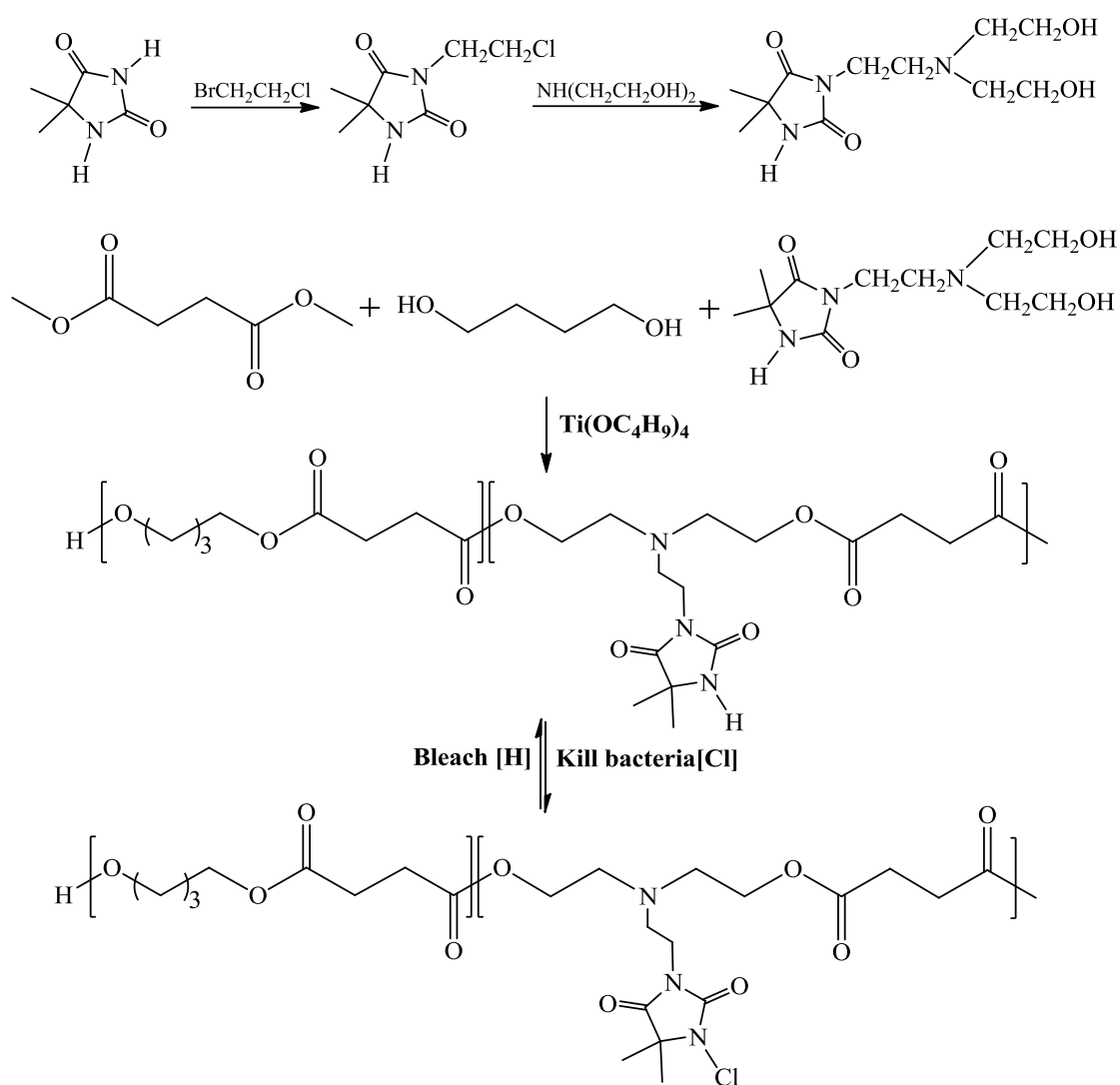
Introduction

bacterial genera, all of which can be found in soil. Green antibacterial agents can also be produced by natural flora, e.g. bamboo or ginkgo etc. Recently a new patent showed that a mixture of bamboo, ginkgo and aloe leaf can be used as natural antimicrobial agent as coating materials.⁹⁶

The second strategy is coating or adsorbing antimicrobial agents onto a (bio)degradable material surface. If the antimicrobial agent has low molecular weight, poor mechanical properties or cannot tolerate the temperature during polymer processing, coating or adsorbing it on the surface of a stable substrate is a very beneficial method. It can not only supply the antibacterial property, but also offer mechanical strength and temperature tolerance from the matrix materials. At the beginning of the development of these materials, fungicides were incorporated into waxes to coat the surface of fruits or quaternary ammonium salts were coated on shrink films to pack vegetables.⁹⁷ Recently, a lot of antimicrobial coatings or adsorbing materials have been studied intensively not only for food industry but also for wound healing and medical devices. For example, a quaternary ammonium-modified triethoxysilane was coated on cotton textile, which shows antimicrobial activity against Gram-positive and Gram-negative bacteria and non-leaching effect.⁹⁸ Kinninmonth *et al.* reported that different essential oils can be used as antimicrobial agents, which are adsorbed on porous silicate materials and then added to polymer materials to produce antimicrobial polymers.⁹⁹ In this thesis, an antimicrobial polymer was also used as a coating material for scaffolds for bone tissue engineering.

Immobilization of antimicrobial agents onto polymers by covalent attachment is another strategy. Jao *et al.* reported that a PBAT film was treated with ozone to activate the surface, onto which the antimicrobial agent chitosan was subsequently grafted. The modified PBAT film exhibits also a superior biocompatibility for clinical applications.¹⁰⁰ In our workgroup L. Tan *et al.* have designed hydantoin-containing polymers based on enzymatic degradable polyesters, prepared by two different routes. The first route involves the dihydroxylation of hydantoin and subsequent transesterification with dimethyl succinate and 1,4-butanediol to synthesize an aliphatic polyester. After chlorination, the copolyester shows antibacterial activity and enzymatic degradability (Scheme 1-9).¹⁰¹

Introduction



Scheme 1-9. Synthesis of monomer and copolyesters containing hydantoin and the chlorination process.

For the second route, a (bio)degradable polyester was synthesized by ring-opening polymerization, which was used to attach antibacterial hydantoin moieties via click chemistry by a copper(I)-catalyzed azide-alkyne cycloaddition reaction.¹⁰² In the first step, cyclohexanone was functionalized with an alkyne group and subsequently expanded via BAeyer-VILLIGER oxidation to give the alkyne-carrying caprolactone derivative. After copolymerization with pure ϵ -caprolactone, the azide-containing hydantoin was attached to the alkyne groups of the copolymer in the presence of a Cu(I) catalyst (Scheme 1-10).

Introduction

For many applications of antimicrobial (bio)degradable materials, good mechanical properties are always important. Therefore, a (bio)degradable matrix polymer with good mechanical properties is required. Incorporation of antimicrobial agents directly through physical blending into a (bio)degradable material, which has good mechanical properties, is one of the most effective methods for providing an antimicrobial (bio)degradable polymer. The antimicrobial agents can be incorporated into matrix polymers by thermal polymer processing, like extrusion or injection molding. For heat-sensitive antimicrobials like enzymes and volatile compounds solution blending is a suitable method. For example, functional nanocomposites with antimicrobial properties were produced by incorporating silver or copper nanoparticles into the (bio)degradable matrix polymers.^{104,105} The nanocomposites are prepared by solution casting and show high antimicrobial activity and (bio)degradability. In addition, the (bio)degradable polymer PBAT was extruded with antimicrobial PHMG and thermoplastic starch (TPS).⁴ Blending with starch led to more hydrophilicity of the material, which increased the rate of biodegradation. The extruded polymer showed antimicrobial activity and biodegradation in soil. However in most cases, the disadvantage is deteriorating mechanical properties with increased amount of additive. PBAT, as a favored matrix material, is usually used for compounding with antimicrobial agents. In chapter 4 of this thesis the commercial polymer material PBAT was utilized as matrix material for a modified simple extrusion process, where PHMG was blended into the matrix as aqueous solution. Highlight of this work are the enhanced mechanical properties of the extruded antibacterial Ecoflex[®]. Although there was no covalent bond formed during the extrusion, the extrudate with high percentage of antimicrobial additive showed little leaching effect.

References

1.5 References

1. Premraj, R. & Doble, M. Biodegradation of polymers. *Indian J. Biotechnology* **4**, 186–193 (2005).
2. Yamamoto, M., Witt, U., Skupin, G., Beimborn, D. & Müller, R.-J. in *Biopolymers Online* (eds. Doi, Y. & Steinbüchel, A.) 299–305 (Wiley-VCH Verlag GmbH & Co. KGaA, 2005). doi:10.1002/3527600035.bpol4011
3. Appendini, P. & Hotchkiss, J. H. Review of antimicrobial food packaging. *Innov. Food Sci. Emerg. Technol.* **3**, 113–126 (2002).
4. Wang, H., Wei, D., Zheng, A. & Xiao, H. Soil burial biodegradation of antimicrobial biodegradable PBAT films. *Polym. Degrad. Stab.* **116**, 14–22 (2015).
5. Knetsch, M. L. W. & Koole, L. H. New Strategies in the Development of Antimicrobial Coatings: The Example of Increasing Usage of Silver and Silver Nanoparticles. *Polymers* **3**, 340–366 (2011).
6. Albertsson, A.-C. & Karlsson, S. in *Chemistry and Technology of Biodegradable Polymers* (Blackie Academic & Professional, 1994).
7. Zhang, Y., Jiang, J. & Chen, Y. Synthesis and antimicrobial activity of polymeric guanidine and biguanidine salts. *Polymer* **40**, 6189–6198 (1999).
8. Thakkar, N. *et al.* Persistent interactions between biguanide-based compound NB325 and CXCR4 result in prolonged inhibition of human immunodeficiency virus type 1 infection. *Antimicrob. Agents Chemother.* **54**, 1965–1972 (2010).
9. Manetti, F. *et al.* Synthesis of new linear guanidines and macrocyclic amidinourea derivatives endowed with high antifungal activity against *Candida* spp. and *Aspergillus* spp. *J. Med. Chem.* **52**, 7376–7379 (2009).
10. Avérous, L. & Pollet, E. *Environmental Silicate Nano-Biocomposites. Green Energy and Technology* **50**, (Springer London, 2012).
11. Tian, H., Tang, Z., Zhuang, X., Chen, X. & Jing, X. Biodegradable synthetic polymers: Preparation, functionalization and biomedical application. *Prog. Polym. Sci.* **37**, 237–280 (2012).
12. Albertsson, A.-C. & Varma, I. K. in *Degradable Aliphatic Polyesters* **157**, 1–40 (Springer Berlin Heidelberg, 2002).
13. Benicewicz, B. C. & Hopper, P. K. Polymers for absorbable surgical sutures. *J. Bioact. Compat. Polym.* **5**, 453–472 (1990).
14. Grijpma, D. W. & Pennings, a. J. (Co)polymers of L-lactide, 1 Synthesis, thermal properties and hydrolytic degradation. *Macromol. Chem. Phys.* **195**, 1633–1647 (1994).

References

15. Holland, S. J., Tighe, B. J. & Gould, P. L. Polymers for biodegradable medical devices. 1. The potential of polyesters as controlled macromolecular release systems. *J. Control. Release* **4**, 155–180 (1986).
16. Menzel, H., Kröger, R. & Hallensleben, M. L. Polymers with Light Controlled Water Solubility. *J. Macromol. Sci. Part A* **32**, 779–787 (1995).
17. Kaplan, D. L., Mayer, J. M., Greenberger, M., Gross, R. & McCarthy, S. Degradation methods and degradation kinetics of polymer films. *Polym. Degrad. Stab.* **45**, 165–172 (1994).
18. Goldberg, D. A review of the biodegradability and utility of poly(caprolactone). *J. Environ. Polym. Degrad.* **3**, 61–67 (1995).
19. Lunt, J. Large-scale production, properties and commercial applications of polylactic acid polymers. *Polym. Degrad. Stab.* **59**, 145–152 (1998).
20. Labet, M. & Thielemans, W. Synthesis of polycaprolactone: a review. *Chem. Soc. Rev.* **38**, 3484–3504 (2009).
21. Amass, W., Amass, A. & Tighe, B. A review of biodegradable polymers: uses, current developments in the synthesis and characterization of biodegradable polyesters, blends of biodegradable polymers and recent advances in biodegradation studies. *Polym. Int.* **47**, 89–144 (1998).
22. Hubbell, D. S. & Cooper, S. L. The Physical Properties and Morphology of Poly- ϵ -caprolactone Polymer Blends. *J. Appl. Polym. Sci.* **21**, 3035–3061 (1977).
23. Siegenthaler, K. O., Künkel, A., Skupin, G. & Yamamoto, M. in *Advances in Polymer Science* 91–136 (2012). doi:10.1007/12_2010_106
24. Artham, T. & Doble, M. Biodegradation of aliphatic and aromatic polycarbonates. *Macromol. Biosci.* **8**, 14–24 (2008).
25. Ranucci, E., Liu, Y., Söderqvist Lindblad, M. & Albertsson, A.-C. New biodegradable polymers from renewable sources. High molecular weight poly(ester carbonate)s from succinic acid and 1,3-propanediol. *Macromol. Rapid Commun.* **21**, 680–684 (2000).
26. Sobczak, M., Oledzka, E. & Kołodziejcki, W. L. NOTE: Polymerization of Cyclic Esters Using Aminoacid Initiators. *J. Macromol. Sci. Part A* **45**, 872–877 (2008).
27. Oledzka, E., Sokolowski, K., Sobczak, M. & Kolodziejcki, W. α -Amino acids as initiators of ϵ -caprolactone and L,L-lactide polymerization. *Polym. Int.* **60**, 787–793 (2011).
28. Stridsberg, K. M., Ryner, M. & Albertsson, A.-C. in *Degradable Aliphatic Polyesters* **157**, 41–65 (Springer Berlin Heidelberg, 2002).
29. Khanna, A., Sudha, Y., Pillai, S. & Rath, S. Molecular modeling studies of poly lactic acid initiation mechanisms. *J. Mol. Model.* 367–374 (2008).

References

30. Nuyken, O. & Pask, S. D. Ring-opening polymerization-An introductory review. *Polymers* **5**, 361–403 (2013).
31. Kim, M. S., Seo, K. S., Khang, G. & Lee, H. B. Ring-opening polymerization of ϵ -caprolactone by poly(ethylene glycol) by an activated monomer mechanism. *Macromol. Rapid Commun.* **26**, 643–648 (2005).
32. Bailey, W. J. in *Comprehensive Polymer Science* (eds. Allen, G. & Bevington, A. G.) **3**, 283–320 (1989).
33. Kanda, N. Syntheses of Z-Phenyl-3-Vinyloxirane Derivatives that Undergo Radical Ringopening Polymerization. **1938**, 1931–1938 (1986).
34. Ochiai, B. & Endo, T. Computational evaluation of radical ring-opening polymerization. *J. Polym. Sci. Part A Polym. Chem.* **45**, 2827–2834 (2007).
35. Cho, I. & Kim, J.-B. Exploratory ring-opening polymerization. VIII. Radical ring-opening polymerization of 2-phenyl-3-vinyloxirane: A C-C bond scission polymerization of the epoxide ring. *J. Polym. Sci. Polym. Lett. Ed.* **21**, 433–436 (1983).
36. Engelberg, I. & Kohn, J. Physico-mechanical properties of degradable polymers used in medical applications: A comparative study. *Biomaterials* **12**, 292–304 (1991).
37. Pitt, C. G. *et al.* Aliphatic Polyesters . I . The Degradation of Poly (ϵ - caprolactone) In Vivo. *J. Appl. Polym. Sci.* **26**, 3779–3787 (1981).
38. Raghavan, D. Characterization of Biodegradable Plastics. *Polym. Plast. Technol. Eng.* **34**, 41–63 (1995).
39. Kricheldorf, H. R., Mang, T. & Jonte, J. M. Polylactones .1. Copolymerization of Glycolide and Epsilon-Caprolactone. *Macromolecules* **17**, 2173–2181 (1984).
40. Hakkarainen, M., Höglund, A., Odelius, K. & Albertsson, A. C. Tuning the release rate of acidic degradation products through macromolecular design of caprolactone-based copolymers. *J. Am. Chem. Soc.* **129**, 6308–6312 (2007).
41. Kwon, S., Lee, K., Bae, W. & Kim, H. Precipitation Polymerization of 2-Methylene-1,3-dioxepane in Supercritical Carbon Dioxide. *Polym. J.* **40**, 332–338 (2008).
42. Darwis, D., Mitomo, H., Enjoji, T., Yoshii, F. & Makuuchi, K. Enzymatic degradation of radiation crosslinked poly(ϵ -caprolactone). *Polym. Degrad. Stab.* **62**, 259–265 (1998).
43. Koleske, J. V. *Polymer Blends*. **2**, (Academic Press, 1978).
44. Göpferich, A. Mechanisms of polymer degradation and erosion. *Biomaterials* **17**, 103–114 (1996).
45. Hakkarainen, M. in *Degradable Aliphatic Polyesters* **157**, 113–138 (Springer Berlin Heidelberg, 2002).

References

46. Artham, T. & Doble, M. Biodegradation of aliphatic and aromatic polycarbonates. *Macromol. Biosci.* **8**, 14–24 (2008).
47. *ASTM Handbook, Standard terminology relating to plastics, D883-92.* (American Society for Testing and Materials, 1992).
48. Smith, R. *Biodegradable polymers for industrial applications.* (Woodhead Publishing Limited, 2005).
49. Scott, G. *Polymers and the environment.* (The Royal Society of Chemistry, 1999).
50. Scott, G. 'Green' polymers. *Polym. Degrad. Stab.* **68**, 1–7 (2000).
51. Tokiwa, Y., Calabia, B. P., Ugwu, C. U. & Aiba, S. Biodegradability of plastics. *Int. J. Mol. Sci.* **10**, 3722–3742 (2009).
52. Wise, D. L. *et al.* Encyclopedic Handbook of Biomaterials and Bioengineering. *Bioengineering* (1995).
53. Chiellini, E., Corti, A., D'Antone, S. & Wiles, D. M. *Handbook of biodegradable polymer.* (Wiley-VCH, 2011).
54. Leja, K. & Lewandowicz, G. Polymer biodegradation and biodegradable polymers - A review. *Polish J. Environ. Stud.* **19**, 255–266 (2010).
55. Zheng, Z., Breedveld, G. & Aagaard, P. Biodegradation of soluble aromatic compounds of jet fuel under anaerobic conditions: Laboratory batch experiments. *Appl. Microbiol. Biotechnol.* **57**, 572–578 (2001).
56. Stanley Dagley. Microbial Degradation of Organic Compounds in the Biosphere. *Am. Sci.* **63**, 681–689 (1975).
57. Sims, R. C. & Overcash, M. R. in *Residue Reviews* (ed. Gunther, F. A.) **88**, 1–68 (Springer New York, 1983).
58. Wilson, L. P. & Bouwer, E. J. Biodegradation of aromatic compounds under mixed oxygen/denitrifying conditions: a review. *J. Ind. Microbiol. Biotechnol.* **18**, 116–130 (1997).
59. Müller, R. Biodegradability of polymers: regulations and methods for testing. *Biopolym. Online* 365–374 (2005). doi:10.1103/Physrevb.74.035409
60. Briassoulis, D., Dejean, C. & Picuno, P. Critical Review of Norms and Standards for Biodegradable Agricultural Plastics Part II: Composting. *J. Polym. Environ.* **18**, 364–383 (2010).
61. Marten, E., Müller, R.-J. & Deckwer, W.-D. Studies on the enzymatic hydrolysis of polyesters. II. Aliphatic–aromatic copolyesters. *Polym. Degrad. Stab.* **88**, 371–381 (2005).

References

62. Gan, Z., Liang, Q., Zhang, J. & Jing, X. Enzymatic degradation of poly(ϵ -caprolactone) film in phosphate buffer solution containing lipases. *Polym. Degrad. Stab.* **56**, 209–213 (1997).
63. Azevedo, H. & Reis, R. in *Biodegradable Systems in Tissue Engineering and Regenerative Medicine* 177–202 (CRC Press, 2004). doi:10.1201/9780203491232.ch12
64. Strantz, A. A. & Zottola, E. A. Stability of Cornstarch-containing Polyethylene Films to Starch-degrading Enzymes. *J. Food Prot.* 736–738 (1992).
65. Coma, V. *et al.* Estimation of the biofragmentability of packaging materials by an enzymatic method. *Enzyme Microb. Technol.* **17**, 524–529 (1995).
66. Kunthadong, P. *et al.* Biodegradable Plasticized Blends of Poly(L-lactide) and Cellulose Acetate Butyrate: From Blend Preparation to Biodegradability in Real Composting Conditions. *J. Polym. Environ.* 107–113 (2014). doi:10.1007/s10924-014-0671-x
67. Vikman, M., Vartiainen, J., Tsitko, I. & Korhonen, P. Biodegradability and Compostability of Nanofibrillar Cellulose-Based Products. *J. Polym. Environ.* **23**, 206–215 (2014).
68. Darwis, D., Mitomo, H., Enjoji, T., Yoshii, F. & Makuuchi, K. Enzymatic degradation of radiation crosslinked poly(ϵ -caprolactone). *Polym. Degrad. Stab.* **62**, 259–265 (1998).
69. Wang, H. *et al.* Oligomeric dual functional antibacterial polycaprolactone. *Polym. Chem.* **5**, 2453 (2014).
70. Carmona-Ribeiro, A. M. & de Melo Carrasco, L. D. Cationic antimicrobial polymers and their assemblies. *Int. J. Mol. Sci.* **14**, 9906–9946 (2013).
71. Littmann, E. R. & Marvel, C. S. Cyclic quaternary ammonium salts from halogenated aliphatic tertiary amines. *J. Am. Chem. Soc.* **52**, 287–294 (1930).
72. Rembaum, A., Baumgartner, W. & Eisenberg, A. Aliphatic ionenes. *Polym. Lett.* **6**, 159–171 (1968).
73. Ilker, M. F., Schule, H. & Coughlin, E. B. Modular Norbornene Derivatives for the Preparation of Well-Defined Amphiphilic Polymers: Study of the Lipid Membrane Disruption Activities. *Macromolecules* **37**, 694–700 (2004).
74. Bazarov, L. U. & Stel'makh, S. A. Molecular-weight characteristics of polyhexamethyleneguanidine hydrochloride. *Russ. J. Appl. Chem.* **81**, 2021–2025 (2008).
75. Vargas, M. & Gonzalez-Martinez, C. Recent Patents on Food Applications of Chitosan. *Recent Pat. Food. Nutr. Agric.* **2**, 121–128 (2010).
76. Salton, M. R. Lytic agents, cell permeability, and monolayer penetrability. *J. Gen. Physiol.* **52**, 227–252 (1968).
77. Denyer, S. P. Mechanisms of action of antibacterial biocides. *Int. Biodeterior. Biodegradation* **36**, 227–245 (1995).

References

78. Zhou, Z., Wei, D., Guan, Y., Zheng, A. & Zhong, J.-J. Extensive in vitro activity of guanidine hydrochloride polymer analogs against antibiotics-resistant clinically isolated strains. *Mater. Sci. Eng. C* **31**, 1836–1843 (2011).
79. Wei, D. *et al.* Condensation between guanidine hydrochloride and diamine/multi-amine and its influence on the structures and antibacterial activity of oligoguanidines. *e-Polymers* **12**, 1–10 (2012).
80. Mattheis, C., Wang, H., Schwarzer, M. C., Frenking, G. & Agarwal, S. Exploring suitable oligoamines for phantom ring-closing condensation polymerization with guanidine hydrochloride. *Polym. Chem.* 707–716 (2012). doi:10.1039/c2py20672b
81. Kusnetsov, J. M., Tulkki, a I., Ahonen, H. E. & Martikainen, P. J. Efficacy of three prevention strategies against legionella in cooling water systems. *J. Appl. Microbiol.* **82**, 763–768 (1997).
82. Cox, N. A., Bailey, J. S. & Berrang, M. E. Bactericidal Treatment of Hatching Eggs I. Chemical Immersion Treatments and Salmonella. *J. Appl. Poult. Res.* **7**, 347–350 (1998).
83. Cox, N. a., Berrang, M. E., Buhr, R. J. & Bailey, J. S. Bactericidal treatment of hatching eggs II. Use of chemical disinfectants with vacuum to reduce Salmonella. *J. Appl. Poult. Res.* **8**, 321–326 (1999).
84. Davis, S. *et al.* The Use of New Antimicrobial Gauze Dressings: Effects on the Rate of Epithelialization of Partial-Thickness Wounds. *WOUNDS* **14**, 252–256 (2001).
85. Payne, J. D. & Kudner, D. W. A durable antiodor finish for cotton textiles. *Text. Chem. Color.* **28**, 28–30 (1996).
86. Mattheis, C., Schwarzer, M. C., Frenking, G. & Agarwal, S. Phantom ring-closing condensation polymerization: Towards antibacterial oligoguanidines. *Macromol. Rapid Commun.* **32**, 994–999 (2011).
87. Li, W. *et al.* Antibacterial 45S5 Bioglass[®]-based scaffolds reinforced with genipin cross-linked gelatin for bone tissue engineering. *J. Mater. Chem. B* **3**, 3367–3378 (2015).
88. Bolton, E. K., Coffman, D. D., Gilman, W. & Golman, L. US 2325586. 1–9 (1943).
89. Wang, B. *et al.* Synthesis and antimicrobial properties of a guanidine-based oligomer grafted with a reactive cationic surfactant through Michael addition. *J. Appl. Polym. Sci.* **130**, 3489–3497 (2013).
90. Iwakura, Y. & Kohji, N. A synthesis of polyguanidines by polyaddition reaction of biscarbodiimines with diamines. *Polym. Lett.* **5**, 821–825 (1967).
91. Lim, H. N., Huang, N. M. & Loo, C. H. Facile preparation of graphene-based chitosan films: Enhanced thermal, mechanical and antibacterial properties. *J. Non. Cryst. Solids* **358**, 525–530 (2012).
92. Makarios-Laham, I. & Lee, T. C. Biodegradability of chitin- and chitosan-containing films in soil environment. *J. Environ. Polym. Degrad.* **3**, 31–36 (1995).

References

93. Zheng, L.-Y. & Zhu, J.-F. Study on antimicrobial activity of chitosan with different molecular weights. *Carbohydr. Polym.* **54**, 527–530 (2003).
94. Roller, S. & Covill, N. The antifungal properties of chitosan in laboratory media and apple juice. *Int. J. Food Microbiol.* **47**, 67–77 (1999).
95. El Ghaouth, A., Arul, J., Ponnampalam, R. & Boulet, M. Chitosan coating effect on storability and quality of fresh strawberries. *J. Food Sci.* **56**, 6–8 (1991).
96. Feng, Y. CN 104830136 A. (2015).
97. Shetty, K. K. & Dwelle, R. B. Disease and sprout control in individually film wrapped potatoes. *Am. Potato J.* **67**, 705–718 (1990).
98. Saif, M. J. *et al.* An eco-friendly, permanent, and non-leaching antimicrobial coating on cotton fabrics. *J. Text. Inst.* **106**, 907–911 (2015).
99. Kinninmonth, M. *et al.* Nano-layered inorganic-organic hybrid materials for the controlled delivery of antimicrobials. *Macromol. Symp.* **338**, 36–44 (2014).
100. Jao, W. C. *et al.* Effect of immobilization of polysaccharides on the biocompatibility of poly(butyleneadipate-co-terephthalate) films. *Polym. Adv. Technol.* **21**, 543–553 (2010).
101. Tan, L. *et al.* Antimicrobial Hydantoin-Containing Polyesters. *Macromol. Biosci.* **12**, 1068–1076 (2012).
102. Tan, L., Maji, S., Mattheis, C., Chen, Y. & Agarwal, S. Antimicrobial Hydantoin-grafted Poly(ϵ -caprolactone) by Ring-opening Polymerization and Click Chemistry. *Macromol. Biosci.* **12**, 1721–1730 (2012).
103. Kanazawa, A., Ikeda, T. & Endo, T. Polymeric phosphonium salts as a novel class of cationic biocides. V. Synthesis and antibacterial activity of polyesters releasing phosphonium biocides. *J. Polym. Sci. Part A Polym. Chem.* **31**, 3003–3011 (1993).
104. Fortunati, E. in *Silver Nanoparticles: Synthesis, Uses and Health Concerns* (eds. Armentano, I. & Kenny, J. M.) 185–202 (2013).
105. Longano, D. *et al.* Analytical characterization of laser-generated copper nanoparticles for antibacterial composite food packaging. *Anal. Bioanal. Chem.* **403**, 1179–1186 (2012).
106. Hench, L. L. The story of Bioglass. *J. Mater. Sci. Mater. Med.* **17**, 967–978 (2006).
107. Jones, J. R. Review of bioactive glass: From Hench to hybrids. *Acta Biomater.* **9**, 4457–4486 (2013).
108. Gorustovich AA, Roether JA, B. A. Effect of bioactive glasses on angiogenesis: a review of in vitro and in vivo evidences. *Tissue Eng. Part B Rev.* **16**, 199–207 (2010).

2. Cumulative Part of Dissertation

This thesis focuses on the preparation and characterization of antimicrobial and (bio)degradable polymeric materials. A balance between antimicrobial activity and (bio)degradability was studied, which can keep the antimicrobial activity, while controlling the rate of (bio)degradation. The dissertation consists three interdependent chapters, in which all new polymeric materials exhibit those two properties: antimicrobial activity and (bio)degradability.

A lot of antimicrobial polymers have cationic and amphiphilic features. The hydrophobic/hydrophilic balance of polymer chains affects the antimicrobial activity and selectivity. In most cases, they are water soluble, therefore if the antimicrobial additive is not immobilized on the (bio)degradable polymer, the material loses the antimicrobial activity during the interaction with microorganisms in humid environment. Hence, the introduction of covalent bonds was chosen as strategy in order to avoid the leaching effect and this strategy is discussed in detail in chapter 3.

However, we obtained only low molecular weight block copolymers of PHMG-*b*-PCL (chapter 3). Because of that, the antimicrobial material exhibits poor mechanical properties and cannot be used for food packaging or medical applications. Therefore, as a new strategy, blending of a high molecular weight polymer and the low molecular weight antimicrobial agent was pursued, whereas the choice of a good matrix material is crucial. (Chapter 4)

Further, in chapter 5 a new antimicrobial biodegradable material “45S5 Bioglass[®]” (45S5 BG) was prepared by loading with antimicrobial additive. The prepared 45S5 BG scaffolds also combine the antimicrobial activity and biocompatibility. They have the potential to become the new general BG scaffolds for bone tissue engineering.

Cumulative Part of Dissertation

2.1 Oligomeric dual functional antibacterial polycaprolactone

This work has already been published:

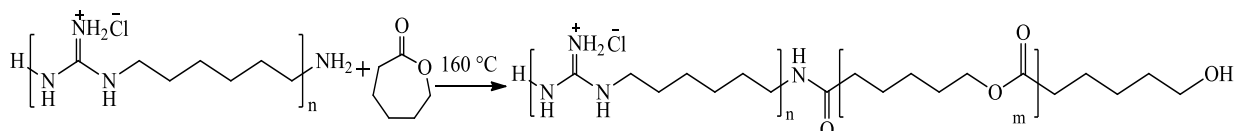
Hui Wang,^a Christopher V. Synatschke,^a Alexander Raup,^b Valérie Jérôme,^b Ruth Freitag^b and Seema Agarwal*^a, “Oligomeric dual functional antibacterial polycaprolactone”, *Polymer Chemistry*, **2014**, *5*, 2453-2460.

Specific contributions by authors:

The planning and the execution of the synthetic and analytical work and antibacterial tests were done by me. The manuscript was written by me. Christopher V. Synatschke helped me to measure the MALDI-ToF MS. Alexander Raup and Valérie Jérôme, from the group of Prof. Ruth Freitag determined the cytotoxicity via MTT-tests. Prof. Seema Agarwal did the final manuscript revision and was in charge for general guidance concept, design and supervision for this project.

Cumulative Part of Dissertation

The aim of this part is the synthesis of a new (bio)degradable polymer with antimicrobial property. In this paper a new synthetic route for ring-opening polymerization of ϵ -CL initiated by PG end groups is presented. Antibacterial oligomeric PHMG with a molecular weight of 3000 Da, carrying primary amine groups at the chain end, was used as macroinitiator, opening the ϵ -caprolactone ring in order to yield the block copolymer polycaprolactone-*b*-polygudnidine hydrochloride (PCL-*b*-PHMG). (Scheme 2-1) PCL as commercial material has been extensively used in agriculture, medicine, pharmacy, biomedical and packaging industry.



Scheme 2-1. Ring opening polymerization of ϵ -polycaprolactone using PHMG as macroinitiator.

With different ratios of PHMG to ϵ -CL as well as with different polymerization times the block length of PCL is controllable. (Table 2-1)

Table 2-1. Details of oligomers synthesized by ROP of CL using poly(hexamethylene guanidine) hydrochloride (PHMG) macroinitiator for 24 h: copolymer composition, molar mass, PDI and yield.

Sample	PHMG:PCL (molar ratio in copolymer)	$M_{n,NMR}$	M_n^b	M_w^b	PDI ^b (M_w/M_n)	Yield %
1	0.72:1	2800	2700	3300	1.2	80
2	0.67:1	2900	2700	3400	1.2	93
3 ^c	2.71:1	1700	2000	2500	1.3	52
4	1.68:1	1900	2200	2900	1.3	94

^a CL:PHMG feed ratio was 77:23 (sample 1), 32:68 (samples 2 and 3), 50:50 (sample 4).

^b determined by MALDI-ToF-MS, ^c Time of polymerization for sample 3 was 8 h.

PHMG has good water solubility and PCL is relatively hydrophobic. Therefore the copolymer shows temperature dependent solubility of an upper critical solution temperature (UCST)-type in polar solvents such as methanol. The formation of copolymer was confirmed by 2D-NMR and MALDI-ToF-MS. A step growth reaction was proven by MALDI-ToF-MS (Figure 2-2). The repeating units of the copolymer can be found in the spectrum.

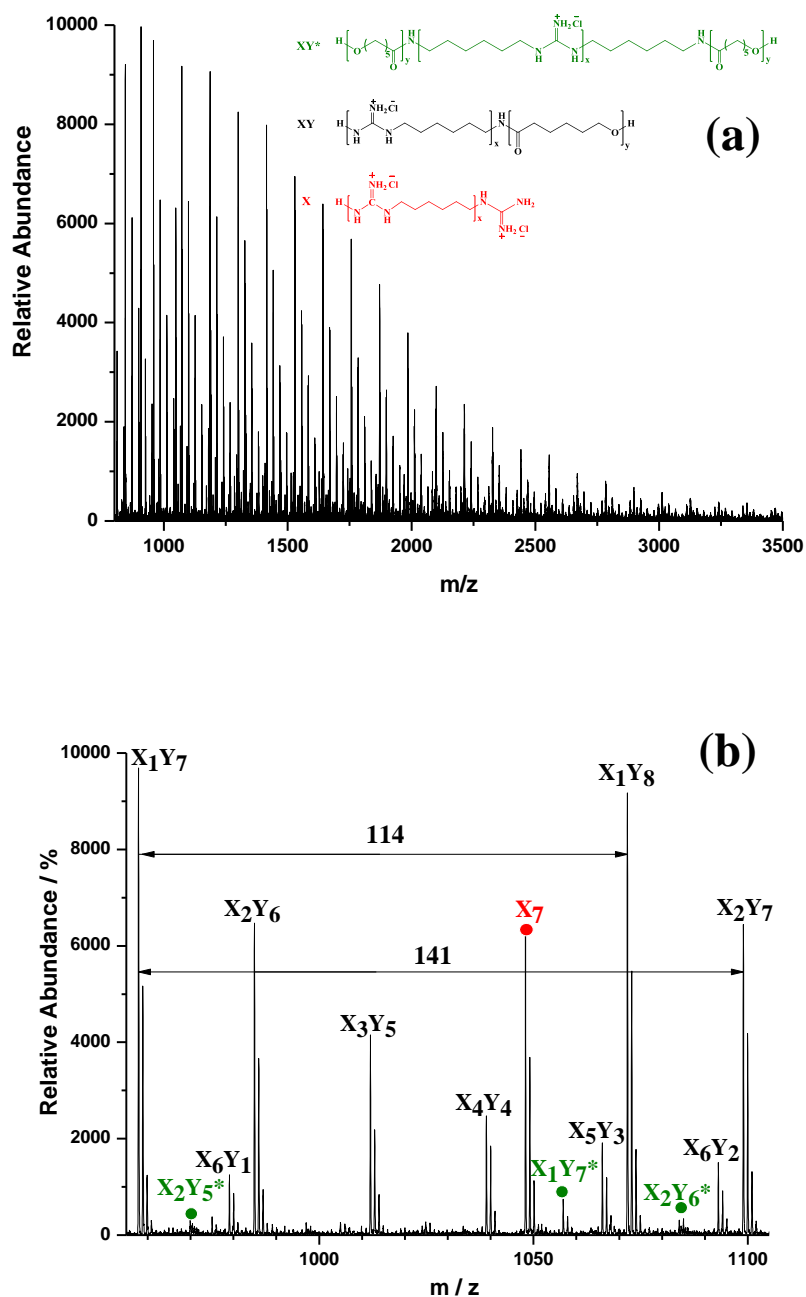


Figure 2-2. (a) Full MALDI-TOF MS spectrum and (b) enlargement of 950-1100 m/z region of sample 2.

The copolymer showed high antibacterial activity and fast antibacterial action against Gram-positive bacteria *B. subtilis* and Gram-Negative bacteria *E. coli*. To produce a stable polymer suspension, 60 mg of the polymer were dissolved in 10 mL DMSO at 40 °C followed by dialysis against Millipore water at room temperature. The different concentrations were prepared by diluting the original suspension with water. Because of the different ratio of PHMG to PCL, sample 3 shows higher antibacterial activity than sample 2, which has a longer PCL block. Sample 2 showed MIC values of 87.5 mg mL⁻¹ and 50 mg mL⁻¹, and MBC of 87.5 mg mL⁻¹ and

Cumulative Part of Dissertation

100 mg mL⁻¹ for *E. coli* and *B. subtilis*, respectively. Sample 3 shows a MIC of 37.5 mg mL⁻¹ and 25 mg mL⁻¹, and MBC to 62.5 mg mL⁻¹ and 50 mg mL⁻¹ for *E. coli* and *B. subtilis*, respectively. Figure 2-3 and 2-4 depict the speed of antibacterial action against *E. coli* and *B. subtilis*. Both samples show fast antibacterial effect. Even sample 2 with the lowest mole percentage of PHMG killed 99% of the bacteria after 30 min at a concentration of 100 µg mL⁻¹ and it even killed 98.0 % of the bacteria after 60 min, at a concentration as low as 10 µg mL⁻¹.

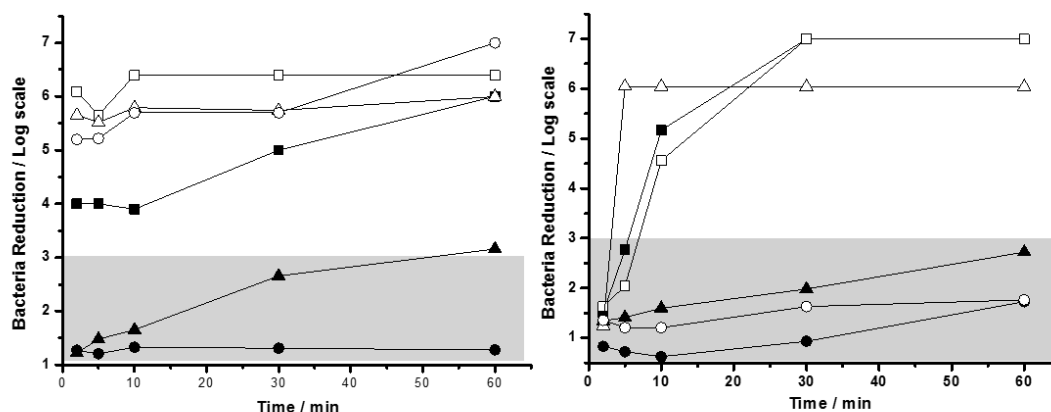


Figure 2-3 and 4. Time-dependent reduction of bacteria in suspension of *B. subtilis* (left) and *E. coli* (right) with an initial cell density of 10⁶ cfu · mL⁻¹ upon contact Samples 2 with concentrations of --■-- 1000 µg · mL⁻¹, --▲-- 100 µg · mL⁻¹, --●-- 10 µg · mL⁻¹ and Samples 3 with concentrations of --□-- 1000 µg · mL⁻¹, --△-- 100 µg · mL⁻¹, --○-- 10 µg · mL⁻¹ at ambient temperature, given in log stages.

(Bio)degradability of this copolymer was confirmed by an enzymatic degradation test. Copolymers were incubated in phosphate buffer with lipase from pseudomonas cepacia at 37 °C. The molar mass of the degrading polymer was monitored by MALDI-ToF-MS. Figure 2-5 shows the degradation after 24 h, while the PCL block was almost completely degraded.

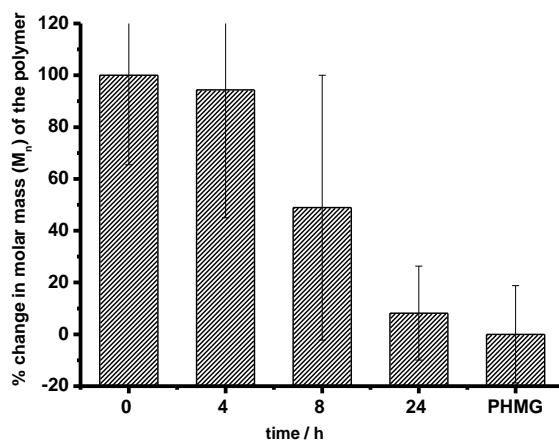


Figure 2-5. Degradation percentage of polymer chain.

A MTT assay was used to determine the cytotoxicity of the copolymer, using L929 cells. Compared to L-PEI 25 kDa and pure antibacterial PHMG, the PHMG-*b*-PCL copolymer showed high LD50 values indicating low cytotoxicity. (Figure 2-6)

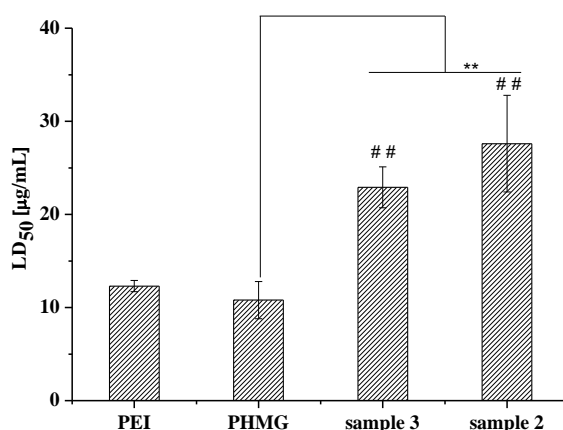


Figure 2-6. (b) LD₅₀ doses for the PHMG-based polymers and l-PEI 25 kDa, used as reference. The data represent mean \pm s.d. from three independent experiments. Polymers yielding cytotoxicity with l-PEI and pairwise are indicated by # and *, respectively.

In conclusion, block copolymers of PHMG-*b*-PCL were prepared by ring-opening polymerization with the antimicrobial macroinitiator PHMG. Chemical structures of the resulting copolymers were confirmed by 2D NMR spectroscopy and MADLI-ToF-MS. The combination of PHMG and PCL exhibited high antibacterial activity, (bio)degradability and low cytotoxicity. Due to the low molecular weight the new material has the potential utilization as compatible antimicrobial additive for (bio)degradable polyesters.

2.2 Biodegradable aliphatic-aromatic polyester with antibacterial property

This work has already been submitted:

Hui Wang, Markus Langner, Seema Agarwal*, “Biodegradable aliphatic-aromatic polyester with antibacterial property”, *Polymer Engineering & Science*, **2016**, DOI: 10.1002/pen.24347.

Specific contributions by authors:

The planning and the execution of the extrusion, analytical work, compost degradation and antibacterial tests were done by me. The manuscript was written by me. Markus Langner assisted to record the SEM images. Prof. Seema Agarwal did the final manuscript revision and gave general guidance concept, design and supervision for this project.

Cumulative Part of Dissertation

PBAT is a commercially available (bio)degradable polyester (commercial name Ecoflex®), which has been extensively used as food packaging material or compost bags. In this work, for the coextrusion of PBAT with PHMG a reactive blending was anticipated, leading to covalent linkages between PBAT and the antimicrobial additive, eventually suppressing leaching of the low molecular weight species during application. The antibacterial aliphatic-aromatic polyester PBAT was extruded using a twin-screw extruder. PHMG ($M_n = 3900$, $M_w = 6000$, $\bar{D} = 1.6$) was employed as antibacterial additive in four different amounts, 1.7, 4.3, 8.5 and 12.9 wt% for the extrusion with Ecoflex®. The corresponding extrudates are referred to as PHMG-Eco1.7, PHMG-Eco4.3, PHMG-Eco8.5 and PHMG-Eco12.9, respectively.

$T_{5\%}$ (temperature at which 5% weight loss took place) of Ecoflex® is higher than 350 °C. The extruded antibacterial Ecoflex® also showed high thermal stability. The $T_{5\%}$ of PHMG-Eco12.9 is at 330 °C. After mixing with PHMG the T_g and T_m of all samples were at -28 °C and 115 °C, respectively. The melting enthalpy and crystallinity of the extrudates decreased with increasing amount of PHMG.

SEM micrographs of PHMG-Eco1.7 and PHMG-Eco12.9 (Figure 2-7) show phase-separated morphology at the surface with some smooth patches.

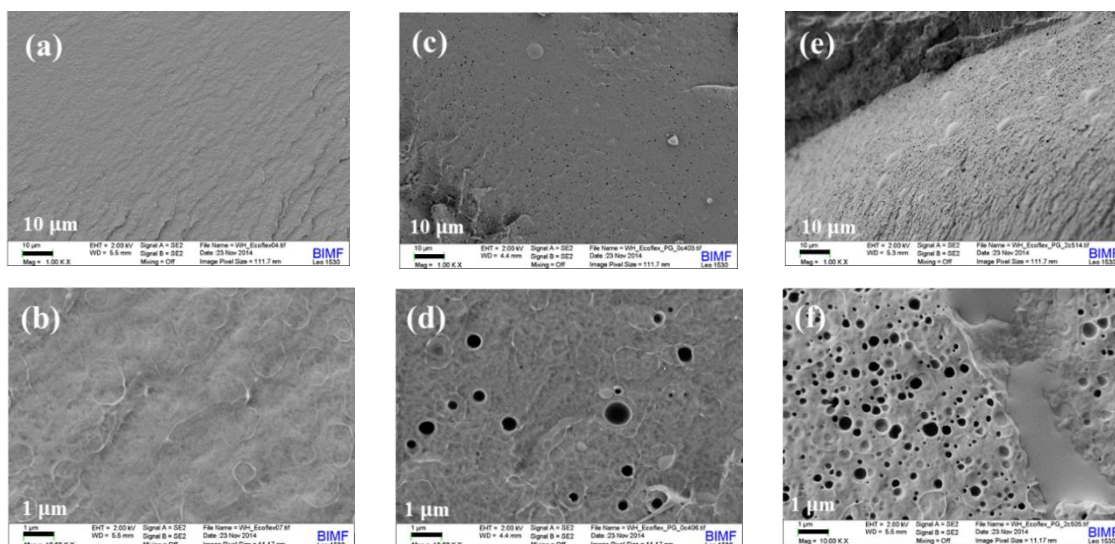


Figure 2-7. SEM micrographs of the extruded PBAT-Eco (a-b), PHMG-Eco1.7 (c-d) PHMG-Eco12.9 (e-f).

Figure 2-8 shows the typical stress-strain curves of extruded samples. After Extrusion the PHMG-Eco samples exhibited increased elongation at break and E-modulus without sacrificing the breaking stress.

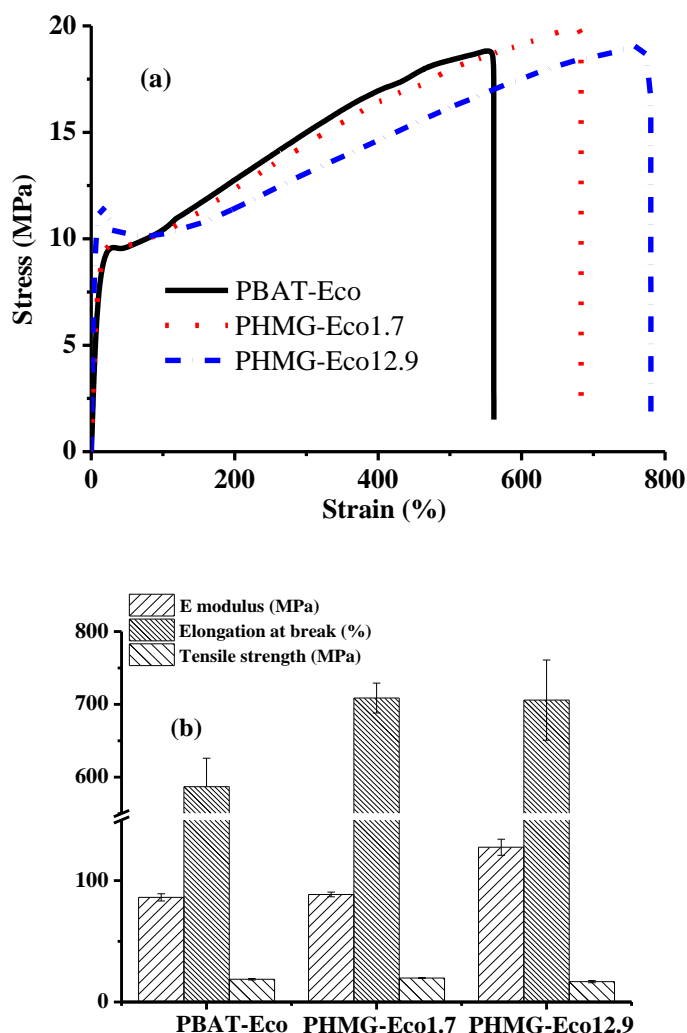


Figure 2-8. Stress-strain curves of PBAT-Eco and PHMG-Eco 1.7 and 12.9 (a) and corresponding bar chart of mechanical properties (b).

All PHMG-Eco samples were tested for antibacterial activity using the Kirby-Bauer test. (Figure 2-9) For Gram-positive bacteria *B. subtilis* PHMG-Eco8.5 showed an inhibitory effect. PHMG-Eco12.9 exhibited strong antibacterial activity against both, Gram-positive and Gram-negative bacteria. Only PHMG-Eco12.9 showed a small inhibition zone indicating leaching of antibacterial material. According to an experiment, which was used to quantify the leaching effect by stirring the samples in water at 37 °C, after 7 days only 3 wt% PHMG leaching was observed, which also explains the long lasting antibacterial activity.

Cumulative Part of Dissertation

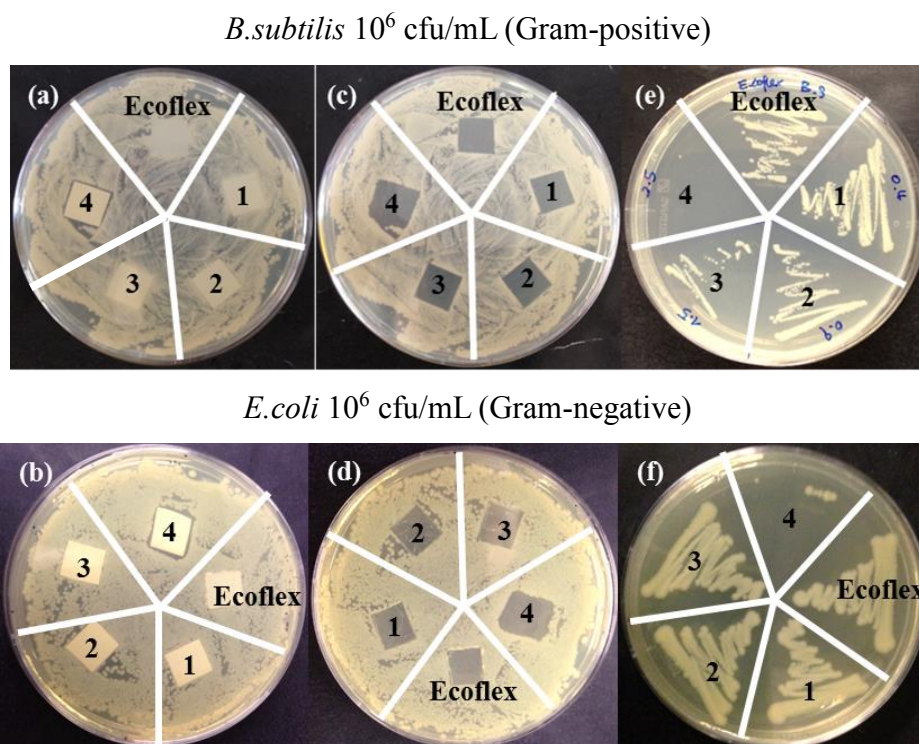


Figure 2-9. Kirby-Bauer test using *B. subtilis* and *E. coli* for sample extruded PBAT-Eco (Ecoflex[®]) and PHMG-Eco1.7 (1), PHMG-Eco4.3 (2), PHMG-Eco8.5 (3), PHMG-Eco12.9 (4). (a) and (b) after 24 hours incubation, (c) and (d) after removing the incubated samples, (e) and (f) bacterial growth on a new agar plate after transferring swab from area under the samples.

The compostability of the extrudates was investigated using highly active compost from an industrial composting plant. As shown in Figure 2-10, after 60 days PBAT-Eco showed some cracks and the film became very brittle. After 100 days PHMG-Eco disintegrated eventually and mixed with the compost. GPC was used to quantify the compostability of the samples. Since the GPC elugram of Ecoflex[®] was not unimodal, we compared the M_p rather than M_n or M_w value. Figure 2-11 shows a decreased M_p of pure Ecoflex[®] and PHMG-Eco12.9 during the composting test. Although for PHMG-Eco12.9 the degradation took longer time, after 30 days, a very significant decrease in molar mass was observed by GPC measurements.

Cumulative Part of Dissertation

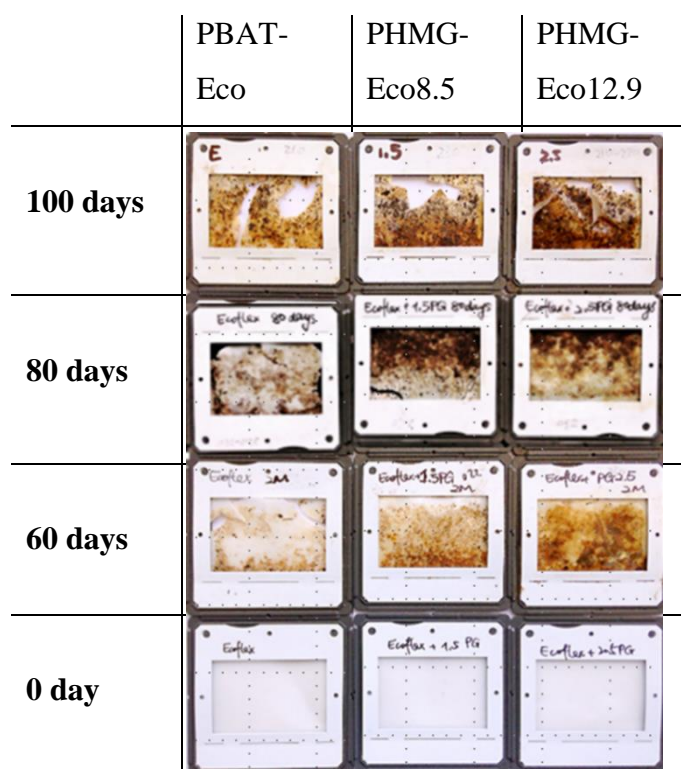


Figure 2-10. The surface of polymer films after at different time by burying in compost at 60 °C.

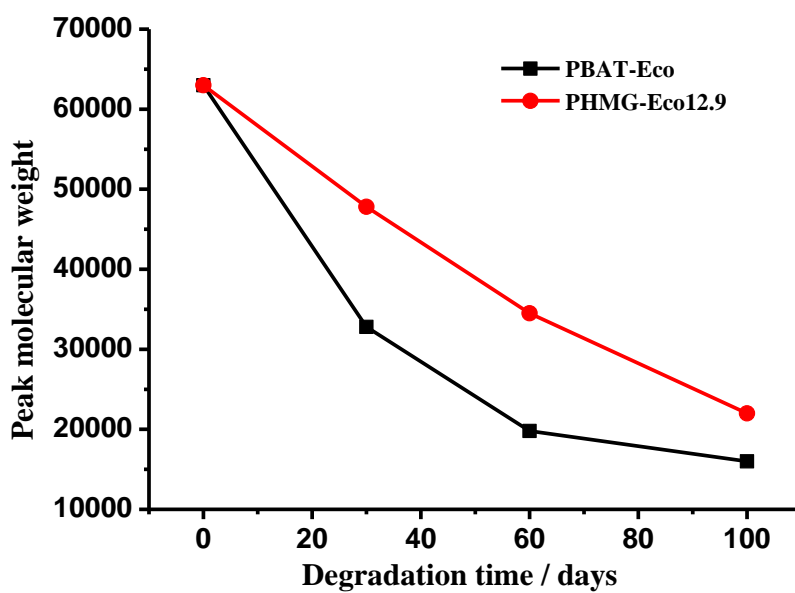


Figure 2-11. Decreased peak average molar mass (M_p) of PBAT-Eco and PHMG-Eco with time during compost test.

Figure 2-12 shows the Kirby-Bauer test for PHMG-Eco12.9 after one and two months of burial in compost. PHMG-Eco12.9 exhibits an excellent permanent antibacterial effect against *B.subtilis* and *E.coli* even after long degradation time.

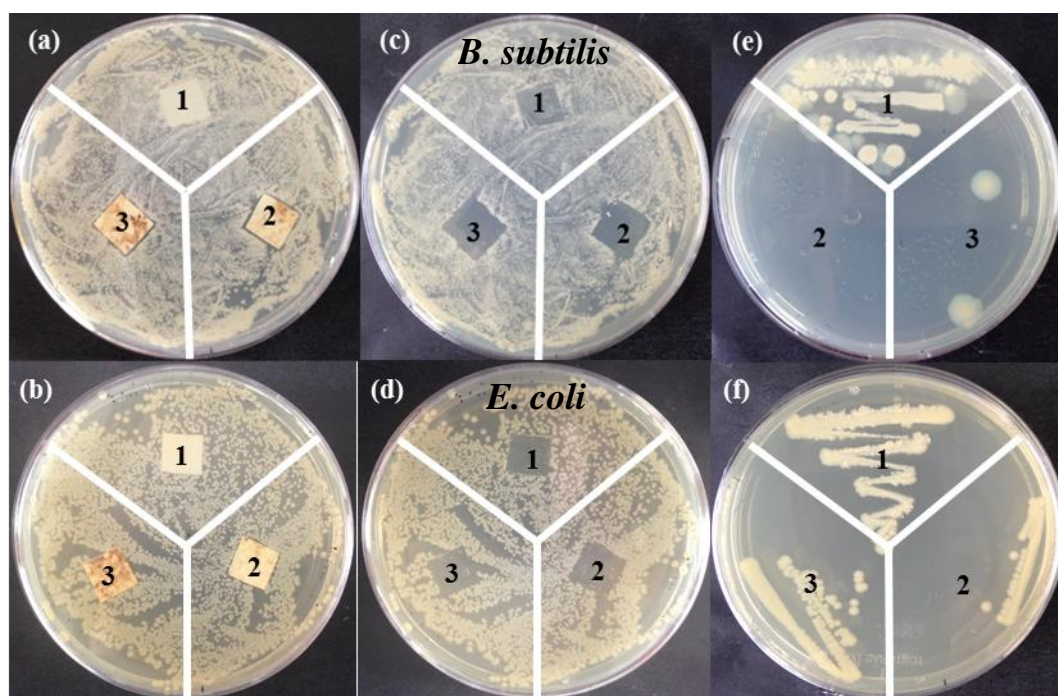


Figure 2-12. Kirby-Bauer test using *E. coli* and *B. subtilis* for sample, 1: PBAT-Eco after degradation one month, 2: PHMG-Eco12.9 after degradation one month, 3: PHMG-Eco12.9 after degradation two months, (a, b) after 24 hours incubation, (c, d) after removing the incubated samples, (e, f) bacterial growth on a new agar plate after transferring swab from area under the samples.

In conclusion, new antibacterial Ecoflex[®] was obtained by non-reactive extrusion blending. Although no covalent bonds were formed, the antimicrobial extrudate, even with high amounts of additive (12.9 wt%), show little leaching effect, because of the hydrophobicity of matrix material. The new material showed (bio)degradability in compost and even after two months degradation it was still showing antibacterial activity. The elongation-at-break and stress to strain of PHMG-Eco samples were also significantly enhanced. The new antibacterial function gives Ecoflex[®] a broader range of applications, e.g. it can be directly used for food packaging or compost bags.

2.3 Antibacterial 45S5 Bioglass[®]-based scaffolds reinforced with genipin cross-linked gelatin for bone tissue engineering

This work has already been published:

Wei Li,^a Hui Wang,^b Yaping Ding,^c Ellen C. Scheithauer,^a Ourania-Menti Goudouri,^a Alina Grünewald,^a Rainer Detsch,^a Seema Agarwal^b and Aldo R. Boccaccini*^a, “Antibacterial 45S5 Bioglass[®]-based scaffolds reinforced with genipin cross-linked gelatin for bone tissue engineering”, *J. Mater. Chem. B*, **2015**, *3*, 3367-3378.

Specific contributions by authors:

The polymer synthesis, characterization, antibacterial tests and XRD measurements of scaffolds were done by me. I wrote parts of the manuscript. Wei Li prepared and characterized the Bioglass[®] scaffold. The degradation test was done by Ellen C. Scheithauer. Cell biology tests were performed by Alina Grünewald and Rainer Detsch. Yaping Ding helped to measure the SEM, FTIR and mechanical properties. Prof. Aldo R. Boccaccini and Prof. Seema Agarwal did the final manuscript revision and gave general guidance and supervision for this project.

Cumulative Part of Dissertation

In this publication a new antimicrobial 45S5 BG was reported, showing a third example of biodegradable materials that were given antimicrobial activity by loading with PG. There exists always a huge risks of contamination and infection during scaffold implantation.⁸⁷ Since 45S5 BG is an ideal material as bone tissue engineering scaffold¹⁰⁶⁻¹⁰⁸ it was chosen as matrix material, which was firstly coated with genipin cross-linked gelatin (GCG) (which maintained high porosity of 93%) to give mechanical strength. Considering the requirement of antimicrobial activity, the scaffolds were furthermore coated with PPXG, to yield a hybrid material being biodegradable and antimicrobial. The highly interconnected pore structure of the GCG coated scaffolds was observed by SEM. Figure 2-13 shows the degradation behavior of the scaffolds. Crosslink gelation significantly decreases the dissolution/degradation rate of gelatin films in SBF at 37 °C. For up to 7 days GCG coated and uncoated 45S5 BG scaffolds have similar weight loss, slowing down after 7 days. The formation of hydroxyapatite (HA) on the scaffold surface compensates the weight loss caused by dissolution, thus reducing the overall degradation rate of the 45S5 BG scaffolds. The 12 wt% higher weight loss of GCG coated scaffolds compared to uncoated scaffolds after 14 days is due to the loss of GCG coating (15 wt%).

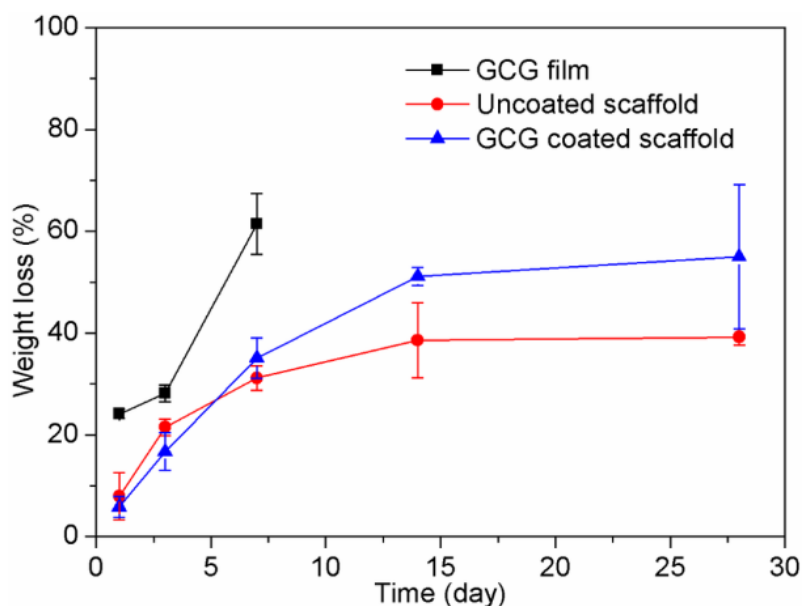


Figure 2-13. Degradation behaviors in SBF of GCG films, uncoated and GCG coated 45S5 BG scaffolds.

For in vitro bioactivity tests the scaffolds were immersed in SBF at 37 °C for 1, 3, 7, 14 and 28 days. Afterwards, FTIR, XRD and SEM were used to characterize the HA formation on the scaffolds. XRD spectra (Figure 2-14) show, that growing HA peaks (e.g. at $2\theta = 25.8^\circ$ and 31.7°) were observed on coated scaffolds after immersion in SBF for 7, 14 and 28 days. The crystallinity of the scaffolds, corresponding to the $\text{Na}_4\text{Ca}_4(\text{Si}_6\text{O}_{18})$ and $\text{Na}_2\text{Ca}_4(\text{PO}_4)_2\text{SiO}_4$

Cumulative Part of Dissertation

phases, decreased with increasing immersion time in SBF. SEM images show, that after 7 days the struts were almost fully covered by HA crystals, which can be clearly recognized by their well-known globular and cauliflower-like shape.

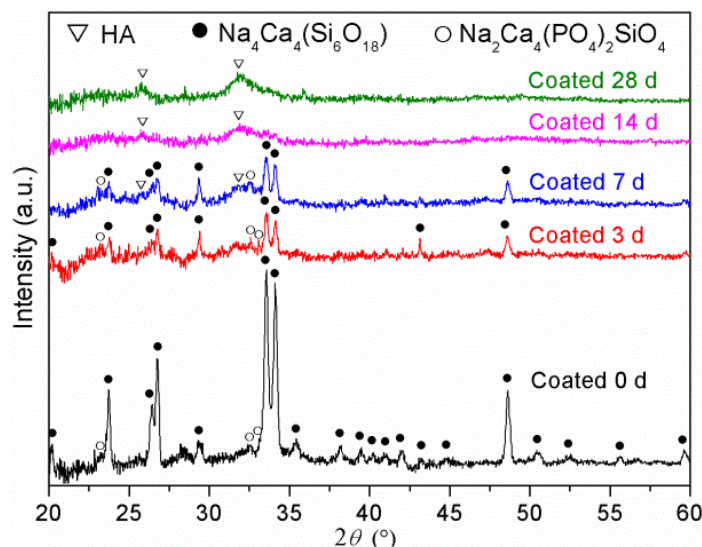


Figure 2-14. XRD spectra of GCG coated 45S5 BG scaffolds before (0 d) and after immersion in SBF for 3, 7, 14 and 28 days.

GCG coated 45S5 BG scaffolds exhibit improved mechanical properties, which were investigated by a uniaxial compressive strength test. The compressive strength of GCG coated scaffolds (1.04 ± 0.11 MPa) is significantly higher than that of uncoated scaffolds (0.04 ± 0.01 MPa). The work of fracture increased from 5.0 ± 1.1 Nmm to 285.6 ± 23.3 Nmm after coating.

Antibacterial properties of the scaffolds were evaluated by the Kirby-Bauer test and time-dependent shaking flask test. With the Kirby-Bauer test (Figure 2-15) the zone of inhibition was visually evaluated on the plate. Both samples without antibacterial polymer PPXG did not show any zone of inhibition to *B. subtilis* and *E. coli*. Furthermore, after the samples were transferred to new agar plate, they did not show any antibacterial activity. GCG coated scaffolds loaded with PPXG showed an increasing zone of inhibition as the PPXG concentration increased. They also showed antibacterial activity against *B. subtilis*. Scaffolds loaded with 30 and 50 $\mu\text{g}/\text{mL}$ PPXG exhibited antibacterial activity against *E. coli*, whereas scaffolds coated with 10 $\mu\text{g}/\text{mL}$ PPXG showed an inhibitor effect against *E. coli*. The time-dependent shaking flask test is used to determine the enduring antibacterial activity of an implant (Figure 2-16). All scaffolds coated with PPXG killed more than 95% of *B. subtilis* and *E. coli* within 2 hours and this antibacterial effect was kept for 6 hours. Even scaffolds loaded with 10 $\mu\text{g}/\text{mL}$ PPXG showed antibacterial activity, however after 2 hours the *E. coli* began to grow.

Cumulative Part of Dissertation

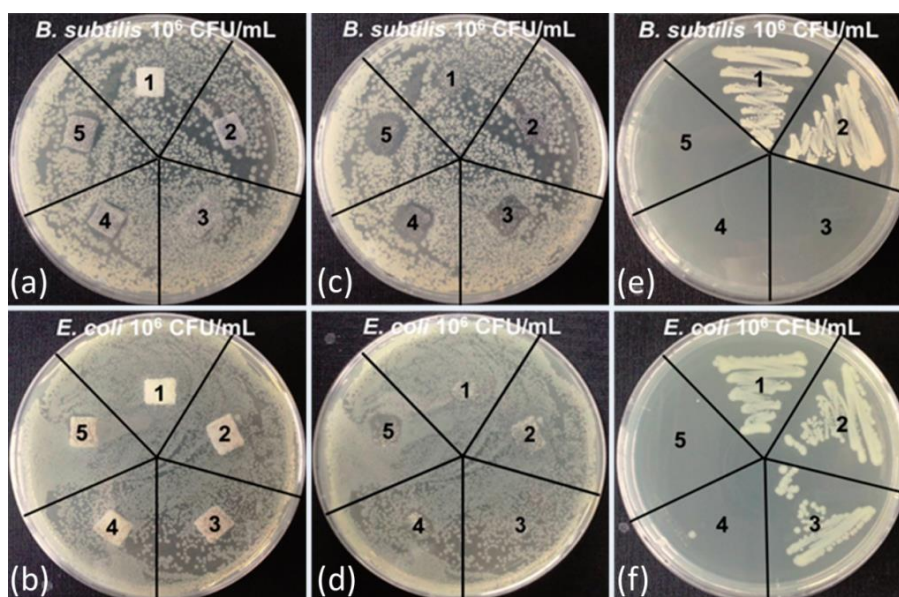


Figure 2-15. Kirby-Bauer test using *B. subtilis* and *E. coli* for samples 1: uncoated scaffold without PPXG, 2: GCG coated scaffold without PPXG, 3: GCG coated scaffold loaded with 10 $\mu\text{g/mL}$ PPXG, 4: GCG coated scaffold loaded with 30 $\mu\text{g/mL}$ PPXG, and 5: GCG coated scaffold loaded with 50 $\mu\text{g/mL}$ PPXG. (a) and (b): after incubation for 24 h, (c) and (d): area under the incubated samples, (e) and (f): smears on agar plate (bacterial growth after transferring swab from area under the samples to a new agar plate).

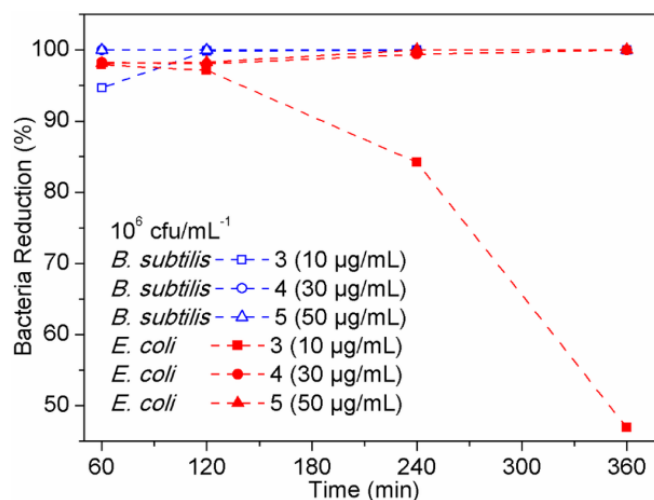


Figure 2-16. Time-dependent shaking flask test results of samples 3: GCG coated scaffold loaded with 10 $\mu\text{g/mL}$ PPXG, 4: GCG coated scaffold loaded with 30 $\mu\text{g/mL}$ PPXG, and 5: GCG coated scaffold loaded with 50 $\mu\text{g/mL}$ PPXG.

Firstly the *in vitro* biocompatibility of PPXG, genipin and GCG was characterized by evaluating the cell proliferation and cell morphology of MG-63 cells. Mitochondrial activity was measured using the water soluble tetrasodium (WST) test. As shown in Figure 2-17, the mitochondrial activity of MG-63 cells significantly decreases with increasing PPXG concentration. The cell shape, cell membrane integrity and nucleus integrity cultured in 10 $\mu\text{g/mL}$ PPXG solution are quite similar to that of the control sample. MG-63 cells exhibited 51% and 59% mitochondrial

Cumulative Part of Dissertation

activity at 50 $\mu\text{g}/\text{mL}$ genipin and a GCG amount of 1 mg/mL , respectively. The mitochondrial activity decreased with an increasing amount of GCG. Compared to the control sample, there is an obvious reduction of viable cells, however the cell shape is still similar to that of the control group.

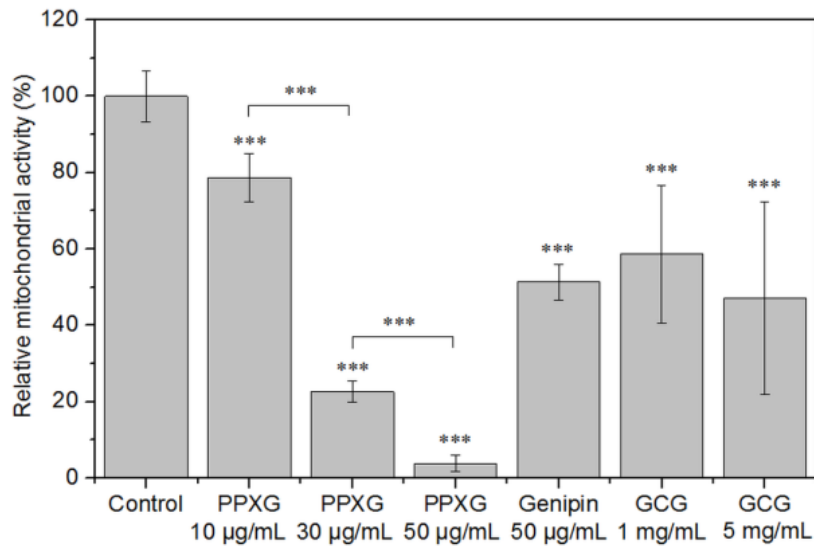


Figure 2-17. Mitochondrial activity measurement of MG-63 cells in the presence of PPXG, genipin and GCG at different concentrations after 2 days of cultivation. The values are mean \pm standard deviation. The asterisks indicate significant difference. *** $P < 0.001$.

Biocompatibility of 45S5 BG scaffolds was also evaluated, as shown in Figure 2-18. The mitochondrial activity of MG-63 cells on GCG coated 45S5 BG scaffolds is higher than on uncoated 45S5 BG scaffolds after 2 weeks of cultivation. Figure 2-19 shows the result of the WST assay, which also indicates, that GCG coating may have a slightly positive effect on the cell proliferation of MG-63 cells (Figure 2-19). As summary of biocompatible tests, GCG coated 45S5 BG scaffolds, as well as the GCG coating itself, show compatibility with MG-63 cells even at a relatively low concentrations.

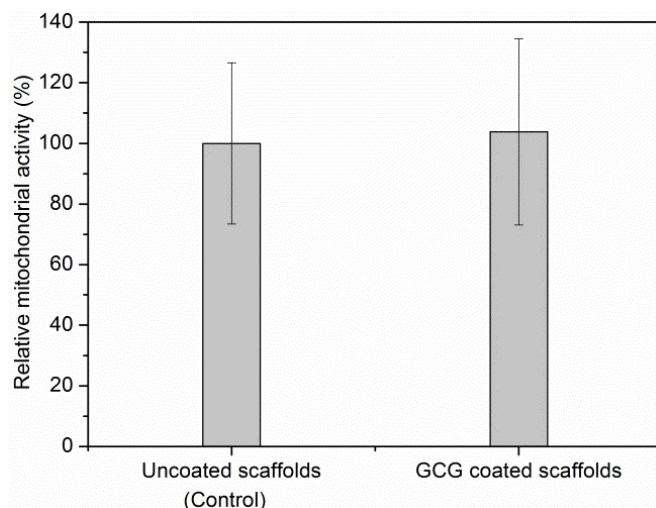


Figure 2-18. Mitochondrial activity measurement of MG-63 cells on GCG coated 45S5 BG scaffolds after 2 weeks of incubation, using uncoated 45S5 BG scaffolds as a control. The values are mean \pm standard deviation.

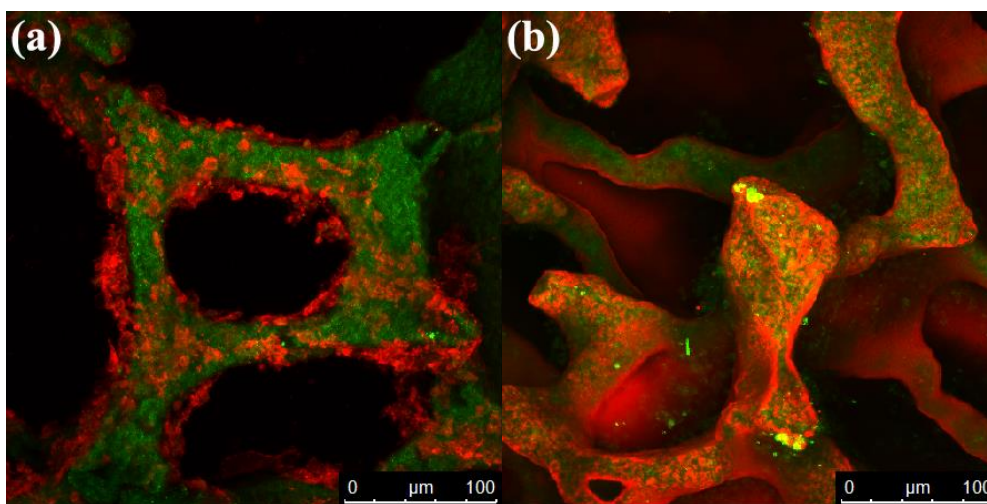
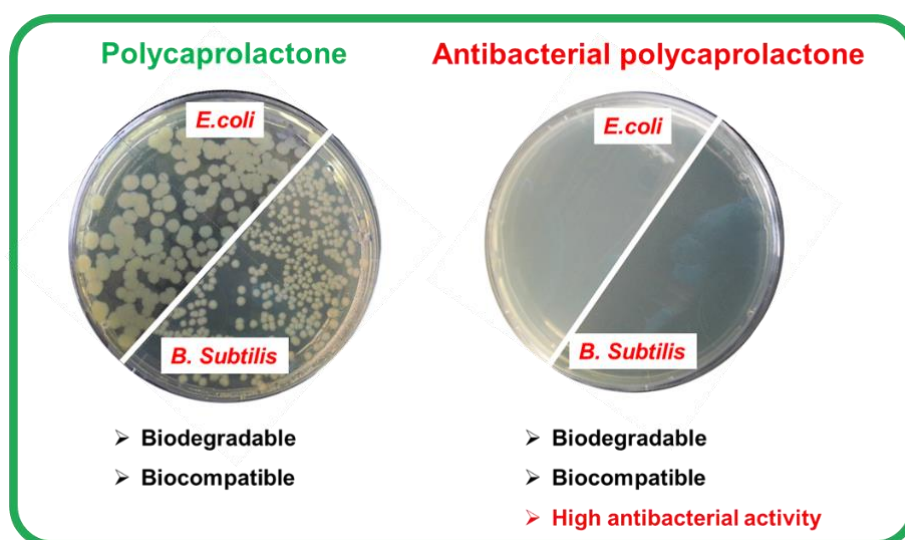


Figure 2-19. CLSM images of MG-63 osteoblast-like cells on the surfaces of (a) uncoated and (b) GCG coated 45S5 BG scaffolds after 2 weeks of cultivation. The cells were stained red and the 45S5 BG surface can be seen in green.

In conclusion, the GCG coated 45S5 BG scaffolds showed the improved mechanical properties and bioactivity. After loading with PPXG, the scaffolds exhibited excellent antibacterial activity against Gram-positive and Gram-negative bacteria. PPXG shows biocompatibility at low concentration, evaluated by an *in vitro* biocompatibility test to MG-63 cells. The new 45S5 BG scaffolds are promising candidates for bone tissue engineering applications.

3. Oligomeric dual functional antibacterial polycaprolactone

Hui Wang,^a Christopher V. Synatschke,^a Alexander Raup,^b Valérie Jérôme,^b Ruth Freitag^b and Seema Agarwal^{*a}



Published in *Polymer Chemistry*, **2014**, 5, 2453-2460. Reproduced by permission of The Royal Society of Chemistry.

Oligomeric dual functional antibacterial polycaprolactone

Hui Wang,^a Christopher V. Synatschke,^a Alexander Raup,^b Valérie Jérôme,^b Ruth Freitag,^b and Seema Agarwal^{*a}

Received 21 Oct 2013, Accepted 01 Dec 2013

DOI: 10.1039/C3PY01467C

Dual functional antibacterial and biodegradable caprolactone (CL) based oligomers were prepared by ring-opening polymerization of caprolactone using polyguanidine macroinitiator. Primary amino (–NH₂) end-groups of linear poly(hexamethylene guanidine) hydrochloride (PHMG) acted as initiating sites for caprolactone polymerization leading to block copolymers which combine antibacterial properties of PHMG with degradability provided by PCL. The block structure of the material was confirmed with 2D NMR and MALDI-ToF-MS. Further, the material exhibited temperature dependent solubility (upper critical solution temperature) in polar solvents like methanol. The oligomers showed high antibacterial activity (reduction of bacterial cells was more than 3 log stages) even at short incubation times depending on the concentration and PHMG:PCL ratio while maintaining enzymatic degradability and biocompatibility.

Introduction

Lot of research efforts are being carried out in the field of antibacterial polymers as microbial contamination is the serious concern in many areas like medical devices, sanitation, food packaging and storage. The most common and widely studied antibacterial polymers are polycations with quaternary ammonium and phosphonium groups. The mechanism of antibacterial action is complex and starts with the interaction of positively charged polymer either with the cytoplasmic membrane of Gram-positive bacteria or the outer membrane of Gram-negative strains followed by the hole-formation killing bacteria.^[1] Depending on molecular weight, spacer length (the length between the active biocidal unit and the polymer backbone), the counter ion and the hydrophilicity / hydrophobicity ratio of the polymeric biocides showed different reaction time against bacteria and universality in killing both Gram-positive and Gram-negative bacteria. For more detailed information, the reader is referred to some excellent reviews.^[1-3] Also, biodegradable polymers with enzymatically or hydrolytically cleavable linkages like polycaprolactone (PCL), polylactide (PLA) etc. (belonging to the class of polyesters) are in high demand for various biomedical applications and as environmental friendly materials for packaging etc.^[4-6] For many application areas of biodegradable polymers like sutures, implants, wound coatings etc. on one side and packaging, food storage etc. on the other side, it is reasonable to have antibacterial functionality besides biodegradability. Such novel dual functional polymers would certainly have an edge over the conventional polyesters

Publications

at present in use for many of such applications. For these applications the antimicrobial moiety should be active while attached to the polymer.

The concept of having a biodegradable antimicrobial polymer with hydrolysable moiety together with antibacterial units in its inactive form is reported in the literature for the smart release of active ingredients on demand. Such systems are important for targeted antibacterial action. They make use of hydrolysable ester units either as linker between the biocide and polymer backbone or in the backbone attaching biocide units together. Poly(vinyl alcohol-peptide linker-gentamicin) is one such polymer, which has degradable peptide units attaching biocide (gentamicin) to the polymer backbone.^[7,8] The enzyme proteinases from wounds infected with bacteria like *Pseudomonas aeruginosa* can cleave the linker releasing the antibiotic. In these cases the biocides are present in their inactive form in the polymers and were released after degradation of either linker or polymer backbone and brought biocides in the active form. There is hardly any literature on dual functional polyesters (hydrolysable and antibacterial) with inherent antimicrobial functionality. One of the broad aims in our research group is to provide dual functional antibacterial and biodegradable polymers. Recently we prepared a dual functional antimicrobial biodegradable polyester using N-halamine as the biocidal unit. Polyesters of dimethyl succinate (DMS), 1,4-butanediol (BDO) and 3-[*N,N*-di(β -hydroxyethyl)aminoethyl]-5,5-dimethylhydantoin (H-diol) were made via a two-step melt polycondensation reaction. (H-diol) was used as antibacterial comonomer. The resulting polyesters were biocompatible as determined by cell viability studies and showed an antibacterial activity against *E. coli*.^[9] N-Halamines are biocidal against a broad range of microorganisms and show regenerable biocidal activity upon exposure to bleach.^[10-12] In another study, the possibility of introducing antibacterial functionality to PCL, a highly studied biomaterial by a combination of ROP and click chemistry is recently shown by us. There a series of novel antibacterial poly(ϵ -caprolactone)-*graft*-hydantoin copolymers were successfully prepared by a copper(I)-catalyzed click reaction of azide-functionalized hydantoin with poly(ϵ -caprolactone) bearing pendent alkyne functionalities and characterized in terms of polymer structure, and thermal, mechanical, antibacterial and biodegradable properties.^[13] Kamigaito and Kuroda *et al.* have recently shown the formation of oligomeric antibacterial biodegradable material with degradable ester linkages in the backbone and quaternary ammonium groups in the side chain by a multi-step reaction scheme. The polymers had low molar mass in the range M_n (number average molar mass) 1200-6000 $\text{g} \cdot \text{mol}^{-1}$ and showed low to good antibacterial activity depending upon the structure without mentioning the time of antibacterial action.^[14]

Publications

We report here a simple method of making highly active and efficient oligomeric antibacterial degradable material with ester linkages and guanidine antibacterial units in the polymer backbone. Both linear and ring polyguanidines are highly efficient and active antibacterial polymers against a wide range of microorganisms, while exhibiting low toxicity.^[15-16] The use of polyguanidines as antibacterial additives for biodegradable polyesters is hindered by the phase-separation and in-homogenous mixing due to the polarity difference between the two. Polyguanidines are synthesized through the condensation of diamines with guanidine hydrochloride and possess different chain ends like primary amino ($-\text{NH}_2$), and guanidine ($-\text{NH}-\text{C}(\text{NH})^+-\text{NH}_2$) groups.^[17-19] The linear oligoguanidine based on hexamethylenediamine and guanidinehydrochloride was used as a macroinitiator for ring-opening polymerization of caprolactone for the formation of polycaprolactone based antibacterial materials in the present work. The guanidine and p-amino functional groups in amino acids L-arginine and L-citrulline previously have been shown as ROP initiator for L-lactide and CL polymerizations.^[20] The resulting amphiphilic block copolymers could be utilised as additives / compatibilizers for polar antibacterial polyguanidines and non-polar degradable polyesters for providing dual functional antibacterial biodegradable polyesters.

Experimental

Materials

Hexamethylenediamine (98%), guanidine hydrochloride (99.5%) and ϵ -caprolactone were purchased from Sigma-Aldrich. Chloroform, pentane and dimethyl sulfoxide were distilled prior to use. Linear PEI (25 kDa) was from Polysciences, Inc. (Warrington, Pennsylvania, USA). 3-(4,5-Dimethylthiazolyl-2)-2,5-diphenyl tetrazolium bromide (MTT), was purchased from Sigma-Aldrich. Cell culture materials, medium and solutions were from PAA Laboratories.

Characterization

Nuclear magnetic resonance (NMR) spectroscopy

^1H (400.13 MHz) and ^{13}C (100.21 MHz) spectra were recorded on a Bruker DRX-400 spectrometer at 60 °C using MeOD (99.8% D, Carl Roth GmbH), D_2O (99.8% D, Carl Roth GmbH) and CDCl_3 (99.8% D, stabilized with Ag, Carl Roth GmbH) as solvent. All chemical shifts (δ) are reported relative to tetramethylsilane (TMS) as internal reference. ^1H - ^{13}C heteronuclear multiple quantum coherence (HMQC) and heteronuclear multiple bond coherence (HMBC) experiments were performed on a Bruker DRX-500 spectrometer, with a

Publications

5mm multinuclear gradient probe at 60 °C using MeOD (99.8% D, Carl Roth GmbH) as solvent.

Matrix-Assisted Laser Desorption/Ionization Time-of-Flight Mass Spectrometry (MALDI-ToF-MS)

MALDI-TOF MS analysis was performed on a Bruker Reflex III apparatus equipped with a N₂ laser ($\lambda = 337$ nm) in linear mode at an acceleration voltage of 20 kV. Indole-3-acetic acid (IAA, Fluka, 99.0%) was used as a matrix material. Samples were prepared with the dried droplet method from Methanol solution by mixing matrix und polymer in a ratio of 20: 5 (v/v) and applying approximately 1 μ L to the target spot.

Homopolymerization of hexamethylenediamine and guanidine hydrochloride (PHMG)^[18]

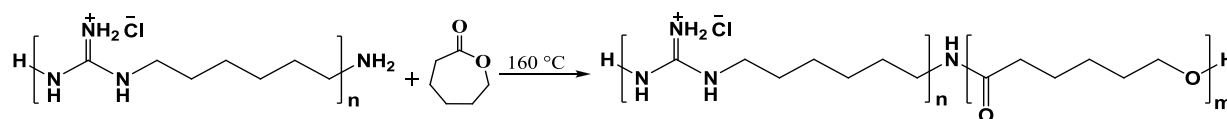
The homopolymerization of hexamethylenediamine and guanidine hydrochloride was carried out by melt polycondensation and the product is designated as PHMG. A mixture of guanidine hydrochloride (8.21 g, 85.00 mmol) and hexamethylenediamine (9.88 g, 85.00 mmol) was combined in a dry 100 mL three necked round bottom flask equipped with a thermometer and a reflux condenser. The reagents were heated up to 150 °C. The ammonia gas at ca. 80 °C started evolving showing start of the polycondensation reaction. The reaction was stopped after 5 hours by cooling in an ice bath and the polymer obtained (yellowish transparent solid) was structurally characterized by NMR. MALDI-TOF MS was used to determine the molar mass and chain ends of PHMG as described in results and discussion part.

¹H NMR: 500 MHz, D₂O; δ (ppm) = 1.40 (*br s*, -CH₂(CH₂)₂NH-); 1.48 (*br s*, -CH₂CH₂NH₂); 1.56 (*br s*, -CH₂CH₂NH-); 2.59 (*br s*, -CH₂NH₂); 3.16 (*br s*, -CH₂NH).

¹³C NMR: 125 MHz, D₂O; δ (ppm) = 25.53 (-CH₂(CH₂)₂NH-); 28.00 (-CH₂CH₂NH-); 30.97 (-CH₂CH₂NH₂); 40.43 (-CH₂NH₂); 41.17 (-CH₂NH-); 155.79, 156.82 (-C(NH)-).

Copolymerization of PHMG and caprolactone (CL)

The copolymers were obtained from ROP of CL using PHMG as macroinitiator (Scheme 3- 1).



Scheme 3-1. Ring opening polymerization of ϵ -polycaprolactone using PHMG as macroinitiator.

Publications

In a typical reaction, Caprolactone (1 mL, 9.5 mmol, 77 wt%) and synthesized Poly(hexanethyleneguanidine) PHMG) (0.5 g, 23 wt%) were placed under argon in a reaction flask. The reaction mixture was stirred at 160 °C for different intervals of time. After a desired time period, the reaction mixture was diluted with CHCl₃ and precipitated in about 200 mL of pentane. The copolymers were dried under vacuum at room temperature to constant weight.

Enzymatic Degradability

In general, 100 mg copolymer was suspended in 5 mL phosphate buffered saline (PBS) buffer (pH = 7.4) and Lipase from *Pseudomonas Cepacia* (0.3 mg·mL⁻¹) NaN₃ solution. It was then placed at 37 °C with shaking for different time periods. The mixture was then lyophilized. The remaining solid was characterized using MALDI-ToF-MS.

Antibacterial activity

Escherichia coli (*E. coli*, DSM No. 1077, K12 strain 343/113, DSMZ) as Gram-negative test-organism and *Bacillus subtilis* (*B. subtilis*, DSM No. 2109, ATCC 11774, ICI 2/4 strain, DSMZ) as Gram-positive representative were used to evaluate the antibacterial activity of copolymers. Tryptic soy broth (Sigma Aldrich) was used as nutrient for *E. coli* (30 g · L⁻¹ in distilled water for liquid nutrient; 15 g · L⁻¹ agar-agar in addition for nutrient agar plates) and peptone/meat extract medium for *B. subtilis* (5 g · L⁻¹ peptone and 3 g · L⁻¹ meat extract in distilled water for liquid nutrient; 15 g · L⁻¹ agar-agar in addition for nutrient agar plates). Both strains were preserved on nutrient agar plates and liquid cultures were grown by inoculation of liquid nutrient with a single bacteria colony using an inoculation loop. The inoculated broth was incubated with shaking at 37 °C until the optical density at 578 nm had increased by 0.125 indicating a cell density of 10⁷-10⁸ cfu · mL⁻¹. To obtain the final bacterial suspensions the inoculated broth was diluted with liquid nutrient to an approximate cell density of 10⁶ cfu · mL⁻¹. Firstly the Antibacterial activity of copolymer was determined by minimal inhibitory concentration (MIC), which is the minimal concentration required to inhibit bacteria growth, and minimal bactericidal concentration (MBC), which corresponds to the minimal concentration needed to kill at least 99.9 % of the bacteria cells.

A water suspension of copolymers was made for antibacterial tests by dissolving 60 mg in 10 mL DMSO at 40 °C followed by dialysis against Millipore water at room temperature. A dilution series of the copolymer suspension each 500 µg · mL⁻¹ were prepared in a sterile 24 well plate (Greiner bio-online) and then equal volume of the 10⁶ cfu · mL⁻¹ inocula of *E. coli* or *B. subtilis* was added. After 24 h of incubation at 37 °C the wells were visually evaluated for bacteria growth. The lowest concentration which remained transparent was taken as MIC. To

Publications

determine the MBC, 100 μL solution was removed from each clear well and spread on nutrient agar plates and incubated for further 24 h at 37 °C. The lowest concentration of biocide at which no colony formation was observed, was taken as MBC. Each test was done in quadruplicate. The speed of antibacterial activity was determined by shaking flask method [21-22]: polymer suspension in water of 10 $\mu\text{g} \cdot \text{mL}^{-1}$, 100 $\mu\text{g} \cdot \text{mL}^{-1}$ and 1000 $\mu\text{g} \cdot \text{mL}^{-1}$ were incubated with equal volumina of bacteria suspension at ambient temperature in microcentrifuge tubes and contact times of 2, 5, 10, 30, and 60 min were chosen. After defined time intervals, 100 μL specimens were drawn and spread on nutrient agar plates. After incubation at 37 °C for 24 h, colonies were counted and the reduction was calculated relative to the initial cell density of the inoculum.

Cytotoxicity Test Using MTT Assay

Mammalian Cell Lines and Culture Conditions

The L929 (CCL-1, ATCC) cell line was used in the cytotoxicity experiments. The L929 cells were maintained in MEM cell culture medium supplemented with 10% fetal calf serum (FCS), 100 $\mu\text{g}/\text{mL}$ streptomycin, 100 $\text{IU} \cdot \text{mL}^{-1}$ penicillin, and 4 mM L-glutamine. Cells were cultivated at 37 °C in a humidified 5% CO_2 atmosphere.

MTT Assay

The cytotoxicity of the polymer (PHMG) and of the samples 2, and 3 in DMSO was tested using L929 murine fibroblasts according to the norm ISO 10993-5 using 1 $\text{mg} \cdot \text{mL}^{-1}$ MTT-stock solution. The polymers were tested in a concentration range from 0 to 1.0 mg/mL in 96-well plates. A of polymers was used as described for antibacterial tests. The cells were seeded at a density of 1×10^4 cells per well 24 h prior to the experiment. As 100% viability control, untreated cells were used. For each dilution step, eight replicates were used. After dissolving the metabolically formed formazan crystals in isopropanol, the absorbance was measured using a plate reader (Genios Pro, Tecan) at a wavelength of 580 nm. For data evaluation, SigmaPlot 11.0 (Systat Software GmbH) software was used, the x-scale was plotted logarithmically, and a nonlinear fit was run to obtain the lethal dose 50 (LD_{50}) values. Group data are reported as mean \pm s.d.

Statistical Analysis

Group data are reported as mean \pm s.d. Statistical evaluation of the MTT results was performed done using the software SigmaPlot 11.0 (Systat Software GmbH). The one-way ANOVA with Bonferroni t-test was used to determine whether data groups differed significantly from each other. Statistical significance was defined as having $P < 0.05$.

Results and Discussion

The antibacterial oligomeric product of melt condensation between hexamethylenediamine and guanidine hydrochloride (PHMG) had a number-average molar mass (M_n), weight average molar mass (M_w) and polydispersity (PDI) of 1300, 1600 and 1.3 respectively, as determined by MALDI-ToF-MS using polystyrene standard of 20kDa. MALDI-ToF-MS was also used to confirm the structure and chain ends of PHMG.^[18] Three different types of oligomeric linear chain structure were found: PHMG with p-amino groups and guanidine groups at both chain-ends respectively, as well as PHMG chain with one guanidine and p-amino group as the chain-ends (Figure 3-1).

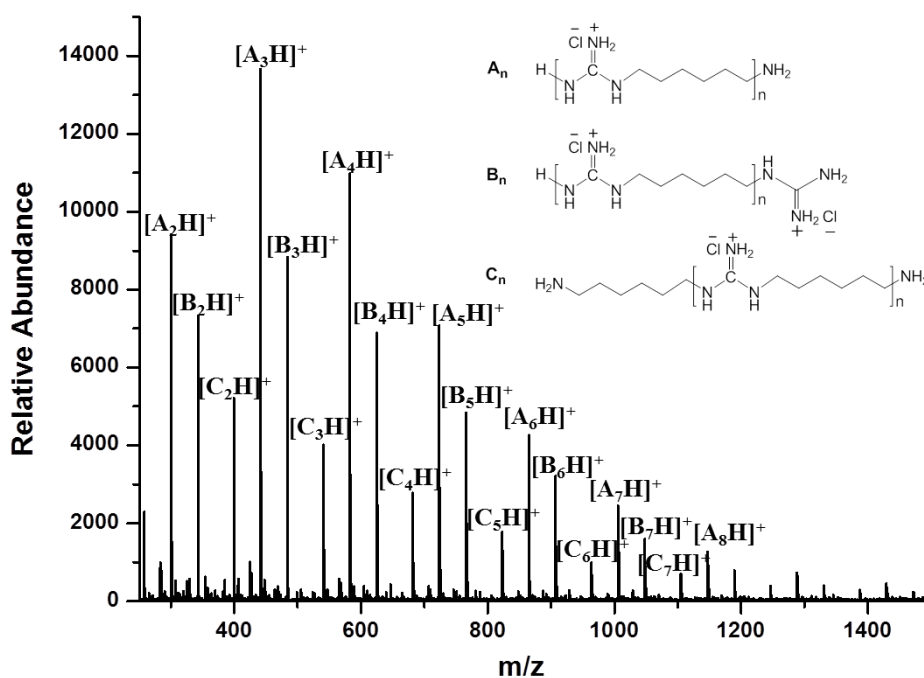


Figure 3-1. MALDI-ToF-MS of PHMG shows a linear structure of poly(hexamethyleneguanidine hydrochloride) (PHMG) with different type of chain ends.

The PHMG was then used as a macroinitiator for ring-opening polymerization (ROP) of caprolactone at 160 °C (Table 3-1). Varying block lengths were prepared through different ratios of PHMG macroinitiator and CL as well as polymerization times. PHMG:CL (32 wt% : 68 wt% in feed) showed an increase in yield from 52 % to about 94 % by increasing the reaction time from 8 to 24 h with increase in molar mass (M_w) from 2500 to 3400 as measured by MALDI-ToF-MS. The PHMG homopolymer was completely soluble in water and methanol. In contrast the reaction product of PHMG with CL showed temperature dependent solubility of

Publications

upper critical solution temperature (UCST)-type in polar solvents like methanol (for temperature dependent solubility please see Figure 3-S1 in supplementary information). A thorough investigation of the temperature dependent solubility aspects of this material are exceeding the scope of the present work and will be conducted in the future.

^1H -NMR spectra of the copolymers were taken in MeOD at 60 °C. A representative ^1H NMR is shown in Figure 3-2. The characteristic proton signals of PHMG and PCL units were present and are marked in the spectrum. The signals of PCL were present at: ppm 4.08 ($-\text{OCH}_2\text{C}(\text{O})-$), 2.23 ($-\text{C}(\text{O})\text{CH}_2-$), ppm 1.64-1.66 ($-\text{C}(\text{O})\text{CH}_2\text{CH}_2\text{CH}_2-$) and ($-\text{CH}_2\text{OC}(\text{O})-$) and ppm 1.41 ($-\text{C}(\text{O})\text{CH}_2\text{CH}_2\text{CH}_2\text{CH}_2-$). The signal centered at ppm 3.23 was from $-\text{NHC}(\text{NH})\text{NHCH}_2-$ of PHMG. The other signals of PHMG were in overlap at ppm 1.64-1.66 and 1.41 with PCL as shown in figure 3-2. The overlap of signals was obvious from the integration ratios between various peaks. The integration ratio was: 2:2:6:4 for signals at ppm 4.08:2.33:1.64:1.41. When it would have been only from PCL then the expected ratio is: 2:2:4:2. 2D HMQC was used for assigning peak position in ^{13}C NMR (Figure 3-3) (For HMQC please see Figure 3-S2 in supplementary information). The overlapping signals of PHMG and PCL in ^1H NMR were analysed using 2D NMR technique like ^1H - ^{13}C heteronuclear multiple bond correlation HMBC (see Figure 4). The signal at ppm 1.41 besides showing 1 and 2 bond correlations of PCL also showed very significant cross-peaks (A) and (B) with carbon signals at ppm 41.22 ($-\text{NHC}(\text{NH})\text{NHCH}_2-$) and ppm 25.96. This confirmed the presence of protons of oligoguanidine ($-\text{NH}-\text{C}(\text{NH})\text{NHCH}_2\text{CH}_2-$) (2) at ppm 1.41 together with $-\text{C}(\text{O})\text{CH}_2\text{CH}_2\text{CH}_2-$ (a) of PCL. The overlapping signal at ppm 1.64-1.66 also showed correlations of both PCL (C,D,E) and oligoguanidines (F) corresponding to PCL protons b and e as well protons 1 of PHMG. The proof of formation of copolymers was the presence of an extra cross-coupling signal (G) by coupling of $-\text{CH}_2\text{NHC}(\text{O})-$ protons (3') of oligoguanidine with carbonyl carbon. The cross-coupling of $-\text{CH}_2\text{NHC}(\text{O})-$ with carbonyl carbon in addition to coupling with carbons 1 and 2 of oligoguanidine (H,I) showed the presence of a linking unit between oligoguanidine and PCL. The copolymer composition was determined to be 0.72:1 (molar ratio) PHMG : PCL. The integration of peaks at ppm 4.08 and 3.23 was used for calculation of copolymer composition. Other copolymers with varied molar ratio of PHMG and PCL were also synthesized (Table 3-1) and analysed in a similar way.

Publications

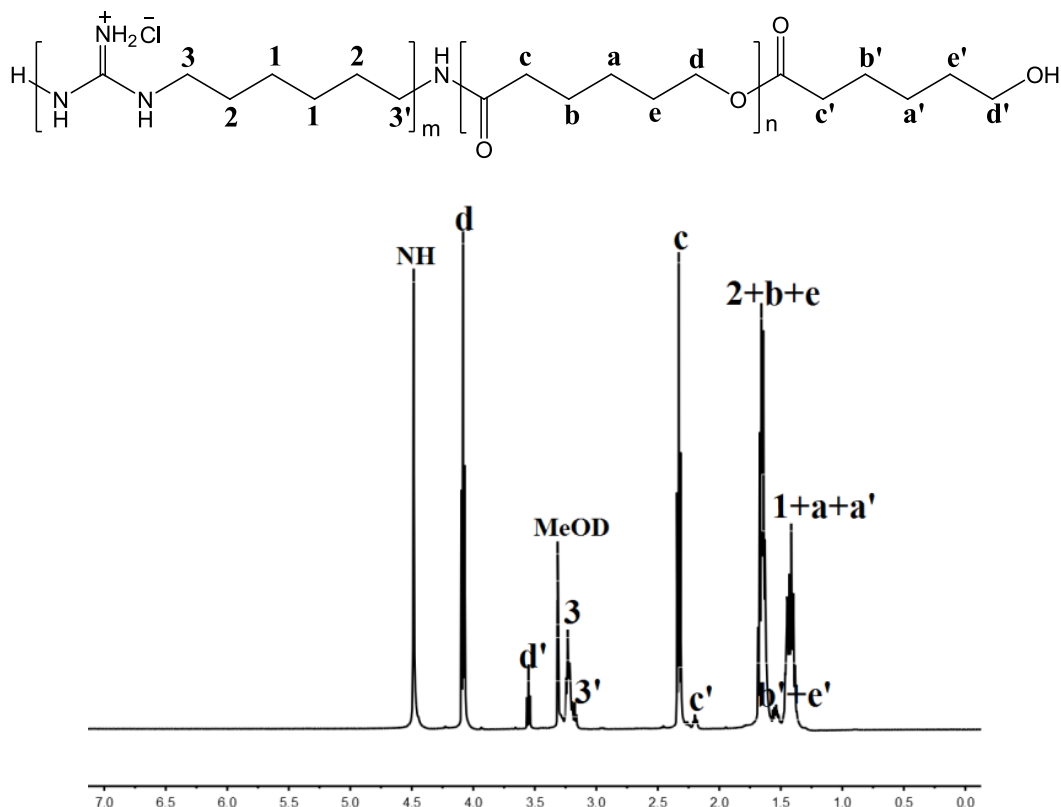


Figure 3-2. ^1H NMR spectrum of PHMG-*b*-PCL (Sample 2, Table 3-1) synthesized by condensation polymerization. The spectrum was measured in MeOD at 60 °C.

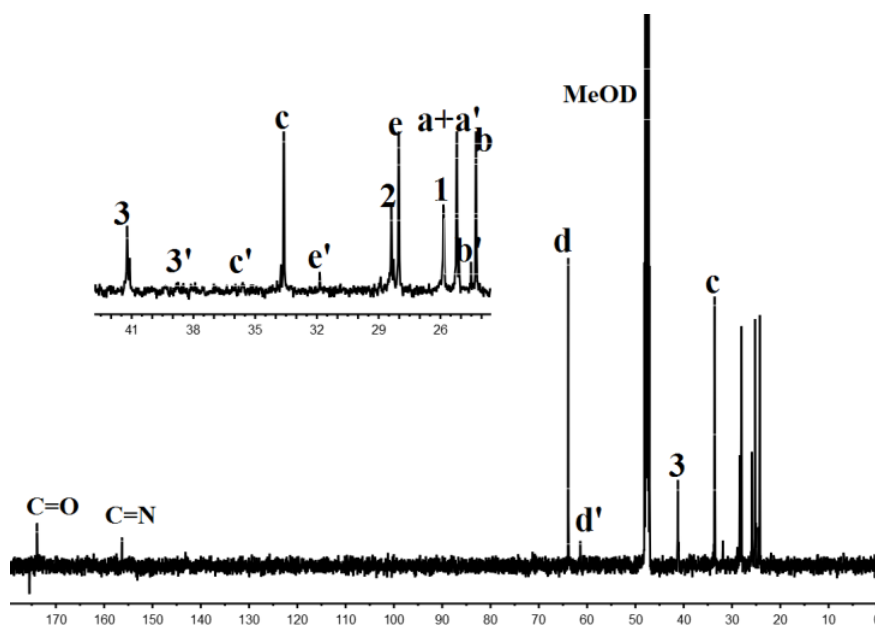


Figure 3-3. ^{13}C NMR spectrum of PHMG-*b*-PCL (Sample 2, Table 3-1) synthesized by condensation polymerization. The spectrum was measured in MeOD at 60 °C.

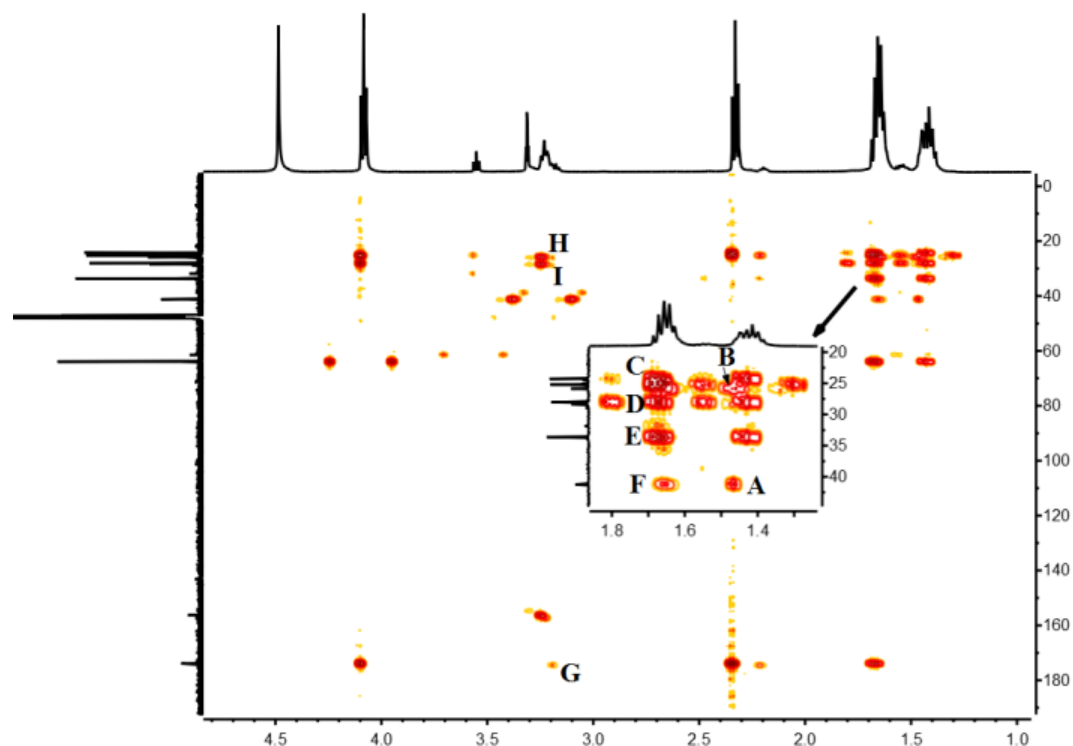


Figure 3-4. 2D ^1H - ^{13}C correlation NMR experiment HMBC in MeOD, at 60 °C of sample 2 with labeled cross resonances.

Table 3-1. Details of oligomers synthesized by ROP of CL using poly(hexamethylene guanidine) hydrochloride (PHMG) macroinitiator for 24 h^a: copolymer composition, molar mass, PDI and yield.

Sample	PHMG:PCL (molar ratio in copolymer)	$M_{n,\text{NMR}}$	M_n^b	M_w^b	PDI ^b (M_w/M_n)	Yield %
1	0.72:1	2800	2700	3300	1.2	80
2	0.67:1	2900	2700	3400	1.2	93
3*	2.71:1	1700	2000	2500	1.3	52
4	1.68:1	1900	2200	2900	1.3	94

^a CL:PHMG feed ratio was 77:23 (sample 1), 32:68 (samples 2 and 3), 50:50 (sample 4).

^b determined by MALDI-ToF-MS

*Time of polymerization for sample 3 was 8 h.

Furthermore, the formation of copolymers was also confirmed by MALDI-ToF-MS (reflectron mode).^[23] The MALDI spectrum of the product showed a step growth reaction resulting in copolymer repeating units as shown in Figure 3-5 and Table 3-2. According to this, the reaction was not hindered and compounds were not a physical blend of PHMG and PCL but block copolymers, formed by ring-opening polymerization. However in this spectrum the signals of homo oligoguanidine (PHMG) with two guanidine hydrochloride end groups were also found as guanidine could not start the ROP of CL.

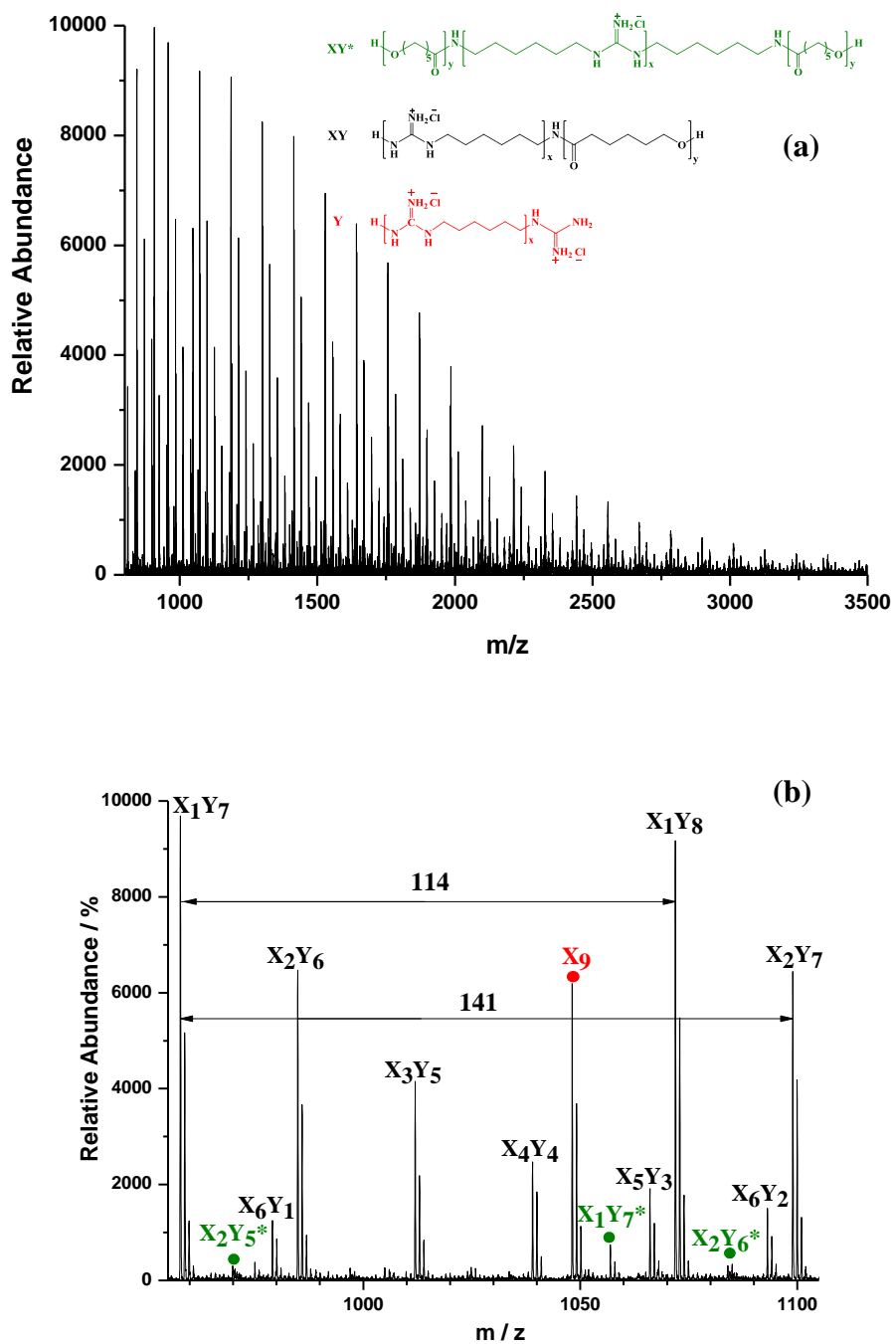


Figure 3-5. (a) Full MALDI-TOF MS spectrum and (b) enlargement of 950-1100 m/z region of sample 2.

Publications

Table 3-2. Experiment and theoretical m/z values for the first peak in the isotopic distributions of the zoom spectrum in Figure 3-5b and their assignments.

m/z_{expt}	ion assignment	formula	m/z_{theor}	$\Delta m/z$
957.8	$[\text{X}_1\text{Y}_7 + \text{H}]^+$	$[\text{C}_{49}\text{H}_{88}\text{N}_4\text{O}_{14}\text{H}]^+$	957.6	0.2
969.9	$[\text{X}_2\text{Y}_5^* + \text{H}]^+$	$[\text{C}_{50}\text{H}_{96}\text{N}_6\text{O}_{10}\text{H}]^+$	969.7	0.2
979.1	$[\text{X}_6\text{Y}_1 + \text{H}]^+$	$[\text{C}_{48}\text{H}_{103}\text{N}_{19}\text{O}_2\text{H}]^+$	978.9	0.2
984.9	$[\text{X}_2\text{Y}_6 + \text{H}]^+$	$[\text{C}_{50}\text{H}_{93}\text{N}_7\text{O}_{12}\text{H}]^+$	984.7	0.2
1012.0	$[\text{X}_3\text{Y}_5 + \text{H}]^+$	$[\text{C}_{51}\text{H}_{98}\text{N}_{10}\text{O}_{10}\text{H}]^+$	1011.8	0.2
1039.0	$[\text{X}_4\text{Y}_4 + \text{H}]^+$	$[\text{C}_{52}\text{H}_{103}\text{N}_{13}\text{O}_8\text{H}]^+$	1038.8	0.2
1048.1	$[\text{X}_7 + \text{H}]^+$	$[\text{C}_{49}\text{H}_{109}\text{N}_{24}\text{H}]^+$	1047.9	0.2
1056.9	$[\text{X}_1\text{Y}_7^* + \text{H}]^+$	$[\text{C}_{55}\text{H}_{101}\text{N}_5\text{O}_{14}\text{H}]^+$	1056.7	0.2
1066.1	$[\text{X}_5\text{Y}_3 + \text{H}]^+$	$[\text{C}_{65}\text{H}_{128}\text{N}_{16}\text{O}_{10}\text{H}]^+$	1065.9	0.2
1071.9	$[\text{X}_1\text{Y}_8 + \text{H}]^+$	$[\text{C}_{55}\text{H}_{98}\text{N}_4\text{O}_{16}\text{H}]^+$	1071.7	0.2
1084.0	$[\text{X}_2\text{Y}_6^* + \text{H}]^+$	$[\text{C}_{56}\text{H}_{106}\text{N}_8\text{O}_{12}\text{H}]^+$	1083.8	0.2
1093.1	$[\text{X}_6\text{Y}_2 + \text{H}]^+$	$[\text{C}_{54}\text{H}_{113}\text{N}_{19}\text{O}_4\text{H}]$	1092.9	0.2
1099.0	$[\text{X}_2\text{Y}_7 + \text{H}]^+$	$[\text{C}_{56}\text{H}_{103}\text{N}_7\text{O}_{14}\text{H}]$	1098.8	0.2

PCL is a well-known biodegradable polymer and we investigated the enzymatic degradation behaviour of the copolymers. The copolymers were incubated at 37 °C in phosphate buffer with lipase from pseudomonas cepacia for different time intervals. The molar mass of the polymer was monitored by MALDI-ToF-MS after different time intervals (4, 8, 24 h). The decrease in molar mass was shown in Figure 6 (MALDI-ToF-MS spectra are shown in Figure 3-S3). After 24 h the PCL part was almost completely degraded, indicating enzymatic degradation of the PCL block.

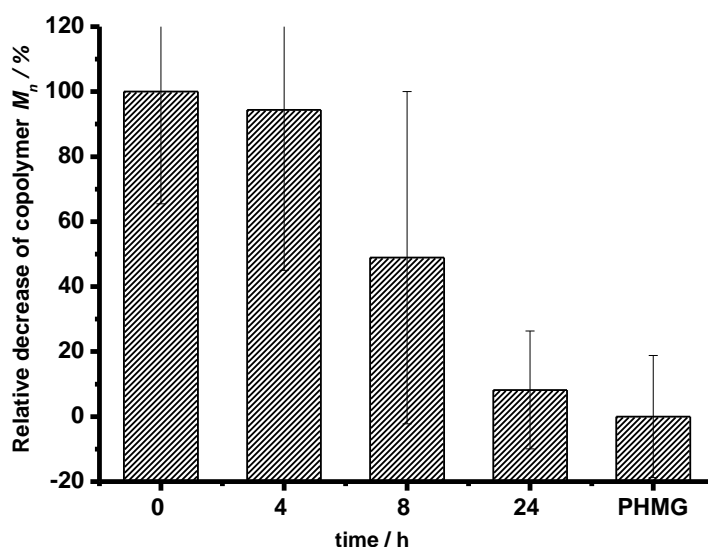


Figure 3-6. Relative decrease of polymer molar mass by lipase from pseudomonas cepacia.

Publications

Furthermore we investigated the antibacterial properties of the materials. The copolymers showed high antibacterial activity as proved by low MIC (minimal inhibitory concentration; the minimal concentration required to inhibit bacteria growth), and MBC (minimal bactericidal concentration; minimal concentration needed to kill at least 99.9 % of the bacteria cells) values. The copolymer with PHMG:PCL molar ratio of 0.67:1 (Table 3-3) showed MIC values of 87.5 $\mu\text{g} \cdot \text{mL}^{-1}$, 50 $\mu\text{g} \cdot \text{mL}^{-1}$ and MBC of 87.5 $\mu\text{g} \cdot \text{mL}^{-1}$, 100 $\mu\text{g} \cdot \text{mL}^{-1}$ for two bacteria, *E.coli* and *B. subtilis*, respectively. The antibacterial effect was dependent upon the ratio of PHMG:PCL. The presence of more PHMG (PHMG:PCL ratio of 2.71:1 (Table 3-3)) reduced MIC to 37.5 $\mu\text{g} \cdot \text{mL}^{-1}$, 25 $\mu\text{g} \cdot \text{mL}^{-1}$ and MBC to 62.5 $\mu\text{g} \cdot \text{mL}^{-1}$, 50 $\mu\text{g} \cdot \text{mL}^{-1}$ for *E. Coli* and *B. subtilis* respectively, indicating a correlation between PHMG content and antibacterial activity. In comparison, the pure PHMG oligomer showed MIC values of 7.81 $\mu\text{g} \cdot \text{mL}^{-1}$, 1.25 $\mu\text{g} \cdot \text{mL}^{-1}$ and MBC values of 7.81 $\mu\text{g} \cdot \text{mL}^{-1}$, 1.96 $\mu\text{g} \cdot \text{mL}^{-1}$ for *E. coli* and *B. subtilis*, respectively.

Table 3-3. MIC and MBC values of PHMG-*b*-PCL regarding 10^5 - 10^6 cfu $\cdot \text{mL}^{-1}$ *E. coli* and *B. subtilis*.

PHMG:PCL (molar ratio)	MIC _{<i>E.Coli</i>} [$\mu\text{g} \cdot \text{mL}^{-1}$]	MBC _{<i>E.Coli</i>} [$\mu\text{g} \cdot \text{mL}^{-1}$]	MIC _{<i>B.subtilis</i>} [$\mu\text{g} \cdot \text{mL}^{-1}$]	MBC _{<i>B.subtilis</i>} [$\mu\text{g} \cdot \text{mL}^{-1}$]
0.67:1	87.5	87.5	50	100
2.71:1	37.5	62.5	25	50

Besides high antibacterial activity, a fast action time is also an important property of biocidal polymers. The speed of antibacterial action, a time dependent test of antibacterial effect was conducted for samples 2 and 3 as generic representative. The reduction of the viable cell count of Gram-positive and Gram-negative bacteria is depicted in logarithmic stages with different concentrations (Figure 3-7 and 3-8). The reduction of bacterial cells was more than 3 log stages, which corresponds to killing 99.9% of bacteria. Figure 3-7 displays the reduction in Gram-positive bacteria by samples 2 and 3. Both polymers killed more than 99.9% *B. subtilis* at 100 $\mu\text{g} \cdot \text{mL}^{-1}$ after 60 minutes. Sample 3 even at concentration of 10 $\mu\text{g} \cdot \text{mL}^{-1}$ after 2 minutes killed more than 99.9% bacteria. Figure 3-8 depicts the speed of antibacterial action towards *E. coli* as Gram-negative bacteria. Both copolymers killed more than 99.9% bacteria at a concentration of 1000 $\mu\text{g} \cdot \text{mL}^{-1}$ after 10 minutes. Even sample 2 with the lowest mole percentage of PHMG killed 99% bacteria after 30 min at concentration of 100 $\mu\text{g} \cdot \text{mL}^{-1}$ and 98.0% *E. coli* after 60 min, at concentration of 10 $\mu\text{g} \cdot \text{mL}^{-1}$. The polymers under study were also qualitatively tested for antibacterial activity during enzymatic degradation process. The antibacterial activity was not disturbed by the presence of lipase from pseudomonas cepacia as shown in the Figure 3-S4 and showed no bacterial colonies on agar plate.

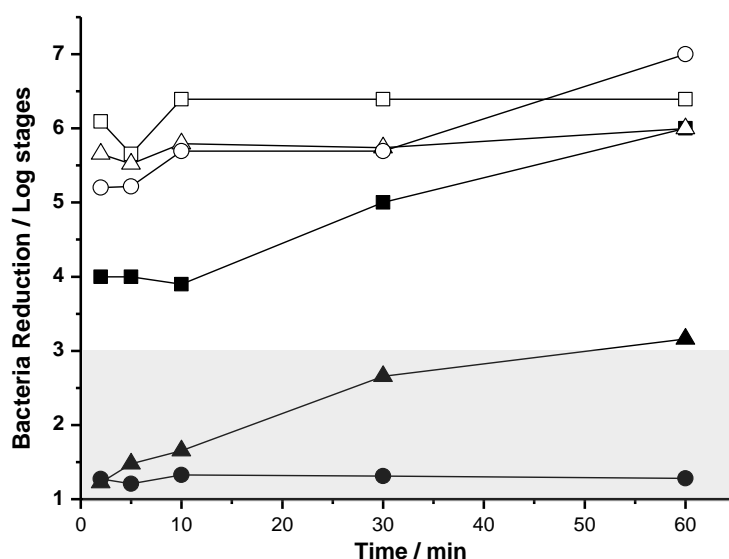


Figure 3-7. Time-dependent reduction of bacteria in a suspension of *B. subtilis* with an initial cell density of 10^6 cfu · mL⁻¹ upon contact Samples 2 with concentrations of --■-- 1000 µg · mL⁻¹, --▲--100 µg · mL⁻¹, --●--10 µg · mL⁻¹ and Samples 3 with concentrations of --□-- 1000 µg · mL⁻¹ --Δ--100 µg · mL⁻¹, --○--10 µg · mL⁻¹ at ambient temperature, given in log stages.

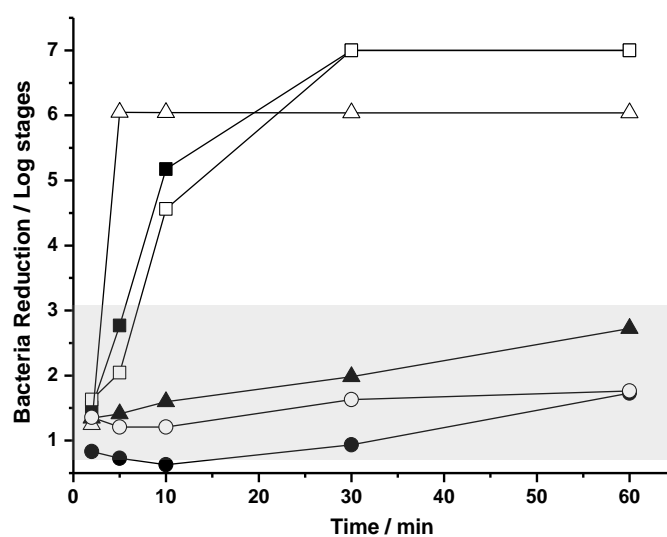


Figure 3-8. Time-dependent reduction of bacteria in a suspension of *E. coli* with an initial cell density of 10^6 cfu · mL⁻¹ upon contact Samples 2 with concentrations of --■-- 1000 µg · mL⁻¹, --▲--100 µg · mL⁻¹, --●--10 µg · mL⁻¹ and Samples 3 with concentrations of --□-- 1000 µg · mL⁻¹ --Δ--100 µg · mL⁻¹, --○--10 µg · mL⁻¹ at ambient temperature, given in log stages.

In order to obtain a first idea concerning the cytotoxicity of these materials towards mammalian cells and tissues the standard MTT assay was performed and compared with 1-PEI 25 kDa as reference. Therefore, the L929 cells were exposed to PHMG and PHMG-*b*-PCL (sample 2 and 3) for 24h. The addition of the polymers in the concentration range 0 to 1 mg · mL⁻¹ affects the

Publications

cellular metabolic activity in a concentration-dependent manner (Figure 3-9). Under these conditions, the LD₅₀ were $10.8 \pm 2.0 \mu\text{g} \cdot \text{mL}^{-1}$, $22.9 \pm 2.2 \mu\text{g} \cdot \text{mL}^{-1}$ and $27.6 \pm 5.2 \mu\text{g} \cdot \text{mL}^{-1}$ for cells treated with the PHMG, sample 2 and 3, respectively. Whereas, PHMG shows cytotoxicity comparable to l-PEI ($12.3 \pm 0.6 \mu\text{g} \cdot \text{mL}^{-1}$), the copolymers have two fold higher LD₅₀ and are therefore less cytotoxic.

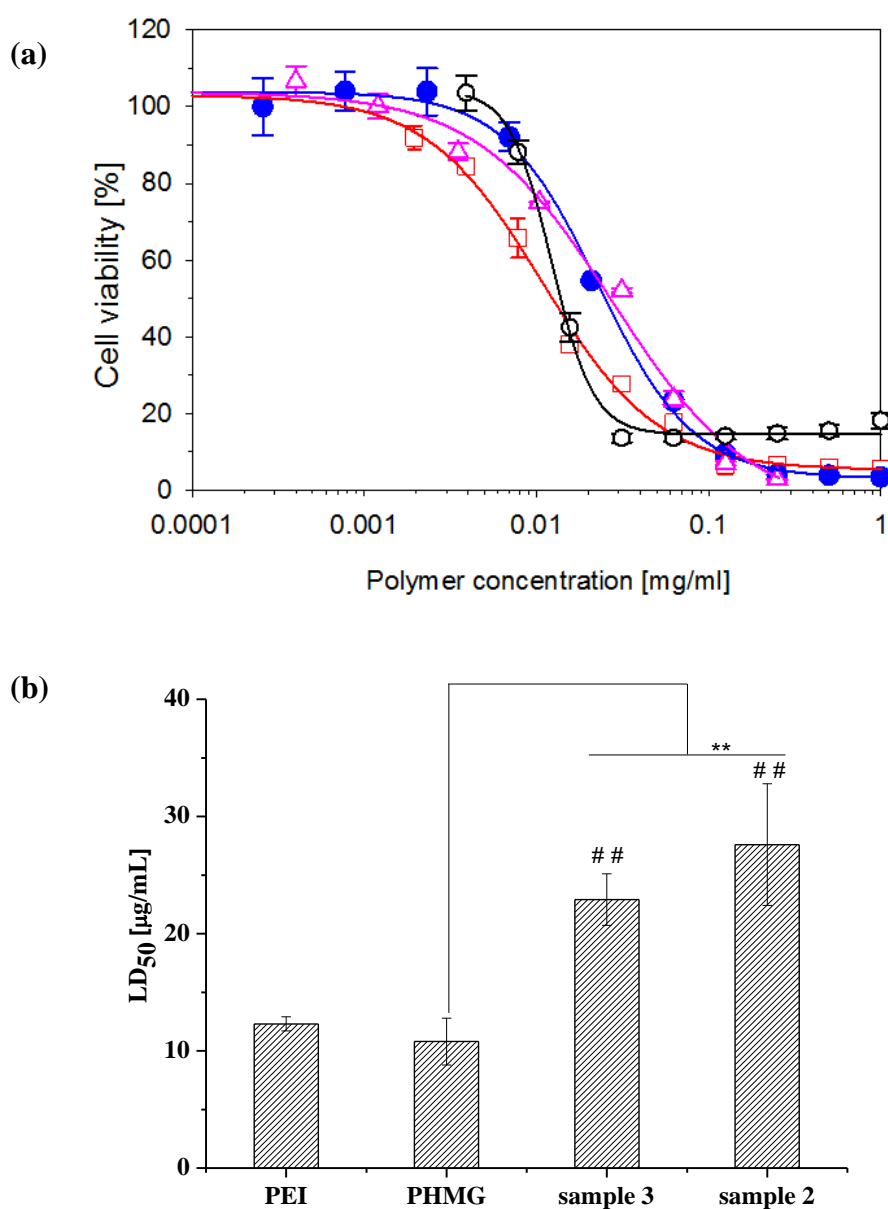


Figure 3-9. Cytotoxicity of the PHMG-based polymers in L929 cells. (a) Incubation period was 24 h and cell seeding density 1×10^4 cells/well. (O) linear PEI, (□) PHMG, (●) sample 2 and (△) sample 3. (b) LD₅₀ doses for the PHMG-based polymers and l-PEI 25 kDa, used as reference. The data represent mean \pm s.d. from three independent experiments. Polymers yielding cytotoxicity with a statistically significant difference (One-way ANOVA, $P < 0.05$) from those obtained with l-PEI and pairwise are indicated by # and *, respectively.

Publications

Conclusions

A simple method of preparing dual functional antibacterial and degradable copolymers (PHMG-*b*-PCL) is shown. The *p*-NH₂ chain-ends of antibacterial homo-polyguanidine (poly (hexamethylene guanidine) hydrochloride) acted as ring-opening polymerization initiator for caprolactone providing amphiphilic block copolymers. Various analytic techniques like 1D and 2D NMR spectroscopy, MADLI-ToF-MS were used to analyze the chemical structure of the polymers. The copolymers showed complete degradation of PCL block at 37 °C in phosphate buffer with lipase from *pseudomonas cepacia* and showed antibacterial action against both Gram-positive and Gram-negative bacteria. These oligomers could be highly interesting antibacterial additive for biodegradable polyesters. The amphiphilic nature (hydrophilic (PHMG) and hydrophobic (PCL polyester) block is expected to provide good compatibility during blending of antibacterial polyguanidines with biodegradable aliphatic polyesters which otherwise are not compatible.

Moreover, MTT data showed that the tested copolymers are significantly less toxicity than l-PEI and thus might therefore also be suitable for putative utilization in the biomedical field.

Notes and references

- [1] F. Siedenbiedel, J. C. Tiller, *Polymers*. 2012, **4**, 46.
- [2] E.R. Kenawy, *J. Appl. Polym. Sci.* 2001, **82**, 1364.
- [3] F. Hui, C. D. Chouvy, *Biomacromolecules*, 2013, **14**, 585.
- [4] Valentina Siracusa, Pietro Rocculi, Santina Romani, Marco Dalla Rosa, *Trends Food Sci. Tech.*, 2008, **19**, 634–643,.
- [5] G. E. Luckachan, C. K. S. Pillai. *J. Polym. Environ.*, 2011, **19**, 637.
- [6] S. Agarwal, *Polymer Science: A Comprehensive Reference*, 2012, **5**, 333.
- [7] G. L. Y. Woo, M. W. Mittelman, J. P. Santerre, *Biomaterials*, 2000, **21**, 1235.
- [8] Y. Suzuki, M. Tanihara, Y. Yoshihiko, K. Suzuki, Y. Kakimaru, Y. Shimizu, *J. Biomed. Mater. Res.* 1998, **42**, 112.
- [9] L. Tan, S. Maji, C. Mattheis, M. Zheng, Y. Chen, E. Caballero-Dí'az, P. R. Gil, W. J. Parak, A. Greiner, S. Agarwal, *Macromol. Biosci.* 2012, **12**, 1068.
- [10] U. Makal, L. Wood, D. E. Ohman, K. J. Wynne, *Biomaterials* 2006, **27**, 1316. ;
- [11] S. J. Grunzinger, P. Kurt, K. M. Brunson, L. Wood, D. E. Ohman, K. J. Wynne, *Polymer* 2007, **48**, 4653.
- [12] H. B. Kocer, A. Akdag, X. Ren, R. M. Broughton, S. D. Worley, T. S. Huang, *Ind. Eng. Chem. Res.* 2008, **47**, 7558.

Publications

- [13] L. Tan, S Maji, C Mattheis, Y Chen, S Agarwal, *Macromol Biosci.* 2012, **12**, 1721.
- [14] M. Mizutani, E. F. Palermo, L. M. Thoma, K. Satoh, M. Kamigaito, K. Kuroda, *Biomacromolecules* 2012, **13**, 1554.
- [15] Z. X. Zhou, D. F. Wie, Y. Guan, A. N. Zheng, J. J. Zhong, *J. Applied microbiology*, 2010, **108**, 898.
- [16] C. Mattheis, M. C. Schwarzer, G. Frenking, S. Agarwal, *Macromol Rapid Commun*, 2011, **32**, 994.
- [17] T. Tashiro, *Macromol. Mater. Eng* 2001, **286**, 63.
- [18] M. Albert, P. Feiertag, G. Hayn, R. Saf, H. Hönig, *Biomacromolecules* 2003, **4**, 1811.
- [19] P. Feiertag, M. Albert, E. M. E. Eckhofen, G. Hayn, H. Hönig, H. W. Oberwalder, R. Saf, A. Schmidt, O. Schmidt, D. Topchiev, *Macromol. Rapid Commun* 2003, **24**, 567.
- [20] Ewa Oledzka,* Kamil Sokolowski, Marcin Sobczak and Wacław Kolodziejewski *Polym Int* 2011, **60**, 787
- [21] C. Mattheis, M. Zheng, S. Agarwal, *Macromol. Bioscience* 2012, **12**, 341.
- [22] C. Mattheis, H. Wang, C. Meister, S. Agarwal* *Macromol. Biosci.*, 2012, **13**, 242.
- [23] L. Li, *MALDI Mass Spectrometry for Synthetic Polymer Analysis*, John Wiley & Sons, New, Jersey 2010.

^a *Macromolecular Chemistry II, Universitätsstraße 30, 95440, Bayreuth, Germany. Fax: 49-921-553393; Tel: 49-921-553398; E-mail: agarwal@uni-bayreuth.de.*

^b *Process Biotechnology, University of Bayreuth, 95440, Bayreuth, Germany.*

Acknowledgements: DFG is acknowledged for the financial support and Fangyao Liu for carrying out temperature dependent solubility measurements.

† Electronic Supplementary Information (ESI) available: [details of any supplementary information available should be included here]. See DOI: 10.1039/b000000x/

Supplementary Information

Oligomeric dual functional antibacterial polycaprolactone

Hui Wang,^a Christopher V. Synatschke,^a Alexander Raup,^b Valérie Jérôme,^b Ruth Freitag,^b and Seema Agarwal^{*a}

Solubility in methanol

Turbidity measurements were performed on a custom-modified Tepper turbidity photometer TP1-D at a wavelength of 670 nm, a cell path length of 10 mm and magnetic stirring. The heating program started at 60 °C and proceeded via cooling to 4 °C at a constant rate of 1.0 °C/min followed by reheating to the starting temperature with the same rate. The inflection point of the transmittance curve was considered as cloud point. It was graphically determined by the maximum of the first derivative of the heating or cooling curve, respectively.

Figure 3-S1 displays the turbidity measurement of the Sample 2 (1.0 wt%) in MeOH. The cloud point upon cooling was about 9 °C. The phase transition upon heating was broad, between 4 °C and 30 °C, which made it difficult to define cloud point. The phase transitions were complete and reversible.

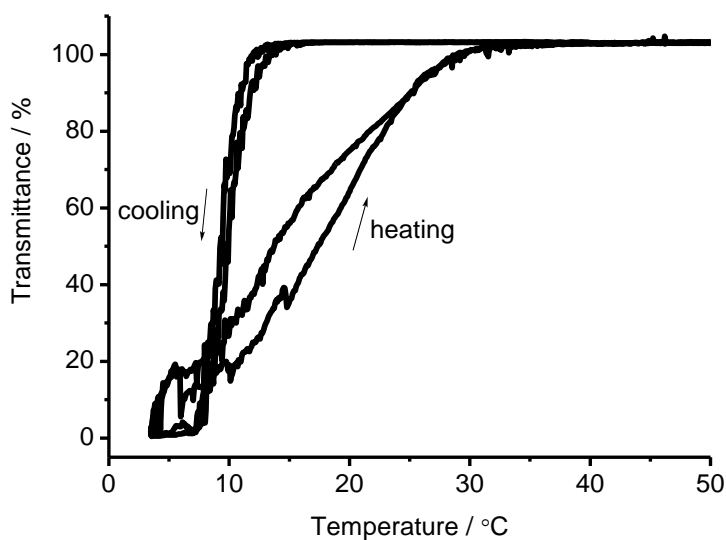


Figure 3-S1: Solubility measurements of 1.0 wt% MeOH solution of the Sample 2 with $M_w = 3400$ g/mol and PDI of 1.2. The heating rate was 1.0 °C/min.

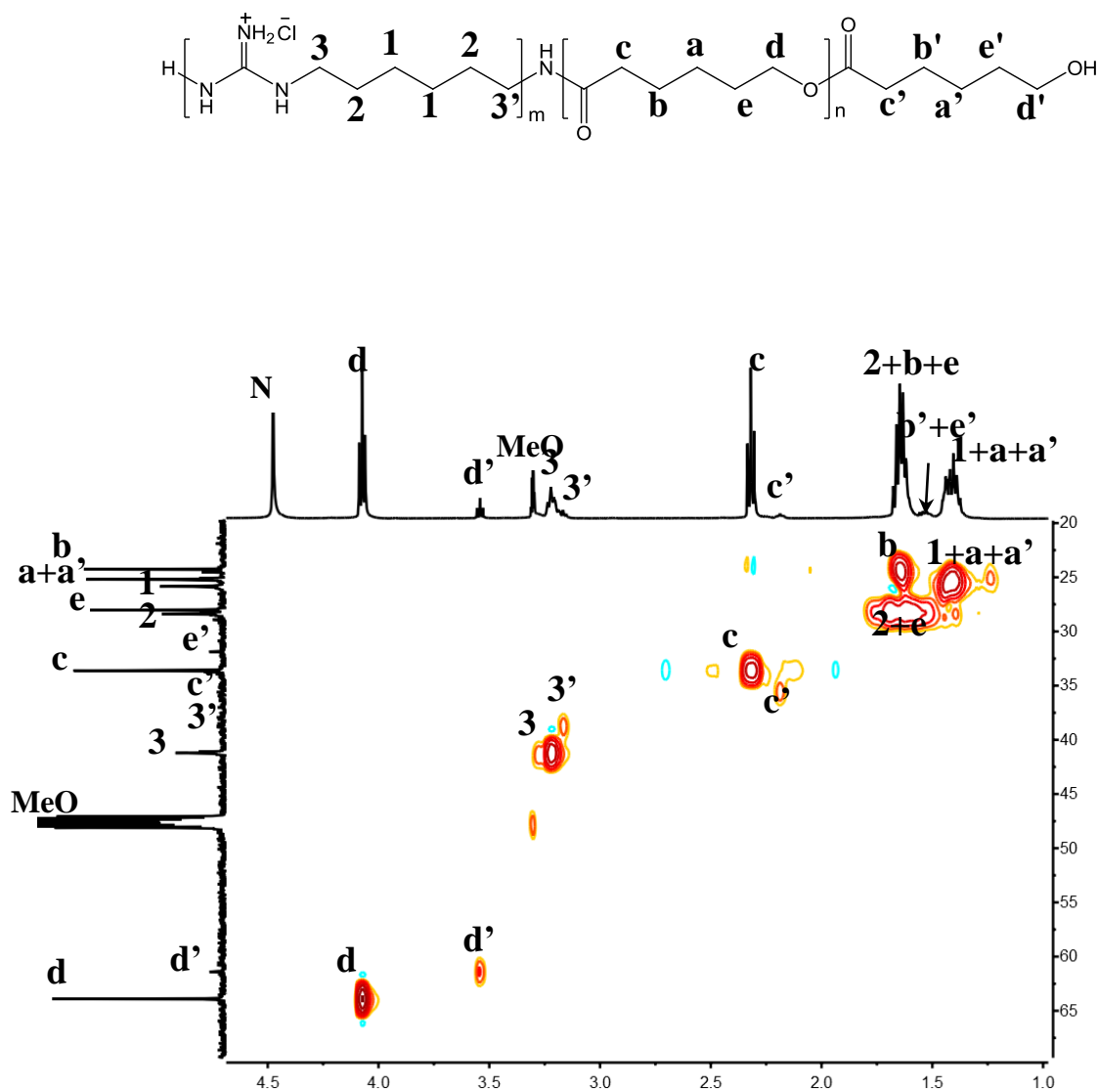


Figure 3-S2. 2D ^1H - ^{13}C correlation NMR experiment (heteronuclear single-quantum coherence HMQC, 600 or 150 MHz, MeOD, at 60 °C of sample 2).

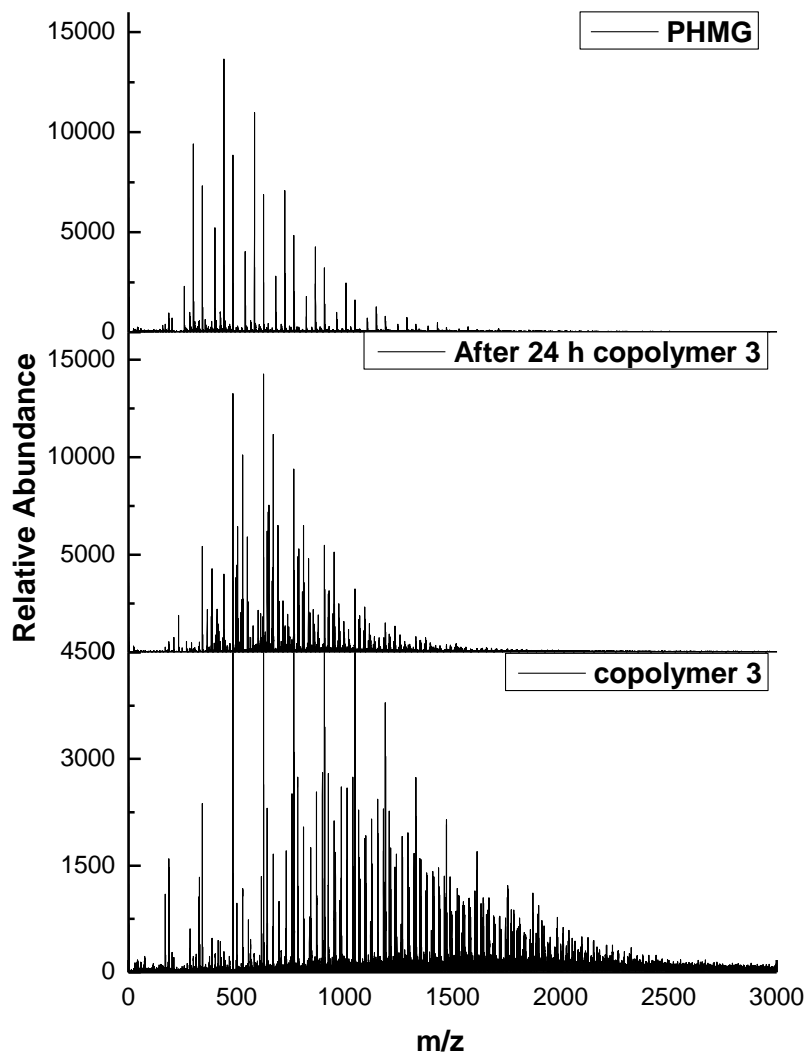


Figure 3-S3. MALDI-TOF MS of copolymer 2 and PHMG after and before enzymatic degradation.

Monitoring of antibacterial activity during enzymatic degradation process

In general, 100 mg copolymer was taken in a suspension of 2 mL phosphate buffered saline (PBS) buffer (pH = 7) with bacteria of cell density of 10^6 cfu \cdot mL⁻¹ (*Escherichia coli* or *Bacillus subtilis*). This mixture was then placed at 37 °C with shaking for different time intervals. After defined time intervals, 100 μ L specimens were drawn and spread on nutrient agar plates. Incubation for 24 h at 37 °C showed no bacterial colonies.

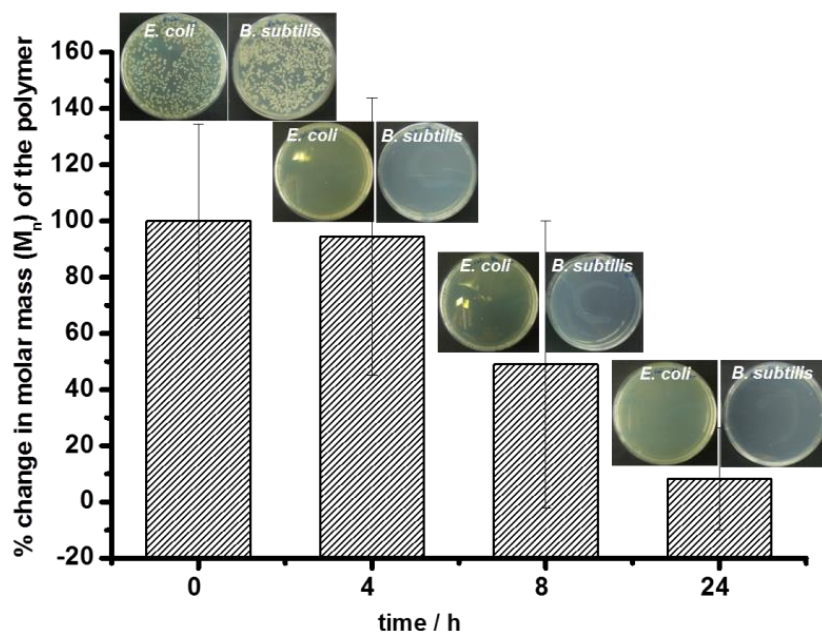
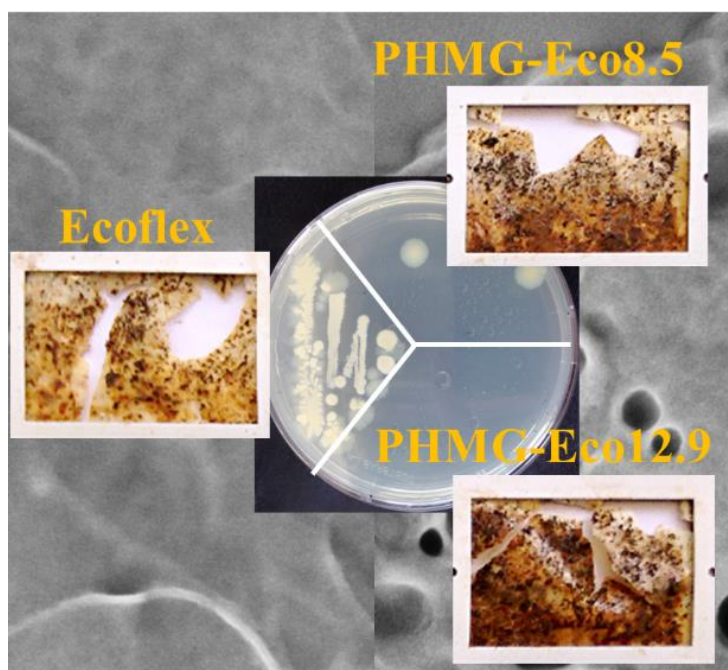


Figure 3-S4: Antibacterial testing during polymer degradation process.

4. Biodegradable aliphatic-aromatic polyester with antibacterial property

Hui Wang, Markus Langner, Seema Agarwal*



Published in *Polymer Engineering & Science*, 2016, DOI: 10.1002/pen.24347.

Publications

Biodegradable aliphatic-aromatic polyester with antibacterial property¹

Hui Wang, Markus Langner, Seema Agarwal*

H. Wang, Markus Langner, Prof. S. Agarwal
Macromolecular Chemistry II and Bayreuth Center for Colloids and Interfaces, Universität Bayreuth, Universitätsstraße 30, 95440 Bayreuth, Germany
E-mail: agarwal@uni-bayreuth.de

Abstract

Fast acting antibacterial property was introduced to aliphatic-aromatic polyester in the present work without sacrificing its compostability, thermal stability and mechanical properties. Antibacterial poly(hexamethylene guanidine) hydrochloride (PHMG) was melt mixed with Ecoflex[®] using a twin-screw extruder in different amounts. The non-reactive blending and uniform mixing was confirmed by nuclear magnetic resonance (NMR), gel permeation chromatography (GPC), scanning electron microscopy (SEM) and energy-dispersive X-Ray spectroscopy (EDX) analysis. The influence of antibacterial agent on compostability, mechanical properties and thermal stability was studied. The presence of PHMG changed slightly the degradation profile of Ecoflex[®] retaining the extent of degradation almost the same. The antibacterial PBAT showed high thermal stability (degradation starts around 330°C), stress at break 17 – 20 MPa, modulus 89 – 127 MPa and elongation at break more than 700% depending upon the amount of PHMG. The combination of antibacterial activity with biodegradability makes this material a very interesting candidate for many different applications including packaging.

Introduction

For the past few decades, intensive research has been carried out in the field of environmentally friendly biodegradable and biocompatible polymers such as polyesters, polyanhydrides, poly(ester amide)s, biodegradable polyurethanes, etc.. Among them, the highly investigated class of biodegradable materials is aliphatic and aliphatic-aromatic polyesters such as poly(caprolactone) (PCL),[1–3] poly(glycolide) (PGA)[4,5] poly(lactide) (PLA)[6,7] and poly(butylene adipate-co-terephthalate) (PBAT). These polyesters find applications in various fields, for example food packaging, [8–10] compost bags, medical sutures, nano- or microscale drug delivery vehicles and temporary scaffolds for tissue regeneration.[11–13] For many of

¹ **Supporting Information** is available online from the Wiley Online Library or from the author.

Publications

these applications, there exists a huge risk of contamination with bacteria coming from the material itself or the surrounding environment. Especially true for food and medical applications. Hence besides biodegradability, antibacterial activity of the engineered material would be add on to the properties profile. Antibacterial activity can be introduced into biodegradable materials using diverse strategies. A simple method is use of biodegradable polymers that are inherently antimicrobial e.g. chitosan. Chitosan (β -(1,4)-2-amino-2-deoxy-D-glucose) has excellent biocompatibility, biodegradability and antibacterial property,[14] therefore it has been widely employed as food packaging material.[15–18]

Furthermore, the synthetic polymers can be modified by covalently attaching antibacterial units. The immobilization of antimicrobial units on polymers by covalent linkages is possible using different methods. For example, the antibacterial polymers can be grafted on biodegradable polymers as shown for grafting of chitosan on poly(butyleneadipate-co-terephthalate) (PBAT).[19] Click chemistry or direct polycondensation can also be used for introducing antibacterial moieties such as hydantoin and quaternary ammonium groups to biodegradable polymers.[20,21] Further, antibacterial additives such as Nisin, a peptide from *Lactococcus lactis* and metal nanoparticles can also be used for imparting antibacterial activity to a biodegradable polymer as shown for PBAT and polylactide.[19,22] In most of the literature studies, antibacterial action is shown but its influence on biodegradability of the original material is not investigated. It is an interesting question that how biodegradability might be influenced by the presence of antibacterial additives. Recently, we combined biodegradable polycaprolactone (PCL) with an antibacterial polyguanidine (poly(hexamethyleneguanidine) hydrochloride, PHMG) in the form of a block copolymer.[23] The amine and guanidine end-groups of PHMG were used for ring-opening polymerization (ROP) of caprolactone for joining antibacterial PHMG block to PCL. The polymers showed antibacterial activity without losing the enzymatic degradability of PCL. Unfortunately, the designed polymers with additional antibacterial units possess low molar mass and therefore could not be used for mechanical characterization. Polyguanidines, in general are highly active antibacterial polymers against Gram-positive and Gram-negative bacteria.[24,25] One of the highly researched and used polyguanidines is PHMG made by condensation of hexamethylene diamine with guanidine hydrochloride.[26–28]

Keeping in view our broad aim of making dual functional (antibacterial-biodegradable) polymers, in the present work we studied in details melt blending of PHMG with a commercially available biodegradable polyester PBAT (commercial name Ecoflex[®]). It was

Publications

interesting to study if the reactive blending via transamination reaction using terminal amine and guanidine groups of PHMG with ester units of PBAT at high temperature in an extruder leading to covalent immobilization was possible or not. The effect of different amounts of PHMG on immobilization as reflected in leaching behavior, antibacterial activity, compostability and mechanical properties of PHMG-Ecoflex[®] system was studied.

Experimental

Materials

Hexamethylenediamine (98%) and guanidine hydrochloride (99.5%) were purchased from Sigma-Aldrich. Ecoflex[®] F A1200 was a gift from BASF, Germany. Hexafluoroisopropanol (HFIP), chloroform and pentane were distilled prior to use. PHMG was made by condensation of hexamethylenediamine and guanidinehydrochloride in the following way: [23,29] A mixture of guanidine hydrochloride (374.9 g, 3.92 mol) and hexamethylenediamine (414.6 g, 3.57 mol) was heated up to 110 °C in a dry three-necked round bottom flask equipped with a thermometer, a KPG-stirrer, and a water condenser. After 1 hour the temperature was raised to 190 °C and stirred at this temperature for 4 hours. After this a vacuum of 250 mbar was applied for 1 hour to remove volatiles by cooling in an ice bath and the polymer obtained (transparent solid) was structurally characterized by NMR. Gel permeation chromatography (GPC) was used to determine the molar mass and molar mass distribution of PHMG as described in results and discussion part.

PHMG was mixed in different amounts with Ecoflex[®] using an 11 mm (diameter) twin-screw extruder (Thermo Scientific Process 11). The barrel had a length/diameter ratio of 40/1 and eight zones with independent temperature control. The diameter of single die is 2 mm. The temperature profile during extrusion was 150/150/160/170/180/180/180/190 °C from the barrel section after the feed throat to the die. Materials were fed separately into the extruder feed throat either gravimetrically (Ecoflex[®]) or volumetrically (PHMG 67 wt% solution). Feed rate for Ecoflex[®] was 634-755 g/h and screw speed was 18 rpm (revolutions per minute). Feed rates for PHMG solution were controlled with a pump (Thermo Scientific Masterflex P/S) at 13.5, 30.4, 50.7, 84.4 g/h, corresponding to screw speeds of 0.4, 0.9, 1.5, 2.5 rpm, respectively.

Publications

Characterization

Molecular characterization

^1H and ^{13}C spectra were recorded on a Bruker DRX-500 using HFIP as a solvent. A capillary with CDCl_3 (99.8% D, stabilized with Ag, Carl Roth GmbH) was inserted in NMR tube. All chemical shifts (δ) are reported relative to tetramethylsilane (TMS) as internal reference.

IR spectra were measured with a Digilab Excalibur FTS-3000 with a Pike Miracle ATR unit (ZnSe crystal) and analysed by WinIRPro software version 3.3.

Elemental (CHN) analyses were carried out on an elemental Vario EL III instrument.

Molar masses and mass distributions of the polymers were determined by GPC in HFIP at 23 °C using an Agilent 1200 series system equipped with a PSS, PGG (7 μm) 50 mm \times 8 mm² pre column and PPS, PFG 300 Å (7 μm) 30 mm \times 0.8 mm² columns with 0.05 M potassium trifluoroacetate as eluent at a flow rate of 0.5 mL min⁻¹ and poly(methyl methacrylate) (PMMA) as standard. The spectra were analysed by software PSS WinGPC Unity, Build 1321.

Thermal Analysis was performed on a Mettler Toledo thermal analyzer comprising 821 DSC and Libra 209 TG modules. By recording thermogravimetric (TG) traces in nitrogen atmosphere with a flow rate of 60 mL \cdot min⁻¹, the thermal stability was determined; a sample size of 12 \pm 2 mg and a heating rate of 10 K \cdot min⁻¹ was used for each measurement. The temperature of thermal decay (T_d) was taken as the inflection point of the TG curve. Differential scanning calorimetry (DSC) was performed in nitrogen atmosphere (flow rate 80 mL min⁻¹) with a heating rate of 20 K min⁻¹; the inflection point of the baseline in the second heating cycle was taken as glass transition temperature (T_g).

Leaching test

The films (~70 mg each) were stirred in water (10 mL) at 37 °C for different intervals of time (24, 72 and 168 hours). After this they were dried *in vacuum* at 60 °C till constant weight. The difference of the original and observed mass was taken as the amount of leachable material.

Degradation test in compost

For the degradation test in compost the extruded polymers were first pressed at 180 °C to 0.2 mm thick plates and cut to size 35 mm \times 22.5 mm. The films were buried in compost at 60 °C with intermediate aeration. A mixture of mature compost was derived from an industrial composting plant in Buchstein, Germany. Samples were taken periodically to determine chemical (by NMR, IR, GPC analysis) and physical (optical inspection) changes.

Publications

Mechanical Testing

Mechanical properties of extrudates were carried out on an Instron 5565 (Instron, Canton, MA) with a speed of 0.3 mm/min to determine E-moduli and then under tension with a crosshead speed of 80 mm/min using 1 kN loading cell at room temperature. At least five samples were tested for each measurement. The dog bone specimens (width: 5.08 mm, thickness: 2.00 mm, length: 30 mm) were injection molded in an injection molding machine. The temperatures of barrel and mold were kept at 180 °C and 40°C respectively, and a specific injection pressure of 10 and 12 bar was applied.

EDX (Energy-dispersive X-ray spectroscopy) and SEM (Scanning electron microscope)

A scanning electron microscope (SEM, Zeiss LEO 1530, EHT= 3 kV) was used to observe the morphology of cross-section of extruded polymers. The pictures were recorded using an optical microscope (VHX 2000). A lithium drifted Silicon (SiLi) detector was used for energy dispersive X-ray analysis.

Antibacterial test

Antibacterial activity was tested by Kirby-Bauer test using *E. coli* (DSM No. 1077, K12 strain 343/113, DSMZ) as the Gram-negative and *B. subtilis* (DSM No. 2109, ATCC 11774, ICI 2/4 strain, DSMZ) as the Gram-positive test organism. For antibacterial tests the extruded polymers were first pressed at 180 °C to 0.2 mm thick plates and cut to size 1 cm². [29,30]

The time dependent antibacterial activity was determined by shaking flask method. 10 mg polymer film was incubated with 1.5 mL bacteria suspension at ambient temperature in micro-centrifuge tubes with contact times of 1 h and 3 h. After defined time intervals, 100 mL specimens were drawn and spread on nutrient agar plates. After incubation at 37 °C for 24 h, colonies were counted and the reduction was calculated relative to the initial cell density of the sample. [23,29]

Results and Discussion

PHMG (number average molar mass (M_n) = 3900, weight average molar mass (M_w) = 6000, molar mass distribution (\mathcal{D}) = 1.6) was melt mixed in different amounts to Ecoflex[®] (M_n = 56600, M_w = 117000, \mathcal{D} = 2.1 (Figure 4-S1)) in an extruder using a 69 wt% solution in water. Pure Ecoflex[®] was also extruded under similar conditions only with water for comparison purposes. The resulting extrudates had 1.7, 4.3, 8.5 and 12.9 wt% of PHMG as determined by elemental analysis. The corresponding extrudates are designated as PHMG-Eco1.7, PHMG-Eco4.3, PHMG-Eco8.5 and PHMG-Eco12.9, respectively in the following text. The Ecoflex[®]

Publications

molar mass was not affected by extrusion with water as observed by GPC, implying hydrolytic stability under extrusion conditions. The PHMG-Eco samples showed bimodal GPC curves with an additional peak at low molar masses which increased with an increase in PHMG in the samples (Figure 4-1). The presence of PHMG was also evident in the extruded samples from ^1H and ^{13}C -NMR characterization (Figures 4-S2 and 4-S3).

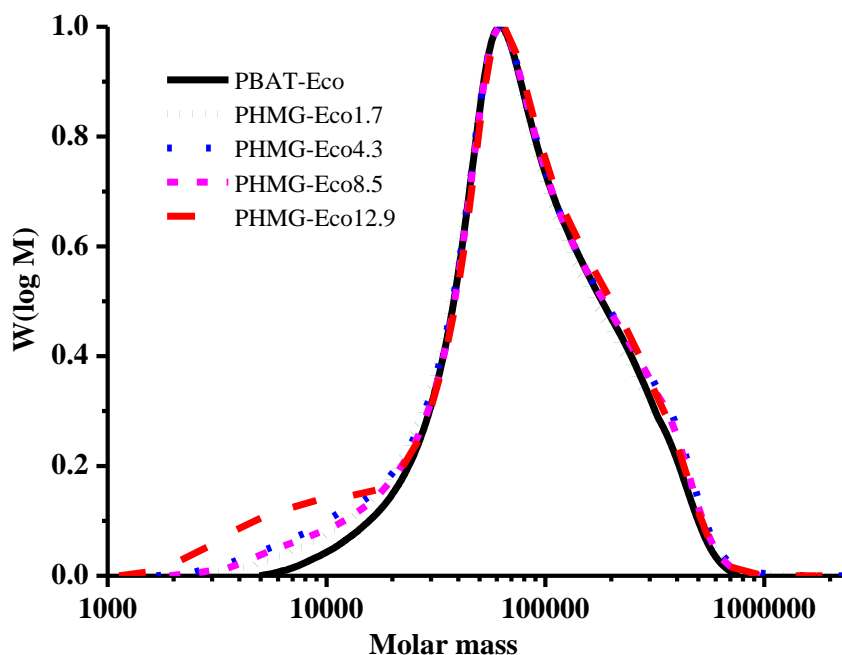


Figure 4-1. GPC curves of Ecoflex[®] and its extrudates with poly(hexamethylene guanidine) hydrochloride.

The PBAT-Eco samples were highly thermally stable. The samples with low amount of PHMG (PHMG-Eco1.7) showed one step degradation with $T_{5\%}$ (temperature at which 5% weight loss took place) more than 350°C (Figure 4-2). The sample with high amounts of PHMG (PHMG-Eco4.3, PHMG-Eco8.5, PHMG-Eco12.9) although showed two step degradation but still with high thermal stability ($T_{5\%}$ 330°C). There was no significant change in the glass transition temperature (T_g) and melting point (T_m) of Ecoflex[®] after mixing with PHMG. (Figure 4-3) The T_g and T_m were observed at -28 °C and 115 °C, respectively for all samples. PHMG is an amorphous polymer with T_g 32 °C. Although all samples were semicrystalline but the presence of PHMG interfered with the crystallization behavior of Ecoflex[®]. The crystallinity of PHMG-Eco was calculated based on the theoretical melting enthalpy of 100% crystalline Ecoflex[®] (melting enthalpy is 114 J/g for 100% crystalline Ecoflex[®]). [31,32] A decrease in melting enthalpy and crystallinity with increased amount of PHMG in extrudates was observed. (Figure 4-4)

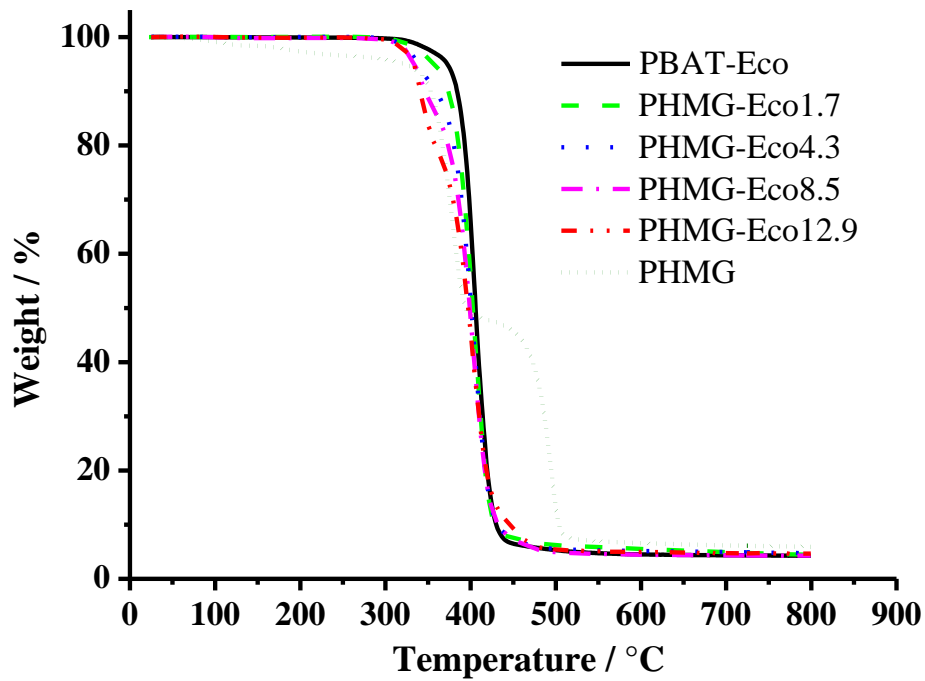


Figure 4-2. TGA traces of Ecoflex[®], PHMG-Eco and PHMG.

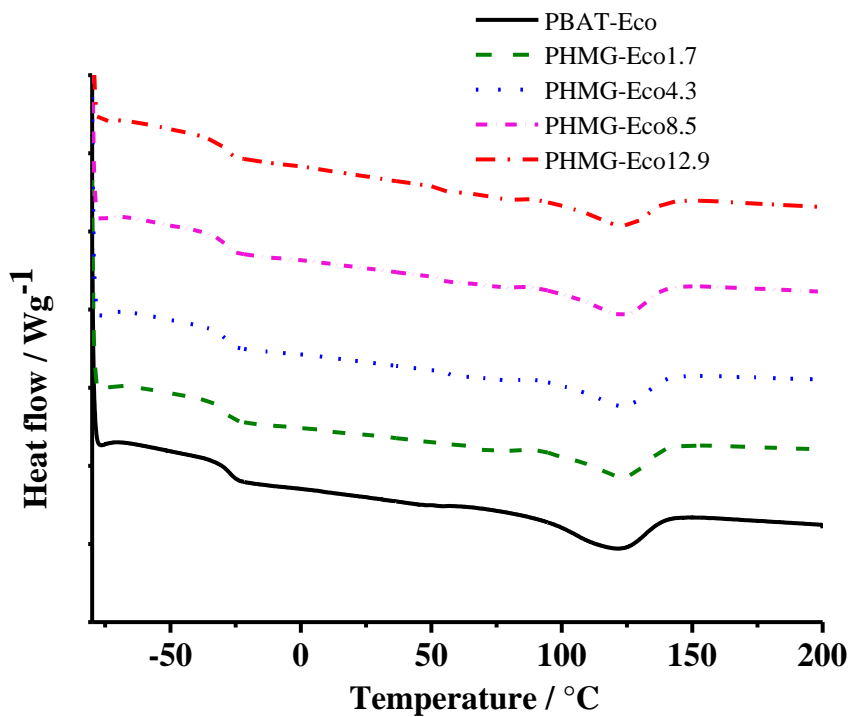


Figure 4-3. DSC traces of samples with different PHMG contents.

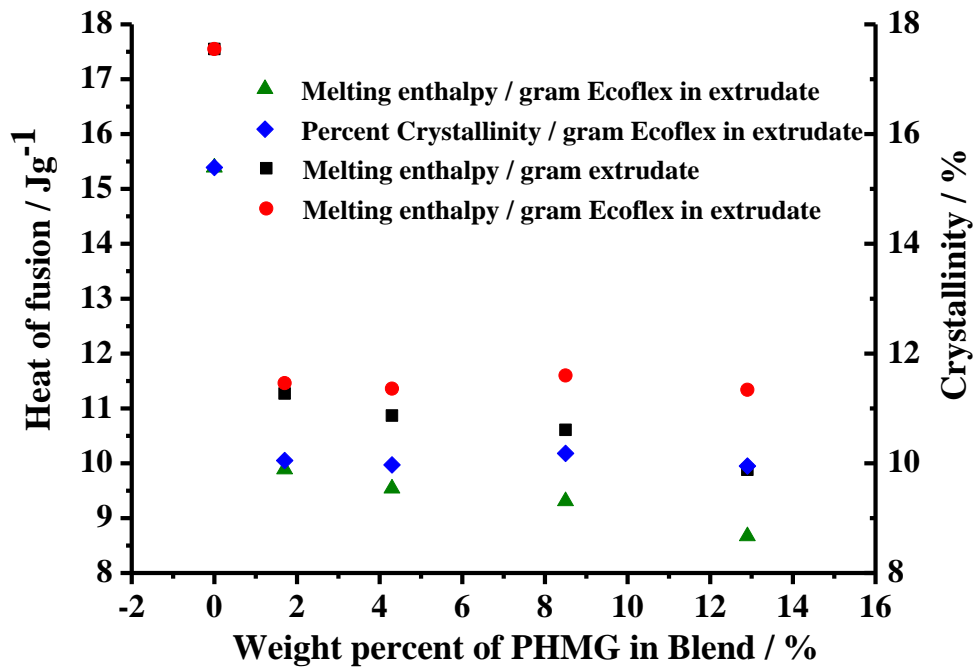


Figure 4-4. Decrease of melting enthalpy and total % crystallinity / g extrudate and / g Ecoflex[®] in samples with increased amount of amorphous PHMG.

Figure 4-5 shows SEM micrographs of the cross-section of PHMG-Eco1.7 and PHMG-Eco12.9. The samples showed phase-separated morphology all over the surface with some smooth patches which was further studied using EDX analysis.

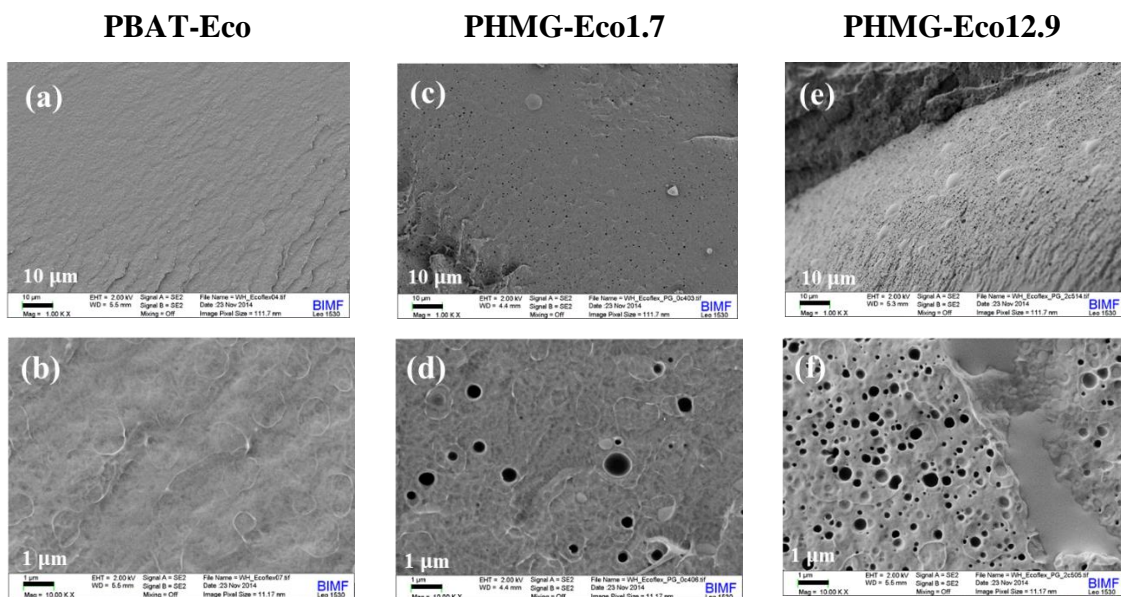


Figure 4-5. SEM micrographs of the extruded PBAT-Eco (a-b), PHMG-Eco1.7 (c-d) PHMG-Eco12.9 (e-f).

Publications

Quantitative EDX results of the compositional weight percent of carbon, nitrogen, oxygen, chlorine on six different positions including single spots and area are shown in Figure 4-6 and Table 4-S1. The most interesting element is chlorine, because the antibacterial additive PHMG contains large amounts of chloride as counter ion. The spots and areas were selected at different places as shown in figure 4-6. The weight percent of chlorine was almost constant (~9-10%) all over the sample and about 25-26% on smooth patches. This suggests presence of PHMG all over the surface with more accumulation at few places.

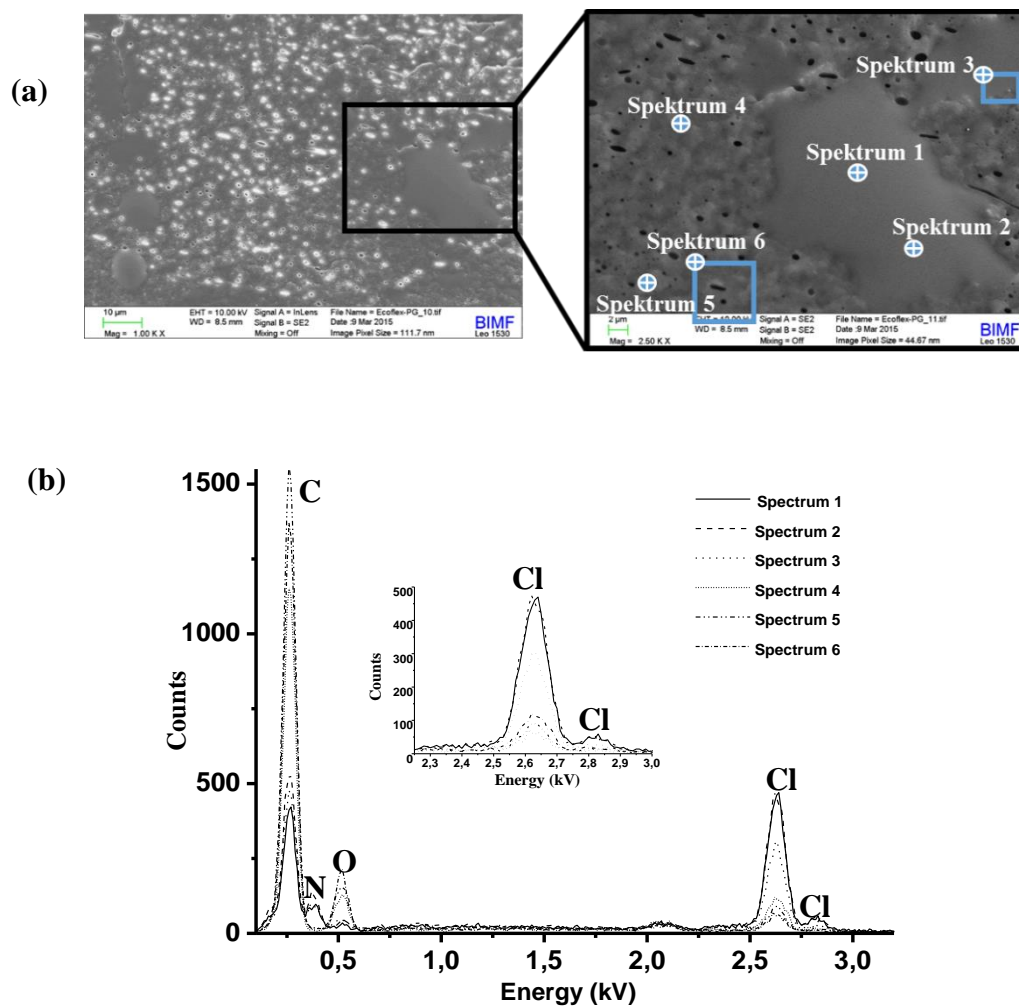


Figure 4-6. SEM photograph of PHMG-Eco12.9 (a) and results of EDX-analysis (b) for the six measuring points of two different phases of the cross-section.

The typical stress-strain curves of extruded pure Ecoflex[®] and PHMG-Eco samples are presented in figure 4-7. Ecoflex[®] showed a breaking stress of 18 MPa and 587 % elongation at break. The addition of PHMG showed increased elongation at break and E-modulus without sacrificing the breaking stress.

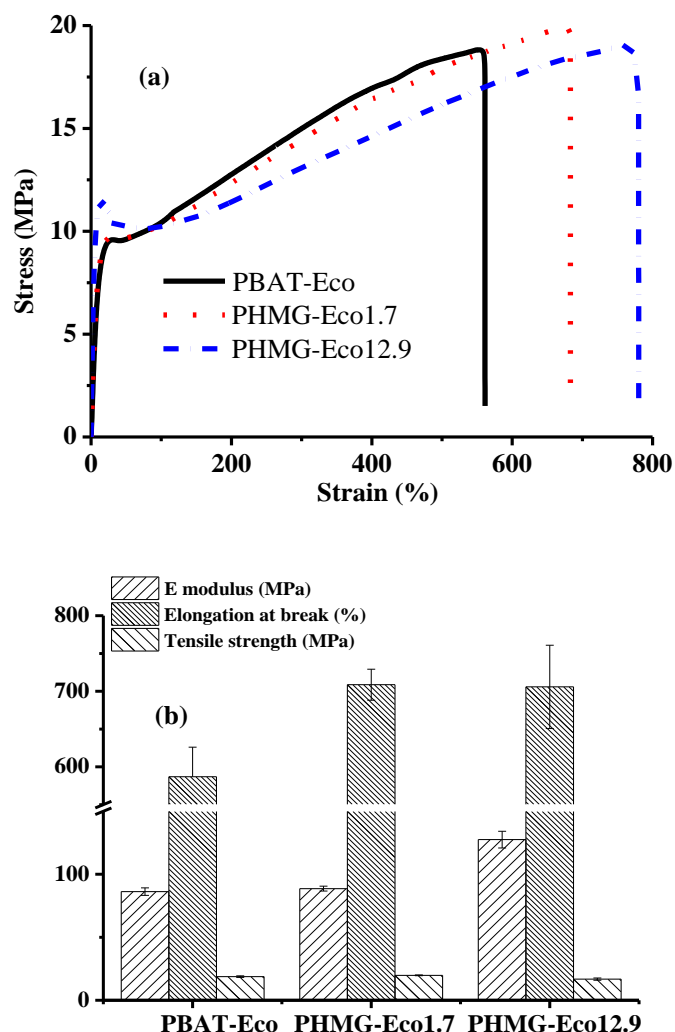


Figure 4-7. Stress-strain curves of PBAT-Eco and PHMG-Eco 1.7 and 12.9 (a) and corresponding bar chart of mechanical properties (b).

Pure PHMG exhibits high antibacterial activity as proved by low MIC (minimal inhibitory concentration) and MBC (minimal bactericidal concentration) values. The PHMG shows MIC values of $3.9 \mu\text{g mL}^{-1}$ and $0.98 \mu\text{g mL}^{-1}$, and MBC values of $3.9 \mu\text{g mL}^{-1}$ and $0.98 \mu\text{g mL}^{-1}$ for *E.coli* and *B.subtilis*, respectively. The extruded samples were tested for antibacterial activity using the Kirby-Bauer Test (Figure 4-8 (a) and (b)) and observed for zone of inhibition. Only PHMG-Eco12.9 showed an obvious small zone of inhibition indicating leaching of antibacterial material and killing both *E. coli* and *B. subtilis*. A separate set of experiment was used to quantify the leaching by stirring the samples in water at 37°C for different intervals of time. 1 and 3 wt% leaching was observed for PHMG-Eco12.9 after 1 and 7 days, respectively. The PHMG-Eco12.9 contains approximately 12.9 wt% of PHMG. The reduced leaching (only 3% leaching in 7 days) might be due to the encapsulation of polar

Publications

PHMG by hydrophobic Ecoflex[®]. There were no signs of covalent linkage of PHMG with Ecoflex[®] after melt mixing in extruder from GPC curves (Figure 4-S1) and NMR spectra (Figure 4-S2 and 4-S3).

A swab from the area under the samples (Figure 4-8 (c) and (d)) after Kirby-Bauer test was further transferred to a new agar plate using a sterile inoculation loop. After 24 hours incubation, the colony formation was visually inspected. As shown in Figure 4-8 PHMG-Eco12.9 showed no growth of bacterial colonies with *B.subtilis* and reduced *E.coli* colonies. The growth of *B.subtilis* was also inhibited using an extrudate with 8.5 wt% of PHMG.

Time dependent antibacterial activity of extruded samples was also determined by shaking flask test. Figures 4-S4 and 4-S5 show colony formation on the Agar-plate after 1 hour and 3 hours incubation in *E. coli* and *B.subtilis* (10^6 cfu mL⁻¹) suspension. For Gram-negative bacteria *E.coli* after 3 hours the colony formations for PHMG-Eco8.5 and PHMG-Eco12.9 are relatively less than blank sample PBAT-Eco showing bacterial inhibition behavior. For Gram-positive bacteria *B.subtilis* after 1 h the bacterial reduction was about 50 % using sample PHMG-Eco 8.5 and PHMG-Eco 12.9. After 3 h PHMG-Eco 8.5 showed the stable bacterial inhibition effect, without increasing of bacterial colony and PHMG-Eco 12.9 showed the antibacterial activity, meanwhile the bacteria reduction attained 77 %.

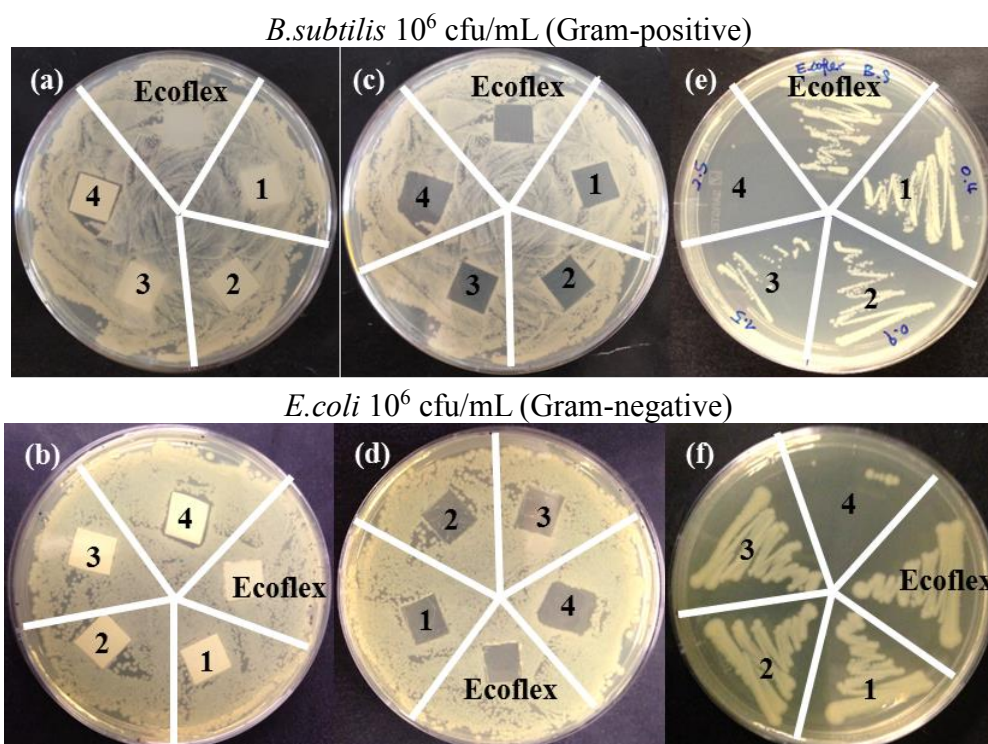


Figure 4-8. Kirby-Bauer test using *B.subtilis* and *E.coli* for sample extruded PBAT-Eco (Ecoflex[®]) and PHMG-Eco1.7 (1), PHMG-Eco4.3 (2), PHMG-Eco8.5 (3), PHMG-Eco12.9 (4). (a) and (b) after 24 hours incubation, (c) and (d) after removing the incubated samples, (e) and (f) bacterial growth on a new agar plate after transferring swab from area under the samples.

Publications

Composability of extruded samples was carried out using highly active compost from a local industrial composting plant in comparison to pure Ecoflex[®]. Qualitative analysis was performed by observation of cracks on the surface of buried films at different time intervals (Figure 4-9). Pure Ecoflex[®] which was taken as positive reference material showed some cracks after 60 days of burial and the film became very brittle. The cracks increased further with time and after about 100 days it broke in small pieces mixed with compost. The molar mass of Ecoflex[®] before and after laying in compost was followed by GPC (Figure 4-10). The peak average molar mass (M_p) decreased from 62100 to 32800, 19800, 16000 in 30, 60, 100 days, respectively (Figure 4-11). Since the GPC curve was not unimodal for Ecoflex[®] we preferred to compare M_p rather than M_n or M_w . PHMG-Eco samples were also compostable. Since antibacterial activity was shown only by PHMG-Eco8.5 and PHMG-Eco12.9, the degradation data of other extruded samples is not provided. Although, it took longer for degradation to be noticed visually in the samples with PHMG but a very significant decrease in molar mass was obvious from GPC measurements even after 30 days.

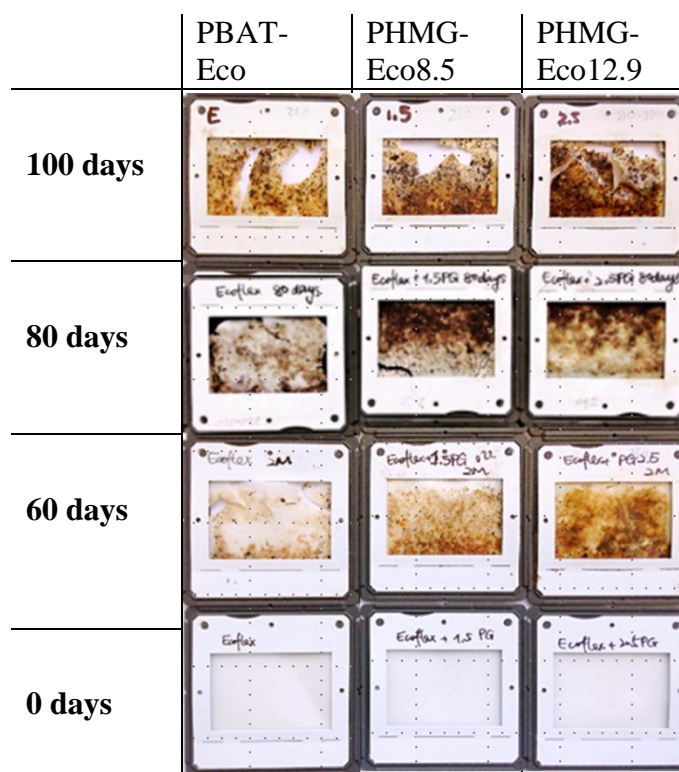


Figure 4-9. The surface of polymer films after different time by burying in compost at 60 °C.

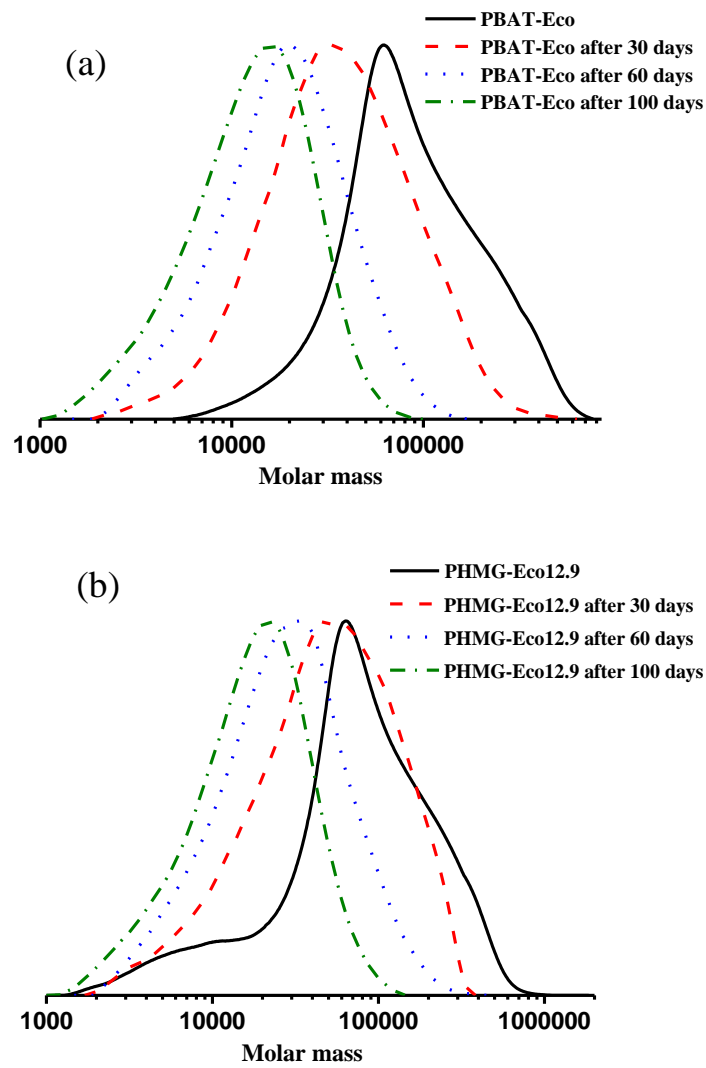


Figure 4-10. GPC profiles of films of PBAT-Eco (a) and PHMG-Eco12.9 (b) before and after 30, 60 and 100 days in compost storage.

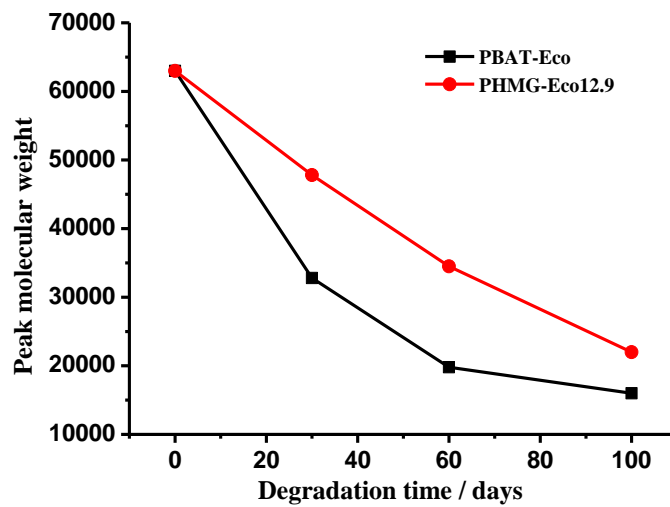


Figure 4-11. Decreased peak average molar mass (M_p) of PBAT-Eco and PHMG-Eco with time during compost test.

Publications

The extruded PHMG-Eco12.9 film showed not only strong antibacterial activity against both types of bacteria (*B.subtilis* and *E.coli*), but also exhibited the excellent permanent antibacterial effect for long periods during degradation. The samples buried in compost were tested after different intervals of time for antibacterial activity. The samples (PHMG-Eco12.9) were taken out from compost after 1 and 2 months, respectively and tested by Kirby-Bauer test for antibacterial activity. The sample was highly active against *B. subtilis* even after 2 months of burial in compost (Figure 4-12). For Gram-negative bacteria *E. coli* the sample PHMG-Eco12.9 showed inhibitory effect. Recently, the blends of Ecoflex[®] and starch-PHMG were tested for degradability in soil burial test and showed only 2.3% Ecoflex[®] weight loss within 3 months but showed antimicrobial growth inhibition against *E. coli*. during the entire three-month bury test period. [33]

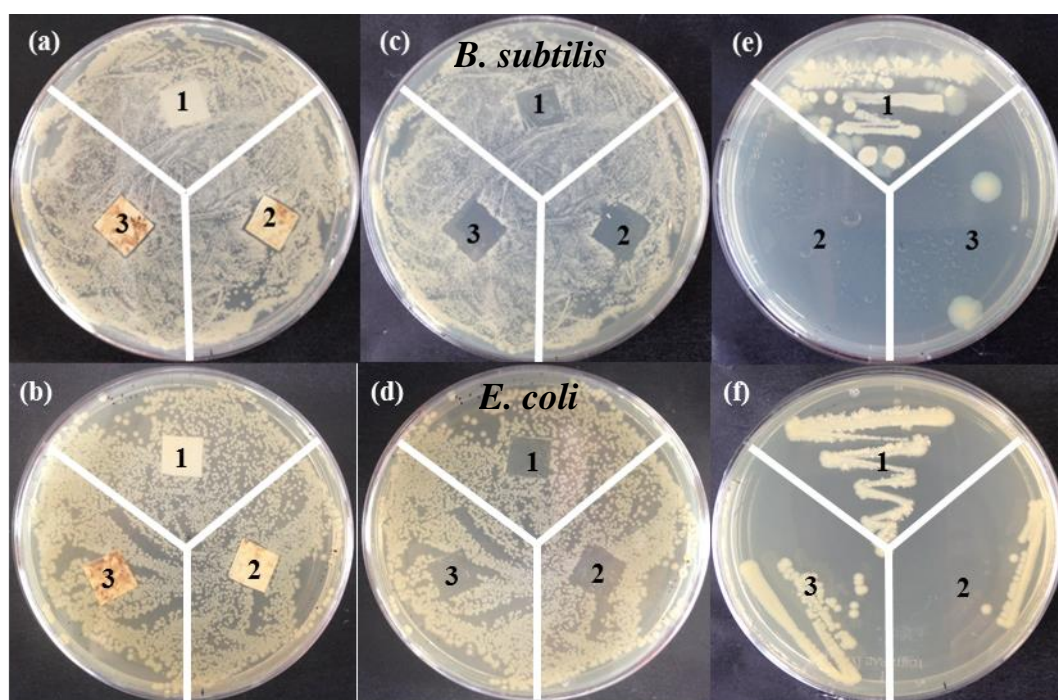


Figure 4-12. Kirby-Bauer test using *E.coli* and *B. subtilis* for sample, 1: PBAT-Eco after degradation one month, 2: PHMG-Eco12.9 after degradation one month, 3: PHMG-Eco12.9 after degradation two months, (a, b) after 24 hours incubation, (c, d) after removing the incubated samples, (e, f) bacterial growth on a new agar plate after transferring swab from area under the samples.

4. Conclusions

Semi-crystalline Ecoflex[®] was mixed with different amounts of amorphous antibacterial PHMG by non-reactive extrusion blending. The extrudates show high antibacterial activity against both Gram-positive and Gram-negative bacteria depending upon the amount of PHMG and are still compostable. Furthermore, the modulus and elongation at break of the blends are improved as the crystallinity is decreased with higher amounts of additive without sacrificing

Publications

thermal stability. The blends possess a significantly higher elongation-to-break and also show higher ratio of stress to strain than pure Ecoflex[®]. The combination of antibacterial activity with biodegradability make this material a very interesting candidate for many different applications including packaging.

Acknowledgements: Authors would like to thank DFG (German Science Foundation) for financial support.

Keywords: Antibacterial material, Biodegradation, Ecoflex[®], compostability

- [1] K. J. Wu, C. S. Wu, J. S. Chang, *Process Biochem.* **2007**, *42*, 669.
- [2] C. H. Tsou, H. T. Lee, H. A. Tsai, H. J. Cheng, M. C. Suen, *Polym. Degrad. Stab.* **2013**, *98*, 643.
- [3] Z. Gan, Q. Liang, J. Zhang, X. Jing, *Polym. Degrad. Stab.* **1997**, *56*, 209.
- [4] G. Sivalingam, G. Madras, *Polym. Degrad. Stab.* **2004**, *84*, 393.
- [5] X.-H. Zong, Z.-G. Wang, B. S. Hsiao, B. Chu, J. J. Zhou, D. D. Jamiolkowski, E. Muse, E. Dormier, *Macromolecules* **1999**, *32*, 8107.
- [6] R. Premraj, M. Doble, *Indian J. Biotechnoogy* **2005**, *4*, 186.
- [7] M. Shima, *Curr. Opin. Biotechnol.* **2001**, *12*, 242.
- [8] M. Yamamoto, U. Witt, G. Skupin, D. Beimborn, R.-J. Müller, in *Biopolym. Online* (Eds.: Y. Doi, A. Steinbüchel), Wiley-VCH Verlag GmbH & Co. KGaA, Weinheim, Germany, **2005**, pp. 299–305.
- [9] E. Marten, R.-J. Müller, W.-D. Deckwer, *Polym. Degrad. Stab.* **2005**, *88*, 371.
- [10] R. Herrera, L. Franco, A. Rodríguez-Galán, J. Puiggali, *J. Polym. Sci. Part A Polym. Chem.* **2002**, *40*, 4141.
- [11] L. S. Nair, C. T. Laurencin, *Prog. Polym. Sci.* **2007**, *32*, 762.
- [12] A. Lendlein, *Chemie unserer Zeit* **1999**, *33*, 279.
- [13] M. Vert, *J. Mater. Sci. Mater. Med.* **2009**, *20*, 437.
- [14] H. N. Lim, N. M. Huang, C. H. Loo, *J. Non. Cryst. Solids* **2012**, *358*, 525.
- [15] A. El Ghaouth, J. Arul, R. Ponnampalam, M. Boulet, *J. Food Sci.* **1991**, *56*, 6.
- [16] S. Roller, N. Covill, *Int. J. Food Microbiol.* **1999**, *47*, 67.
- [17] J.-W. Lee, H.-H. Lee, J.-W. Rhim, *Korean J. Food Sci. Technol.* **2000**, *32*, 828.
- [18] J. Rhoades, S. Roller, *Appl. Environ. Microbiol.* **2000**, *66*, 80.

Publications

- [19] W. C. Jao, C. H. Lin, J. Y. Hsieh, Y. H. Yeh, C. Y. Liu, M. C. Yang, *Polym. Adv. Technol.* **2010**, *21*, 543.
- [20] L. Tan, S. Maji, C. Mattheis, Y. Chen, S. Agarwal, *Macromol. Biosci.* **2012**, *12*, 1721.
- [21] M. Mizutani, E. F. Palermo, L. M. Thoma, K. Satoh, M. Kamigaito, K. Kuroda, *Biomacromolecules* **2012**, *13*, 1554.
- [22] L. Bastarrachea, S. Dhawan, S. S. Sablani, J. H. Mah, D. H. Kang, J. Zhang, J. Tang, *J. Food Sci.* **2010**, *75*, DOI 10.1111/j.1750-3841.2010.01591.x.
- [23] H. Wang, C. V. Synatschke, A. Raup, V. Jérôme, R. Freitag, S. Agarwal, *Polym. Chem.* **2014**, *5*, 2453.
- [24] D. Wei, Y. Guan, Q. Ma, X. Zhang, Z. Teng, H. Jiang, A. Zheng, *e-Polymers* **2012**, *12*, 1.
- [25] Y. Zhang, J. Jiang, Y. Chen, *Polymer* **1999**, *40*, 6189.
- [26] Y. Iwakura, K. Noguchi, *J. Polym. Sci. Part A-1 Polym. Chem.* **1969**, *7*, 801.
- [27] Kuno Wagner, K. Findeisen, W. Schafer, W. Dietrich, *Angew. Chem. Int. Ed. Engl.* **1981**, *20*, 819.
- [28] E. K. Bolton, D. D. Coffman, W. Gilman, L. Golman, *US 2325586*, **1943**, U.S. Patent, 2 325 586.
- [29] W. Li, H. Wang, Y. Ding, E. C. Scheithauer, O.-M. Goudouri, A. Grünewald, R. Detsch, S. Agarwal, A. R. Boccaccini, *J. Mater. Chem. B* **2015**, *3*, 3367.
- [30] C. Mattheis, H. Wang, M. C. Schwarzer, G. Frenking, S. Agarwal, *Polym. Chem.* **2012**, 707.
- [31] D. S. Rosa, D. Grillo, M. a G. Bardi, M. R. Calil, C. G. F. Guedes, E. C. Ramires, E. Frollini, *Polym. Test.* **2009**, *28*, 836.
- [32] L. Avérous, F. Le Digabel, *Carbohydr. Polym.* **2006**, *66*, 480.
- [33] H. Wang, D. Wei, A. Zheng, H. Xiao, *Polym. Degrad. Stab.* **2015**, *116*, 14.

Supporting Information

Biodegradable aliphatic-aromatic polyester with antibacterial property

Hui Wang, Markus Langner, Seema Agarwal*

H. Wang, Markus Langner, Prof. S. Agarwal
Macromolecular Chemistry II and Bayreuth Center for Colloids and Interfaces, Universität
Bayreuth, Universitätsstraße 30, 95440 Bayreuth, Germany
E-mail: agarwal@uni-bayreuth.de

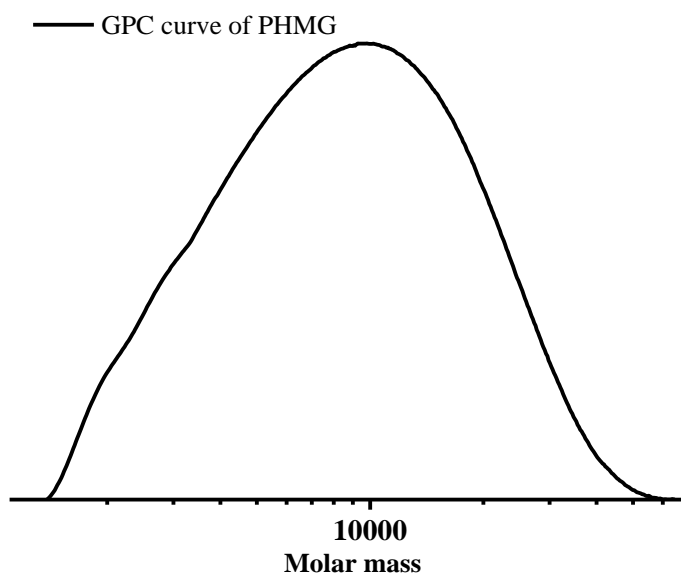


Figure 4-S1. GPC curve of PHMG.

Publications

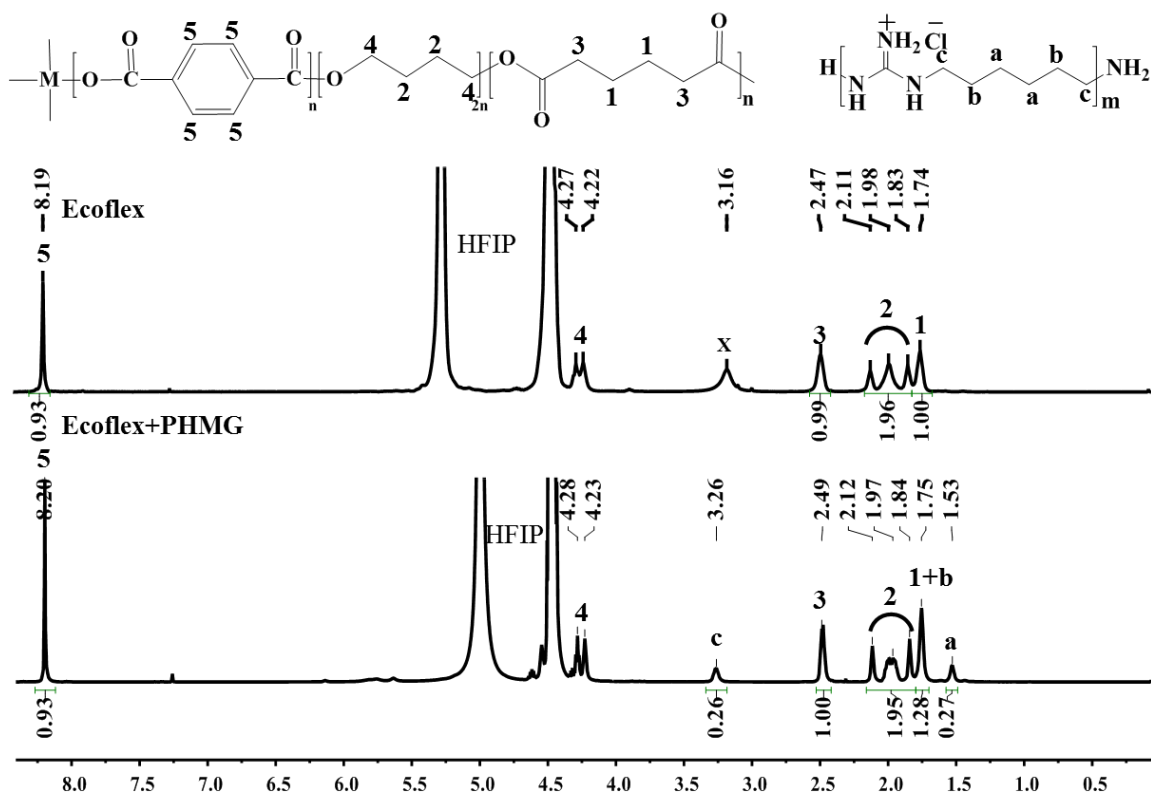


Figure 4-S2. ¹H NMR spectra of Ecoflex[®] and PHMG-Eco12.9.

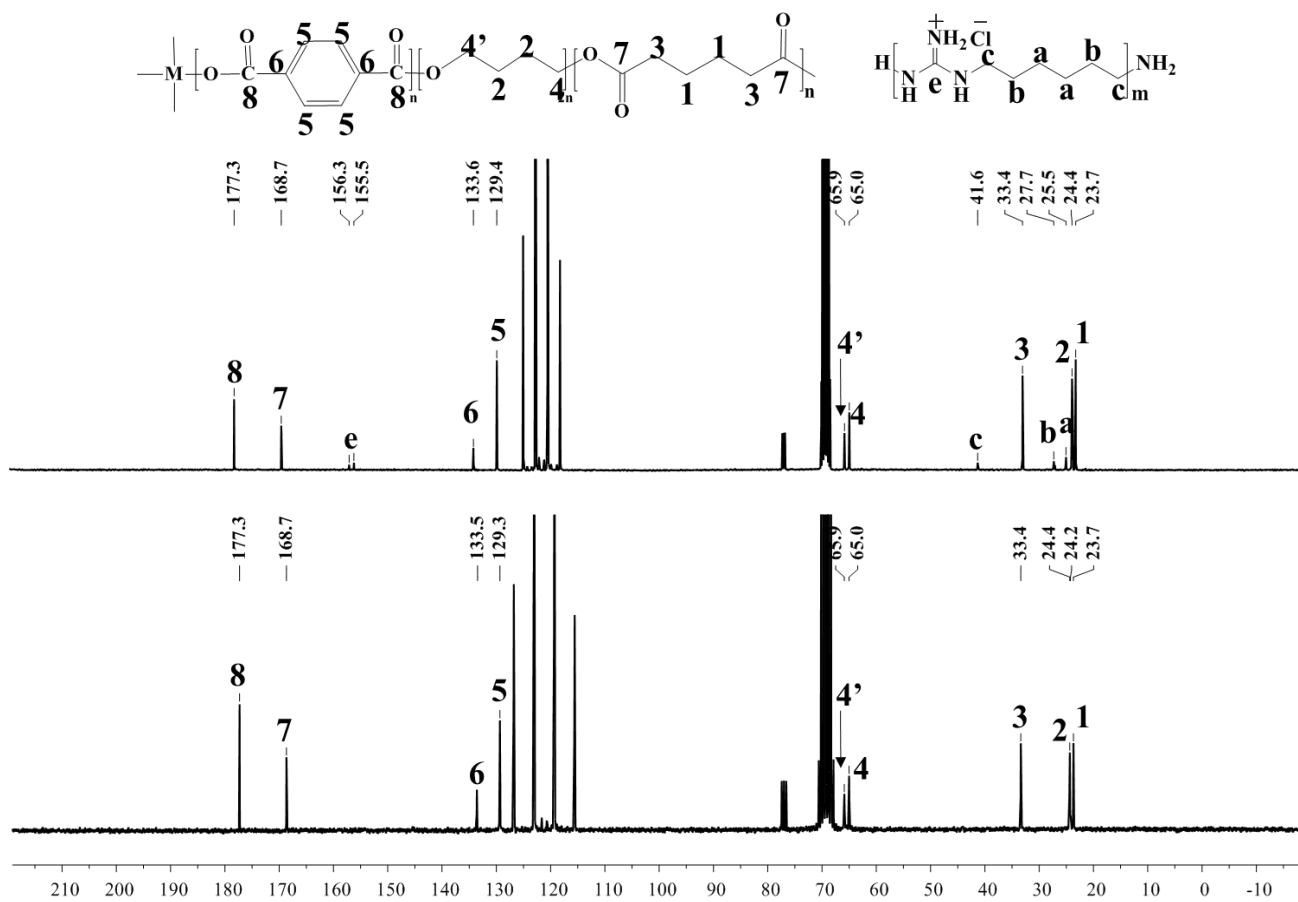


Figure 4-S3. ¹³C NMR spectra of Ecoflex[®] and PHMG-Eco12.9.

Publications

Table 4-S1. Elemental composition of PHMG-Eco12.9 in weight percent of carbon and chlorine of six spectra determined by EDX-analysis.

	C / wt%	Cl / wt%
spectrum 1	50	26
spectrum 2	49	23
spectrum 3	51	20
spectrum 4	80	10
spectrum 5	80	10
spectrum 6	79	9

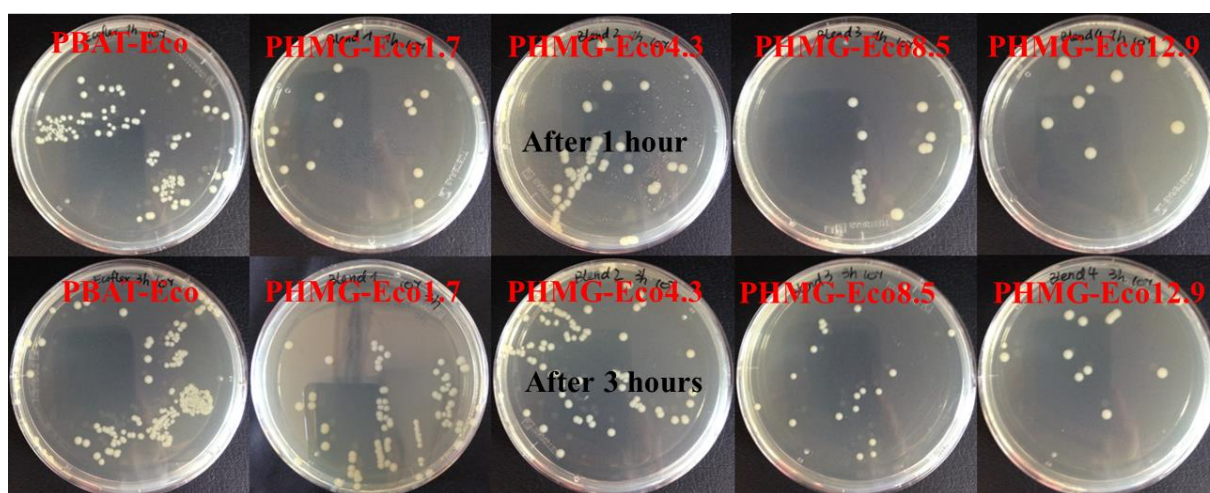


Figure 4-S4. Reduction of bacteria in a suspension of *E.coli* with an initial cell density of 10^6 cfu mL⁻¹ upon contact after 1 and 3 hours.

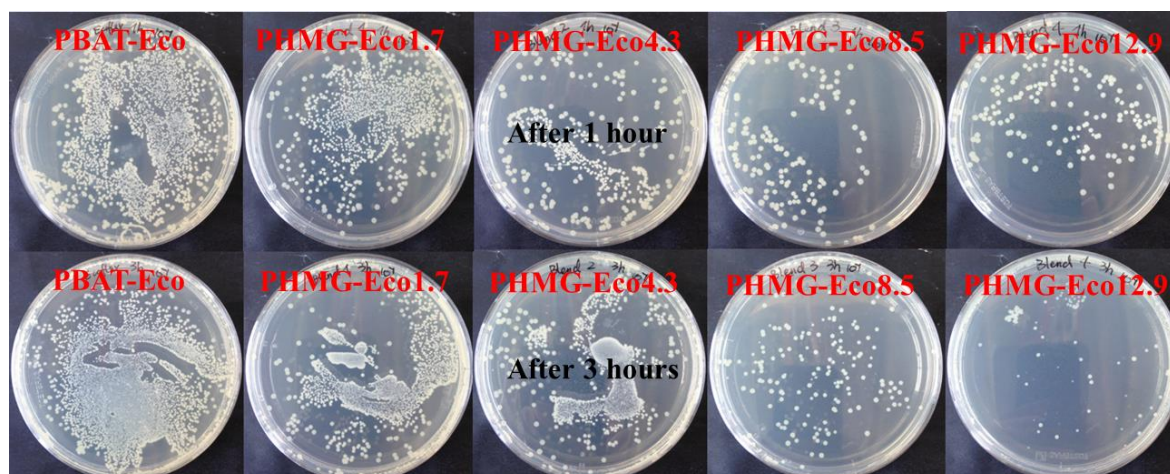


Figure 4-S5. Reduction of bacteria in a suspension of *B.Subtilis* with an initial cell density of 10^6 cfu mL⁻¹ upon contact after 1 and 3 hours.

Publications

For mechanical properties at least five samples were tested for each measurement.

PBAT-Eco:

	E modulus (Mpa)	Tensile strength (Mpa)	Elongation at break (%)
1	81	18	551
2	86	19	619
3	89	19	634
4	88	18	580
5	87	19	549
mean value	86	19	587
Standard deviation	2.99	0.64	39.03

PHMG-Eco1.7

	E modulus (Mpa)	Tensile strength (Mpa)	Elongation at break (%)
1	85	20	733
2	89	20	697
3	89	19	683
4	91	20	726
5	89	20	705
mean value	89	20	709
Standard deviation	1.95	0.33	20.53

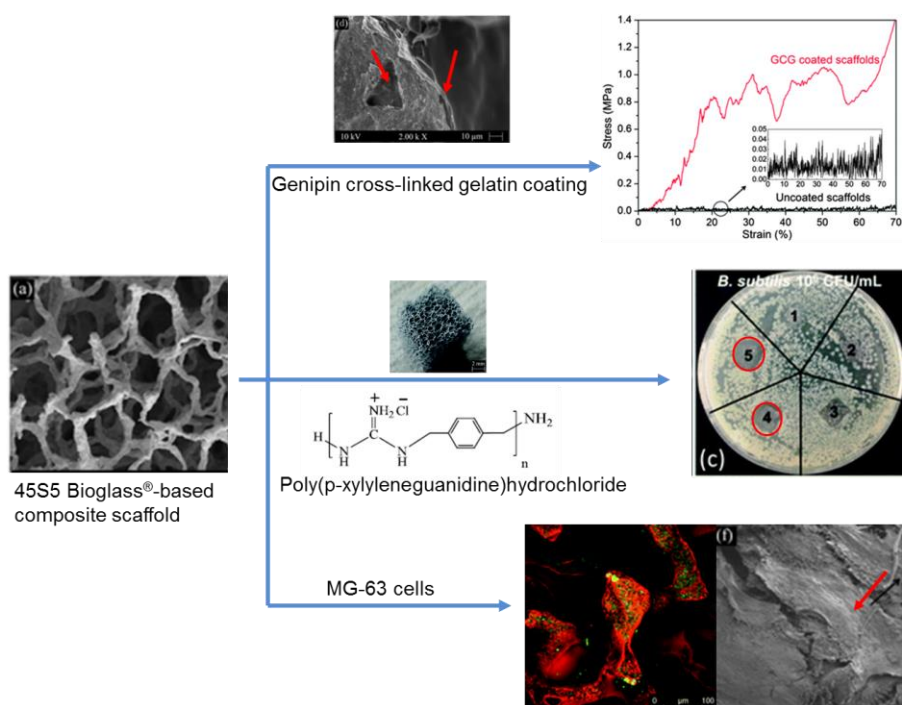
Publications

PHMG-Eco12.9

	E modulus (Mpa)	Tensile strength (Mpa)	Elongation at break (%)
1	136	150	645
2	125	18	734
3	133	16	780
4	124	17	710
5	120	17	659
mean value	128	17	706
Standard deviation	6.62	0.89	55.10

5. Antibacterial 45S5 Bioglass[®]-based scaffolds reinforced with genipin cross-linked gelatin for bone tissue engineering

Wei Li, Hui Wang, Yaping Ding, Ellen C. Scheithauer, Ourania-Menti Goudouri, Alina Grünewald, Rainer Detsch, Seema Agarwal and Aldo R. Boccaccini*



Published in *J. Mater. Chem. B*, **2015**, 3, 3367-3378. Reproduced by permission of The Royal Society of Chemistry

Publications

Antibacterial 45S5 Bioglass[®]-based scaffolds reinforced with genipin cross-linked gelatin for bone tissue engineering

Wei Li^{a,1}, Hui Wang^{b,1}, Yaping Ding^c, Ellen C. Scheithauer^a, Ourania-Menti Goudouri^a, Alina Grünewald^a, Rainer Detsch^a, Seema Agarwal^b, Aldo R. Boccaccini^{a,*}

^a Institute of Biomaterials, Department of Materials Science and Engineering, University of Erlangen-Nuremberg, Cauerstrasse 6, 91058 Erlangen, Germany

^b University of Bayreuth, Macromolecular Chemistry II and Bayreuth Center for Colloids and Interfaces, Universitaetsstrasse 30, 95440 Bayreuth, Germany

^c Institute of Polymer Materials, Department of Materials Science and Engineering, University of Erlangen-Nuremberg, Martensstrasse 7, 91058 Erlangen, Germany

* Corresponding author at: Institute of Biomaterials, Department of Materials Science and Engineering, University of Erlangen-Nuremberg, Cauerstrasse 6, 91058 Erlangen, Germany. Tel.: +49 9131 85 28601; fax: +49 9131 85 28602. E-mail address: aldo.boccaccini@ww.uni-erlangen.de (A.R. Boccaccini).

¹ These two authors contributed equally to the experimental part.

† Electronic supplementary information (ESI) available.

Publications

Abstract

45S5 Bioglass® (BG) scaffolds with high porosity (>90%) were coated with genipin cross-linked gelatin (GCG) and further incorporated with poly(*p*-xylyleneguanidine) hydrochloride (PPXG). The obtained GCG coated scaffolds maintained the high porosity and well interconnected pore structure. A 26-fold higher compressive strength was provided to 45S5 BG scaffolds by GCG coating, which slightly retarded but did not inhibit the *in vitro* bioactivity of 45S5 BG scaffolds in SBF. Moreover, the scaffolds were made antibacterial against both Gram-positive and Gram-negative bacteria by using polyguanidine, i.e. PPXG in this study. Osteoblast-like cells (MG-63) were seeded onto PPXG and GCG coated scaffolds. PPXG was biocompatible to MG-63 cells at a low concentration (10 µg/mL). MG-63 cells were shown to attach and spread on both uncoated and GCG coated scaffolds, and the mitochondrial activity measurement indicated that GCG coating had no negative influence on the cell proliferation behavior of MG-63 cells. The developed novel antibacterial bioactive 45S5 BG-based composite scaffolds with improved mechanical properties are promising candidates for bone tissue engineering.

Keywords: 45S5 Bioglass®, scaffold, antibacterial, polyguanidine hydrochloride, bone tissue engineering

Introduction

Tissue and organ failure is a major health problem. Among them, bone is one of the most common tissues necessitating replacement or repair as bone failure can widely result from trauma, tumor, bone related diseases or aging.¹ Using scaffolds made from engineered biomaterials is an effective approach to restore function of damaged bone or to regenerate bone tissues.² An ideal scaffold should act as a temporary template to support cell activity and to induce extracellular matrix deposition until new bone forms in the defect sites.^{3,4} The essential properties that an ideal scaffold should possess for bone tissue engineering applications have been comprehensively discussed in detail in the literature,^{2,5-7} and include suitable mechanical properties, bioactivity and 3D pore architecture.

45S5 BG-based scaffolds fabricated by the foam replication method meet several important properties of an ideal bone tissue engineering scaffold, due to the intrinsic bioactivity, biocompatibility, osteogenic and angiogenic effects of 45S5 BG, and the high porosity and interconnected large pore structure derived from the foam replication method.⁸⁻¹² The high porosity and large pore size of such scaffolds are favorable for osteogenesis and vascularization throughout the entire 3D structure.^{12,13} However, the high porosity also limits the mechanical properties of the scaffolds.¹¹ Besides the concern of mechanical properties, antibacterial action should also be taken into consideration since the risk of infection exists during scaffold

Publications

implantation which may eventually lead to implantation failure. To this end, in previous efforts 45S5 BG scaffolds have been coated with polymers (e.g. poly(3-hydroxybutyrate-co-3-hydroxyvalerate) (PHBV)¹⁴ or polycaprolactone (PCL)/chitosan¹⁵), and these polymers were shown to not only enhance the mechanical properties of the scaffolds without significantly sacrificing the porosity and pore size but also impart an antibiotic release function to the scaffolds. It is worth noting that the compressive strength of these coated scaffolds (0.1–0.2 MPa) although improved, still falls close to the lower bound of the values for cancellous bone.¹⁶ Therefore, the relatively low mechanical properties still limit the potential application of these coated scaffolds.

The present research aims at developing 45S5 BG-based scaffolds with a novel coating based on gelatin for increased mechanical properties (compressive strength and work of fracture) and antibacterial effect. Gelatin, a water soluble natural polymer, has been shown to be able to considerably improve the mechanical properties of bioactive glass/ceramic scaffolds due to its strengthening and toughening effects which can be linked to a micron-scale crack-bridging mechanism.^{17, 18} However, gelatin, in its original state, dissolves/degrades rapidly in aqueous solution,^{19, 20} which may lead to the quick loss of its reinforcing effects on scaffolds. In order to decrease the dissolution/degradation rate, gelatin has been chemically cross-linked with crosslinking reagents, such as glutaraldehyde or genipin.¹⁹⁻²¹ Genipin was reported to be much less cytotoxic than glutaraldehyde.²² Therefore, in the present study, genipin is selected as the crosslinking agent for gelatin which will be used for coating the 45S5 BG scaffolds prepared by the foam replication method.

As mentioned above, an antibiotic release function can be incorporated into the scaffolds in order to reduce and combat bacterial infection, which is one of the major complications associated with implants.^{23, 24} However, the emergence of resistance of bacteria to antibiotics becomes a common phenomenon, because inappropriate antibacterial treatment and overuse of antibiotics accelerate the evolution of resistant strains.²⁵ Therefore, there is a particular interest in the development of new biocides in order to fight infections. Biocidal cationic polymers, such as polyguanidines, have attracted considerable attention for their high antibacterial activity and low toxicity to humans, and they have been widely investigated or used as disinfectants or biocides in ophthalmology, water systems, topical wounds and environments.²⁶⁻²⁹ The antibacterial action of the polyguanidines starts with the interaction of positively charged polymer molecules with the bacteria which carry a net negative charge on their surface due to negatively charged lipids in the cell membrane, and followed by the hole-formation i.e.,

Publications

perturbations of the polar headgroups and hydrophobic core region of the lipids membranes killing the bacteria.^{30, 31}

Based on the facts discussed above, in order to incorporate an effective antibacterial function to the gelatin coated 45S5 BG-based scaffolds, poly(*p*-xylyleneguanidine) hydrochloride (PPXG), which belongs to the polyguanidines, was used as the antibacterial agent. To the best of our knowledge, polyguanidine has not been used as antibacterial agent in bone tissue engineering scaffolds, this work was thus dedicated to fabricate and characterize 45S5 BG scaffolds which were coated with genipin cross-linked gelatin (GCG) and then incorporated with PPXG. This study is focused on the investigation of the antibacterial effect and biocompatibility that PPXG can confer to the 45S5 BG scaffolds. In addition, the influence of GCG coating on the mechanical properties and bioactivity of the 45S5 BG scaffolds was also studied.

Materials and methods

Preparation of 45S5 BG scaffolds

Commercially available melt-derived 45S5 BG powder (mean particle size ~5 μm) and polyurethane (PU) foams (45 pores per inch, Eurofoam, Troisdorf, Germany) were used for preparing the scaffolds by foam replication method.^{11, 32} In brief, the slurry was prepared by dissolving 6% w/v polyvinyl alcohol (PVA) ($M_w \sim 30,000$, Merck, Darmstadt, Germany) in water, and followed by adding 45S5 BG powder to the PVA solution up to a concentration of 50 wt%. PU foams were immersed and rotated in the slurry, and then taken out from the slurry. The extra slurry was completely squeezed out from the foams. The foams were left to dry at room temperature followed by repeating the procedure described above one more time. The obtained green bodies were heated at 400 $^{\circ}\text{C}$ for 1 h to decompose the PU foams, and then at 1100 $^{\circ}\text{C}$ for 2 h to densify the glass network. The heating and cooling rates used were 2 $^{\circ}\text{C}/\text{min}$ and 5 $^{\circ}\text{C}/\text{min}$, respectively.

Synthesis and antibacterial activity of PPXG

PPXG was synthesized by condensation polymerization of *p*-xylylenediamine and guanidine hydrochloride in melt according to the literature.^{29, 33} A dry 100 mL three necked round bottom flask equipped with a thermometer and a reflux condenser was charged with guanidine hydrochloride (6.18 g, 50.00 mmol) and *p*-xylylenediamine (4.78 g, 50.00 mmol). The reagents were heated up to 150 $^{\circ}\text{C}$. The polycondensation reaction was stopped after 5 hours by cooling

Publications

the reaction flask in an ice bath and the polymer was obtained as a colorless transparent solid. The polymer was structurally characterized using 1D (^1H and ^{13}C), 2D heteronuclear single quantum coherence (HSQC) NMR and atmospheric pressure chemical ionization (APCI) spectroscopic techniques (Figures 5-S1 and 5-S2; see electronic supplementary information (ESI)). The molecular weight of the polymer (M_n : 2200, M_w : 2500, PDI: 1.12) was determined by MALDI-TOF MS (Figure 5-S3). In addition, the thermal behavior of the polymer was analyzed using differential scanning calorimetry (DSC) and thermogravimetry (TG) (Figures 5-S4 and 5-S5).

Minimal inhibitory concentration (MIC) and minimal bactericidal concentration (MBC) were evaluated to determine the antibacterial activity of PPXG. A dilution series of the PPXG solution starting from 1000 $\mu\text{g/mL}$, each 500 μL was prepared in a sterile 24 well plate (Greiner bio-online). Equal volume of bacteria (*Bacillus subtilis* (*B. subtilis*) or *Escherichia coli* (*E. coli*); 10^6 cfu/mL) were added and incubated for 24 h at 37 °C. After this the wells were visually evaluated for bacteria growth. The lowest concentration which remained transparent was taken as the MIC. To determine the MBC, 100 μL of solution was removed from each clear well and spread on nutrient agar plates and incubated for a further 24 h at 37 °C. The lowest concentration of biocide at which no colony formation was observed was taken as the MBC. Each test was done in quadruplicate.

Incorporation of GCG coating and PPXG

Gelatin-genipin solution at a concentration of 5 % w/v was prepared by dissolving gelatin (type A, Sigma-Aldrich, St. Louis, MO, USA) and genipin (Wako, Osaka, Japan) together in a distilled water-ethanol mixture (5 vol% ethanol) under magnetic stirring at 50 °C. The amount of genipin in the gelatin-genipin mixture was 1 wt%. The 45S5 BG scaffolds were then completely immersed in the gelatin-genipin mixture solution for 1 min under a vacuum condition, and then dried at room temperature for 1 day and subsequently the above coating procedure was repeated one more time.

In order to load different amount of PPXG directly into the GCG coated scaffolds, PPXG was dissolved in methanol at concentrations of 40, 120 and 200 $\mu\text{g/mL}$, respectively. Then 0.5 mL PPXG solution of each concentration was dripped onto the GCG coated scaffolds from different sides, followed by drying at room temperature for 1 day.

Publications

Characterization of scaffolds

Morphology and porosity

The microstructure of scaffolds before and after GCG coating was characterized using scanning electron microscopy (SEM) (LEO 435 VP, Cambridge, UK and Ultra Plus, Zeiss, Germany). Samples were sputter coated with gold in vacuum. SEM was also used to observe the scaffold surfaces after immersion in simulated body fluid (SBF) and after cell cultivation.

The porosity of scaffolds before (p_1) and after (p_2) coating with GCG was calculated by equations (1) and (2):

$$p_1 = 1 - M_1/(\rho_{BG}V_1) \quad (1)$$

$$p_2 = 1 - (M_1/\rho_{BG} + (M_2 - M_1)/\rho_{GCG})/V_2 \quad (2)$$

where M_1 and M_2 are the mass of the scaffolds before and after coating, respectively; V_1 and V_2 are the volume of the scaffolds before and after coating, respectively; ρ_{BG} ($= 2.74 \text{ g/cm}^3$) is considered as the density of sintered Bioglass[®] and ρ_{GCG} ($= 1.3 \text{ g/cm}^3$) is the density of genipin cross-linked gelatin.³⁴

Structural analysis

The chemical structure of the scaffold surfaces was investigated by FTIR (Nicolet 6700, Thermo Scientific, USA). Spectra were recorded in the absorbance mode in the range of 2000 and 400 cm^{-1} with a resolution of 4 cm^{-1} . For FTIR measurements, the scaffolds were ground, mixed with KBr (spectroscopy grade, Merck, Germany) and pressed into pellets. The pellets consisted of 1 mg of sample and 200 mg of KBr. Scaffolds were also characterized using XRD (Bruker D8 ADVANCE Diffractometer, Cu $K\alpha$). Data were collected over the 2θ range from 20° to 60° using a step size 0.02°. For XRD measurements, the scaffolds were also ground and measured in powder form.

Mechanical properties

Zwick/Roell Z050 mechanical tester was used to determine the mechanical properties of the scaffolds before and after coating with GCG. The crosshead speed was 0.5 mm/min. Due to the wide range of compressive strength, load cells with 50 N and 1 kN loading capacity were used for measuring the uncoated and GCG coated scaffolds, respectively. The samples were in dimensions of 10 mm \times 8 mm \times 8 mm. During compressive strength test, the scaffolds were pressed in the 10 mm direction until the strain reached 70%. The maximum stress of the obtained stress–strain curve before densification was used to determine the compressive strength. The work of fracture (W_{ab}) of the scaffolds, which is related to the energy necessary

Publications

to deform a sample to a certain strain, was estimated from the area under the load-displacement curve until 70% strain. At least five samples were tested, and the results were given as mean \pm standard deviation.

***In vitro* bioactivity and degradation tests**

The *in vitro* bioactivity test was performed using the standard procedure described by Kokubo *et al.*³⁵ The scaffolds with dimensions of 10 mm \times 8 mm \times 8 mm were immersed in 50 mL of SBF and maintained at 37 °C in a shaking incubator (90 rpm) for 1, 3, 7, 14 and 28 days. The SBF was replaced twice a week during the test. Once removed from the incubator, the scaffolds were rinsed with deionized water and left to dry at room temperature. Afterwards, SEM, XRD and FTIR were used to assess the hydroxyapatite (HA) formation on the scaffolds. Weight loss of the samples was calculated by equation (3):

$$\text{Weight loss (\%)} = (M_1 - M_2)/M_1 \times 100\% \quad (3)$$

where M_1 and M_2 are the mass of the samples before and after immersion in SBF, respectively.

In addition to uncoated 45S5 BG scaffolds, the degradation behavior of pure GCG films was also studied in SBF following the procedure as described above for comparison with the degradation behavior of GCG coated 45S5 BG scaffolds. GCG films were prepared by drying the GCG solution used for coating scaffolds in a petri dish.

Antibacterial test

Antibacterial activity was characterized by Kirby-Bauer test and time-dependent shaking flask test. *E. coli* (DSM No. 1077, K12 strain 343/113, DSMZ) as Gram-negative and *B. subtilis* (DSM No. 2109, ATCC 11774, ICI 2/4 strain, DSMZ) as Gram-positive test organism were used.²⁹ Tryptic soy broth (TSB) (Sigma-Aldrich, Germany) was used as nutrient for *E. coli* (30 g·L⁻¹ in distilled water for liquid nutrient; 15 g·L⁻¹ agar-agar in addition for nutrient agar plates) and peptone/meat extract medium for *B. subtilis* (5 g·L⁻¹ peptone and 3 g·L⁻¹ meat extract in distilled water for liquid nutrient; 15 g·L⁻¹ agar-agar in addition for nutrient agar plates). Both strains were preserved on nutrient agar plates and liquid cultures were grown by inoculation of liquid nutrient with a single bacteria colony using an inoculation loop. The inoculated broth was incubated under shaking at 37 °C until the optical density at 578 nm had increased by 0.125 indicating a cell density of 10⁷–10⁸ cfu·mL⁻¹. To obtain the final bacterial suspensions the inoculated broth was diluted with liquid nutrient to an approximate cell density of 10⁶ cfu·mL⁻¹.

Publications

Kirby-Bauer test

To determine the antibacterial activity, samples of approximate 10 mm (width) × 10 mm (length) were placed on a nutrient agar plate previously inoculated with 100 µL inoculum and incubated at 37 °C for 24 h. The plates were visually evaluated for a zone of inhibition and colony formation on the surface of the sample. The samples were removed from the incubated agar plate and a swab from the area under the samples with a sterile inoculation loop was transferred to a new TSB agar plate. After incubation for 24 h at 37 °C, the colony formation was visually checked.

Time-dependent shaking flask test

The time-dependent antibacterial activity was determined by the shaking flask method: samples incorporated with different amount of PPXG were incubated with equal volume of bacteria suspension at ambient temperature in microcentrifuge tubes, and contact times of 60, 120, 240 and 360 min were chosen. After each time interval, 100 µL specimens were drawn and spread on nutrient agar plates. After 24 h at 37 °C incubation, colonies were counted and the reduction was calculated relative to the initial cell density of the inoculum.²⁹

***In vitro* biocompatibility test**

In vitro biocompatibility tests were carried out using human osteosarcoma cell line MG-63 (Sigma-Aldrich, Germany). Cells were cultured at 37 °C in a humidified atmosphere of 95% air and 5% CO₂ in DMEM (Dulbecco's modified Eagle's medium, Gibco, Germany) containing 10 vol.% fetal bovine serum (FBS, Sigma-Aldrich, Germany) and 1 vol.% penicillin/streptomycin (Gibco, Germany). Cells were grown to confluence in 75 cm² culture flasks (Nunc, Denmark), and afterwards harvested using Trypsin/EDTA (Gibco, Germany) and counted by a hemocytometer (Roth, Germany).

PPXG is water soluble and dissolves in aqueous medium rather quickly. Since the pH of BG scaffolds needs to be regulated in aqueous medium before seeding the cells, PPXG preloaded on GCG coated 45S5 BG scaffolds will not be present on the scaffold anymore after the pH regulation step. Therefore, in this study, the *in vitro* biocompatibility tests were carried out in two steps rather than directly on GCG coated 45S5 BG scaffolds loaded with PPXG. Firstly, a preliminary test was performed on PPXG, genipin and GCG in order to understand the behavior of MG-63 cells in the presence of these individual components of the GCG coated 45S5 BG scaffolds. This test was carried out in a short term (2 days), because these components will rather quickly dissolve in the cell culture medium which thus makes long term test impossible

Publications

as the cell culture medium needs to be changed every few days. Cell cultivation in the well plate without any material was used as a control. Secondly, MG-63 cells were directly cultured onto the uncoated and GCG coated 45S5 BG scaffolds. Uncoated 45S5 BG scaffolds were used as a control.

For preparing the samples, PPXG, genipin and GCG were sterilized by filtering their respective solution through a 0.22 μm syringe filter. PPXG was dissolved in distilled water, while genipin or gelatin-genipin mixture was dissolved in a distilled water-ethanol mixture solution (5 vol% ethanol). Uncoated 45S5 BG scaffolds were sterilized at 160 $^{\circ}\text{C}$ for 2 h in a furnace (Nabertherm, Germany). GCG coated 45S5 BG scaffolds were prepared by using sterilized GCG solution and sterilized uncoated 45S5 BG scaffolds.

In vitro biocompatibility of PPXG, genipin and GCG

Various amounts of PPXG (6 μg , 18 μg and 30 μg), genipin (30 μg) and GCG (0.6 mg and 3 mg) were obtained by adding different volumes of their respective solution into a 48-well cell culture plate and left to dry in the sterile bench. 60000 MG-63 cells in 0.6 mL cell culture medium were seeded into each well, and cells were cultivated for 2 days without change of the culture medium. Therefore, the tested concentration of PPXG was 10 $\mu\text{g}/\text{mL}$, 30 $\mu\text{g}/\text{mL}$ and 50 $\mu\text{g}/\text{mL}$, genipin was 50 $\mu\text{g}/\text{mL}$, and GCG was 1 mg/mL and 5 mg/mL. Water soluble tetrasodium (WST) test, a colorimetric assay, was used to assess the cell viability. After cell cultivation, cell culture medium was removed and samples were washed with 0.5 mL phosphate buffered saline (PBS). Afterwards, 0.25 mL WST medium (containing 1 vol% of WST reagent (Cell Counting Kit-8, Sigma) and 99 vol% of DMEM medium) was added and incubated for 2 h. After incubation, 0.1 mL of the supernatant was transferred to a 96-well culture plate and spectrometrically measured using a microplate reader (PHOmo, anthos Mikrosysteme GmbH, Germany) at 450 nm. To analyze the adherent growth of cells on the samples, green Calcein AM (Molecular Probes, The Netherlands) cell-labelling solution were used for staining the cytoplasm of the cells. After removing the cell culture medium, 0.25 mL staining solution (0.5 vol% of dye labelling solution and 99.5 vol% of PBS) was added and incubated for 30 min. Afterwards, the solution was removed and the samples were washed with 0.5 mL PBS. Cells on the surfaces were fixed by 3.7 vol.% paraformaldehyde. Samples were washed again and blue fluorescent DAPI (4',6-diamidino-2-phenylindole dihydrochloride, Roche, Basel, Switzerland) was added to label the nuclues. After 5 minutes of incubation, the solution was removed and the samples were left in PBS for microscopic viewing using a fluorescence microscope (Axio Scope, ZEISS, Germany).

Publications

In vitro biocompatibility of scaffolds

Scaffolds (6 mm × 6 mm × 4 mm) were soaked in DMEM medium to regulate the pH value. To evaluate the cell behavior of osteoblast-like cells on the scaffolds, 0.3 million MG-63 cells in 0.6 mL cell culture medium were seeded on each scaffold, and cells were cultivated for 2 weeks with change of culture medium every 2–3 days. After cell cultivation, mitochondrial activity, cell distribution, cell attachment and cell morphology were determined. Mitochondrial activity was measured using WST test as described in section 2.7.1. To visualize the adherent grown cells on the scaffolds, Vybrant™ cell-labelling solution (Molecular Probes, The Netherlands) was used. After incubation, cell culture medium was removed and staining solution (5 µL dye labelling solution to 1 mL of growth medium) was added and incubated for 15 min. Afterwards the solution was removed, the samples were washed with PBS and cells on the surfaces were fixed by 3.7 vol.% paraformaldehyde. Samples were washed again and left in PBS for microscopic viewing with a confocal scanning laser microscope (CSLM, Leica TCS SP5 II, Germany). The CLSM images were taken from the outside surface of the scaffolds. For cell morphology characterization, cells on scaffolds were fixed in 3 vol.% paraformaldehyde, 3 vol.% glutaraldehyde (Sigma-Aldrich, Germany) and 0.2 M sodiumcacodylate (Sigma-Aldrich, Germany). After dehydration through incubation with a series of graded ethanol series (30, 50, 70, 80, 90, 95 and 100 vol.%), the samples were critical point dried with CO₂ (EM CPD300, Leica, Germany) and sputtered with gold. The cell morphology was analyzed by SEM.

Statistical analysis

All quantitative data were expressed as the mean ± standard deviation. Statistical analysis was performed with one-way analysis of variance (ANOVA) using Microsoft Excel 2010 (Microsoft, Redmond, WA, USA). A value of $P < 0.05$ was considered statistically significant.

Results and discussion

Morphology of scaffolds

Typical morphologies of the uncoated (Figure 5-1(a)–(b)) and GCG coated (Figure 5-1(c)–(d)) 45S5 BG scaffolds were observed by SEM. The uncoated scaffolds (Figure 5-1(a)) exhibited a highly interconnected pore structure. The porosity and pore size were determined to be 95% and 200–550 µm, respectively. After coating with GCG (Figure 5-1(c)), the interconnected pore structure of the scaffolds was maintained since only very few pores were clogged by the coating, and the porosity slightly decreased to 93%. The amount of GCG in the coated scaffolds was determined to be 15 ± 2 wt%. As shown in the cross section image at a high magnification, the strut of the scaffold is homogeneously covered by the GCG coating (Figure 5-1(d)), and the

Publications

GCG coating firmly adheres to the strut (Figure 5-1(d)–(e)), which is qualitatively confirmed by the fact that the GCG coating did not peel off during cutting the scaffolds. Moreover, it is worth noting that the voids of the hollow struts, which result from the burning out of polyurethane during the foam replication method (Figure 5-1(b)),¹¹ were mostly filled with the GCG (Figure 5-1(d)). This filling effect could be attributed to the infiltration of the polymer solution into the hollow struts under the applied vacuum condition for coating the scaffolds, and it means many defects and cracks on the struts can be "repaired" by the GCG coating, as evidenced by the quite smooth surface of the GCG coated strut (Figure 5-1(e)), thus expecting a positive contribution to the mechanical behavior of the scaffolds.

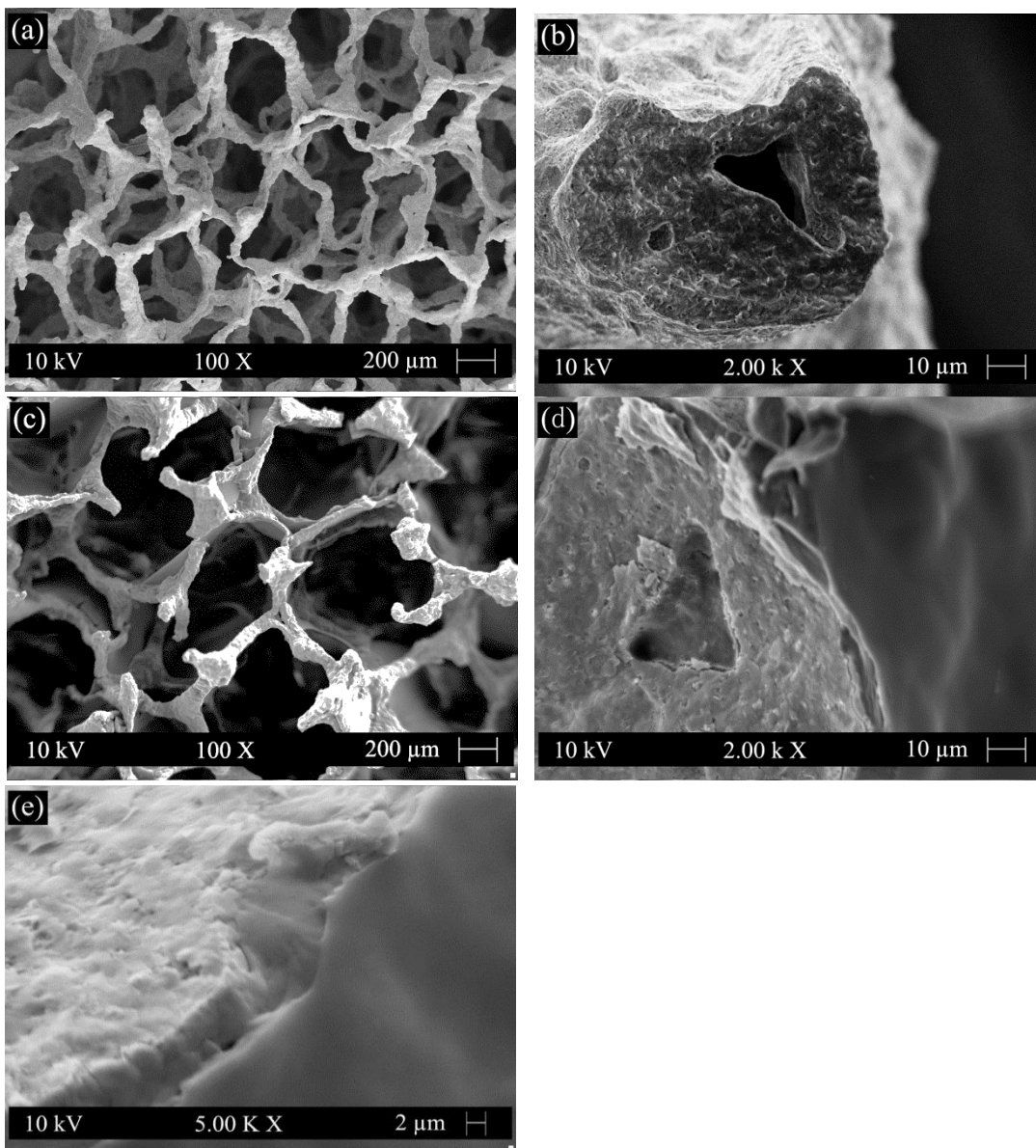


Figure 5-1. SEM images of 45S5 BG scaffolds (a)–(b) before and (c)–(e) after coating with GCG.

Publications

Degradation behavior

Gelatin films without any crosslinking completely dissolved at 37 °C in SBF within a few minutes, which would lead to the loss of their potential strengthening and toughening effects as coating on scaffolds. Therefore, the main aim to crosslink gelatin is to decrease its dissolution/degradation rate. GCG films only exhibited 24% weight loss after immersion in SBF for 1 day, and their weight loss increased to 62% after 7 days (Figure 5-2). GCG films were still present in SBF after 14 days, but they already broke up into small gelatinous blue pieces which therefore made the weight loss measurement impossible. Also, only small gelatinous blue pieces were visible in the SBF solution after 28 days. The decrease of dissolution/degradation rate of gelatin after crosslinking with genipin has also been reported in other studies.²¹ It should be pointed out that although the dissolution/degradation behavior of GCG film cannot be considered as GCG coating existed on the 45S5 BG scaffolds equally, it still could represent the gradual dissolution/degradation trend of GCG coating. Actually, this gradually dissolution/degradation trend of GCG coating on 45S5 BG scaffolds can be proved by the FTIR results of GCG coated scaffolds before and after immersion in SBF for different times. As shown in Figure 5-3, compared to the spectra of uncoated 45S5 BG scaffolds, two new bands can be observed at 1660 cm⁻¹ and 1540 cm⁻¹. These bands are identified as amide C=O stretching vibration (amide I) and amide N–H bending vibration (amide II),^{21, 36, 37} which indicate the presence of gelatin, in this particular case genipin cross-linked gelatin (GCG). The intensity of the amide I band (1660–1650 cm⁻¹) and amide II band (1540 cm⁻¹) decreased and almost disappeared as immersion time in SBF increased, suggesting the gradual dissolution/degradation of the GCG coating.

As shown in Figure 5-2, the weight loss of uncoated 45S5 BG scaffolds increases with immersion time; however the degradation rate is reduced with immersion time. The degradation of bioactive glass/ceramic-based scaffolds consists of the partial dissolution of the glass and crystalline phases and the formation of HA on the scaffold surface.³⁸ The rapid weight loss at initial immersion times is due to the fast dissolution of 45S5 BG surface upon immersion in SBF. As the immersion time increases, HA begins to form on the 45S5 BG scaffolds,¹⁴ which compensates the weight loss caused by dissolution and therefore reduces the overall degradation rate of the 45S5 BG scaffolds. The weight loss of GCG coated 45S5 BG scaffolds was similar to that of uncoated 45S5 BG scaffolds for up to 7 days, and then increased faster after 7 days. The weight loss caused by the dissolution of the 45S5 BG surface should be slower in the presence of GCG coating at the initial immersion stage; however the GCG coating begins to

Publications

gradually dissolve upon immersion in SBF which therefore results in the overall weight loss of the GCG coated 45S5 BG scaffolds increasing and eventually it becomes similar to that of the uncoated 45S5 BG scaffolds. As suggested by the dissolution/degradation behavior of the GCG film, the GCG coating on the 45S5 BG scaffolds is also likely to largely dissolve/degrade in SBF after 7 days. Moreover, as HA forms on both uncoated and GCG coated 45S5 BG scaffolds after 7 days, the higher weight loss of GCG coated scaffolds over uncoated scaffolds is assumed to be mainly attributed to the loss of the GCG coating. To a certain extent, this assumption is confirmed by the fact that the 12 wt% difference of the weight loss of uncoated and GCG coated scaffolds after 14 days of immersion in SBF is close to the amount (15 wt%) of GCG in the coated scaffolds.

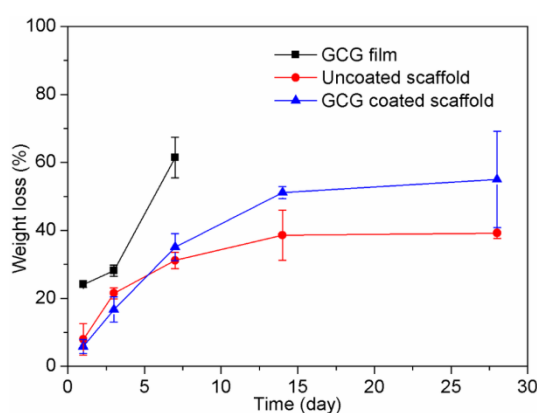


Figure 5-2. Degradation behaviors in SBF of GCG films, uncoated and GCG coated 45S5 BG scaffolds.

***In vitro* bioactivity of GCG coated 45S5 BG scaffolds**

As an assessment of bioactivity, HA formation on the surface of scaffolds upon immersion in SBF was characterized by FTIR, XRD and SEM. Figure 5-3 shows FTIR spectra of GCG coated 45S5 BG scaffolds before and after immersion in SBF. The FTIR spectra of GCG coated scaffolds after 3, 7, 14 and 28 days of immersion in SBF present dual bands at 564 cm^{-1} and 602 cm^{-1} corresponding to the bending vibration of P–O bond, which is characteristic of a crystalline phosphate phase.^{14, 39-41} Furthermore, the band at 876 cm^{-1} and the dual broad bands at $1423\text{--}1455\text{ cm}^{-1}$ can be assigned to the stretching vibration of C–O bond, suggesting the formed HA is carbonated hydroxyapatite (cHA) rather than stoichiometric hydroxyapatite.^{14, 39, 40, 42, 43} It should be noted that, for GCG coated 45S5 BG scaffolds, the characteristic bands of cHA after 3 days of immersion in SBF were relatively weaker in comparison to that after 7 days. As shown in our previous study¹⁴, for uncoated 45S5 BG scaffolds, the characteristic bands of cHA did not appear after 1 day of immersion in SBF, while these bands occurred after 3 days and their relative intensities were quite close to those that appeared after 7 days. This

Publications

comparison between the FTIR spectra of uncoated and GCG coated 45S5 BG scaffolds after immersion in SBF suggests that the bioactivity of 45S5 BG scaffolds was maintained after coating with GCG, although the GCG coating may slightly retard the formation rate of cHA at the initial stage of immersion in SBF.

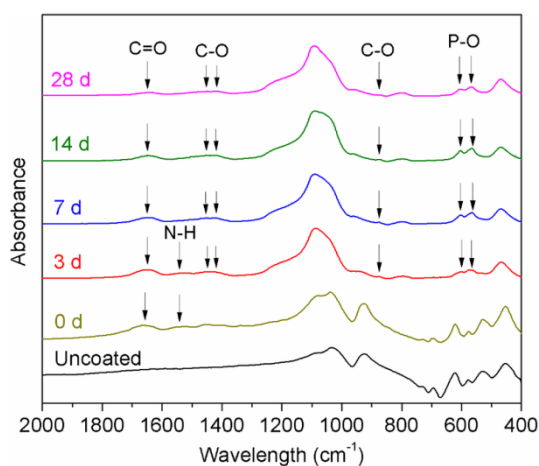


Figure 5-3. FTIR spectra of uncoated 45S5 BG scaffolds (labelled as uncoated), and GCG coated 45S5 BG scaffolds before (0 d) and after immersion in SBF for 3, 7, 14 and 28 days.

Figure 5-4 shows the XRD spectra of GCG coated scaffolds before and after immersion in SBF. The peaks in scaffolds before immersion in SBF correspond to the $\text{Na}_4\text{Ca}_4(\text{Si}_6\text{O}_{18})$ and $\text{Na}_2\text{Ca}_4(\text{PO}_4)_2\text{SiO}_4$ phases, which have also been found in previous studies.^{14, 44} Growing HA peaks (e.g. at $2\theta = 25.8^\circ$ and 31.7°) were observed on coated scaffolds after immersion in SBF for 7, 14 and 28 days. In addition, the crystallinity of the sintered scaffolds decreased with increasing immersion time in SBF as indicated by the gradual disappearance of the sharp peaks of the $\text{Na}_4\text{Ca}_4(\text{Si}_6\text{O}_{18})$ phase.

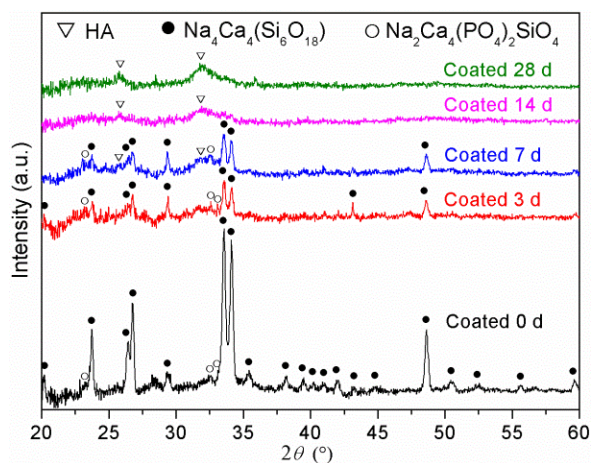


Figure 5-4. XRD spectra of GCG coated 45S5 BG scaffolds before (0 d) and after immersion in SBF for 3, 7, 14 and 28 days.

Publications

SEM images of GCG coated scaffolds after immersion in SBF for different times are shown in Figure 5-5. After 3 days immersion in SBF, there were some apatite-like precipitates on the surface of struts. As the immersion time increased to 7 days, the struts were almost fully covered by HA crystals which can be clearly recognized by their well-known globular and cauliflower-like shape.

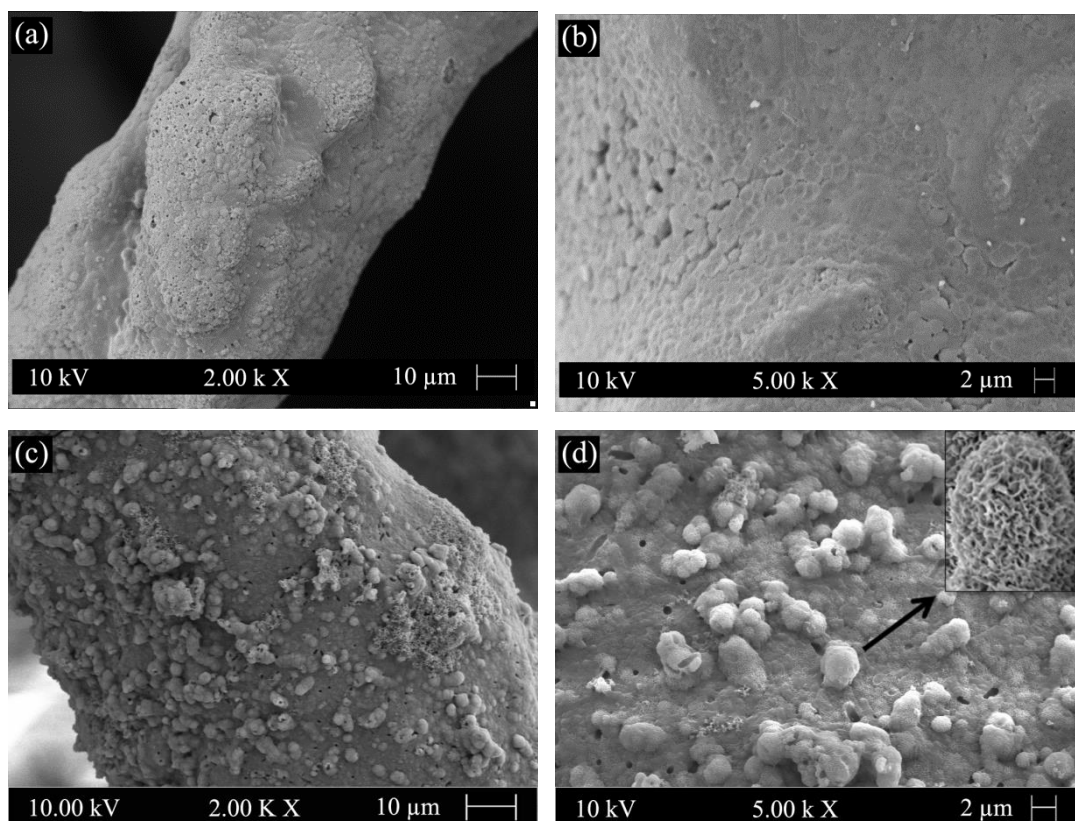


Figure 5-5. SEM images showing HA formation on the surfaces of GCG coated 45S5 BG scaffolds after immersion in SBF for (a)–(b) 3 days and (c)–(d) 7 days.

Based on the XRD, FTIR and SEM results described above, the bioactivity of the 45S5 BG scaffolds is confirmed to be maintained after coating with GCG. The explanation for HA formation on polymer coated bioactive glass/ceramic scaffolds was given in our previous studies.^{14, 17} Briefly, some areas of the struts are not fully covered by the polymer as a result of the surface roughness of the original struts. Thus, uncoated areas of the struts provide paths for SBF to penetrate the area underneath the coating. Besides, in the present study, GCG will gradually dissolve/degrade in the SBF which enables coated areas of the struts to be increasingly exposed to SBF. Thus, the established direct contact between SBF and the surface of bioactive glass/ceramic struts is essential to retain the intrinsic bioactivity of the scaffolds.

Publications

Mechanical properties

The mechanical properties of uncoated and GCG coated 45S5 BG scaffolds were investigated by the uniaxial compressive strength test. As indicated by the typical compressive stress-strain curves of these scaffolds (Figure 5-6), the compressive strength of GCG coated scaffolds (1.04 ± 0.11 MPa) was significantly higher than that of uncoated scaffolds (0.04 ± 0.01 MPa). The area under the load-displacement curve (related to work of fracture) of GCG coated scaffolds was calculated to be 285.6 ± 23.3 N·mm, whereas it was only 5.0 ± 1.1 N·mm for the uncoated scaffolds. It is worth pointing out that the uncoated scaffolds were completely broken into little pieces during compressive strength test, while the GCG coated scaffolds were able to partly maintain their cuboid shape despite being compressed (Figure 5-7). Taking into consideration the high porosity (93%) of the fabricated GCG coated scaffolds, the achieved compressive strength (1.04 MPa) is obviously higher than the lower bound of the values for human cancellous bone (>0.15 MPa, porosity $\sim 90\%$).¹⁶

It is well-known that polymer coatings can not only fill microcracks on the strut surfaces but also fill the void of hollow struts.^{14, 18, 45} In other words, the polymer coatings turn the original weak and brittle struts into strong and tough composite struts, thus significantly improving the mechanical stability of the flaw sensitive glass/ceramic struts. As a consequence, the compressive strength and toughness of the uncoated scaffolds in the present study are considerably improved after coating with GCG. The strengthening and toughening effects in the present study are in broad agreement with other studies about polymer coated scaffolds,^{14, 17, 45, 46} and they can be explained by the micron-scale crack-bridging mechanism.⁴⁶⁻⁴⁸

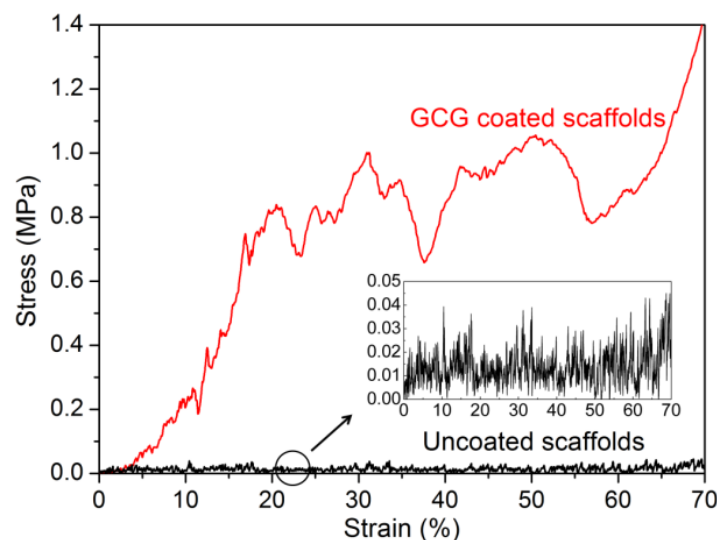


Figure 5-6. Typical compressive stress-strain curves of uncoated and GCG coated 45S5 BG scaffolds, showing remarkable improvement of mechanical properties by the presence of the GCG coating.

Publications

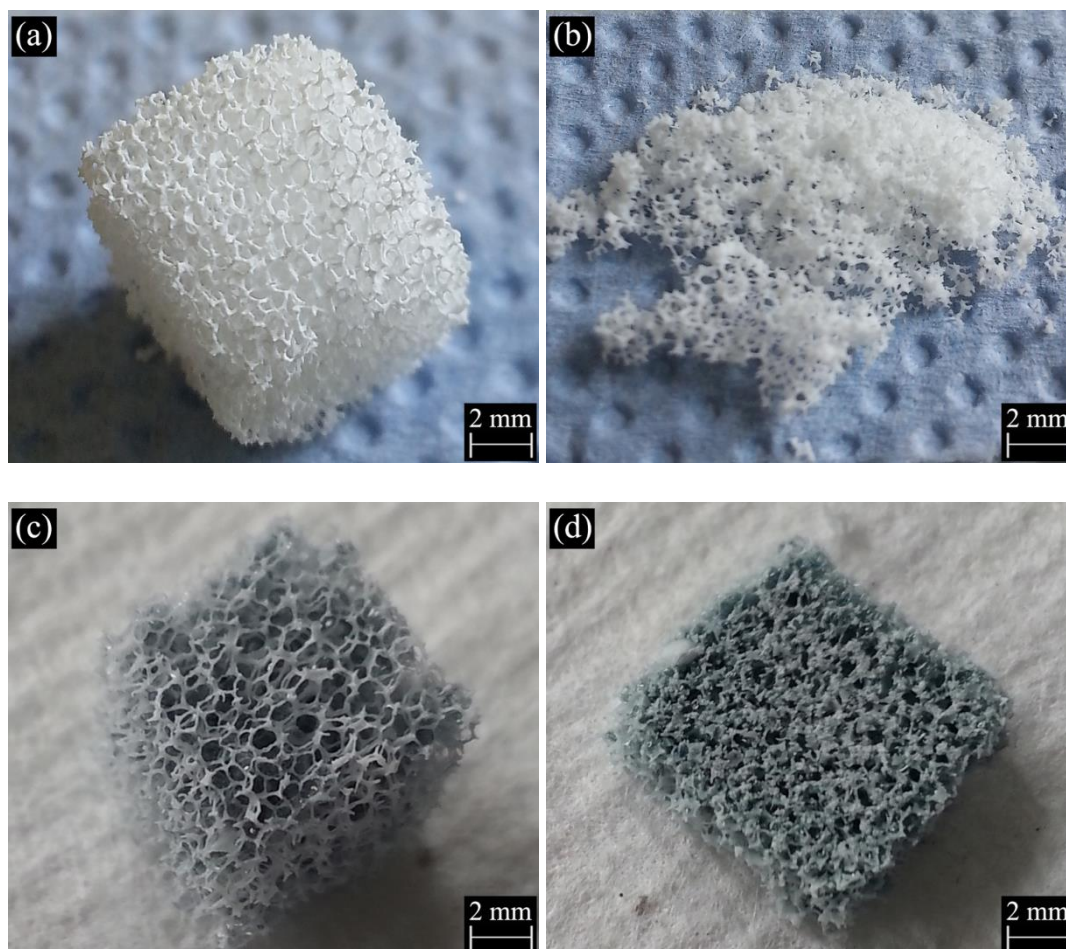


Figure 5-7. Digital photographs of (a)–(b) uncoated and (c)–(d) GCG coated 45S5 BG scaffolds before ((a), (c)) and after ((b), (d)) compressive strength test.

It is worth mentioning that the GCG coating provides much more significant strengthening and toughening effects than PHBV or PCL/chitosan coating on 45S5 BG scaffolds.^{14, 49} Similarly, significant strengthening and toughening effects were also observed on non-cross-linked gelatin coated Biosilicate[®] scaffolds.¹⁷ The different degrees of strengthening and toughening effects obtained from different polymer coatings are likely to be determined by the of polymer solution on the scaffold struts and the adhesion ability of the obtained polymer coating on the scaffold struts. Obviously, low viscosity gelatin aqueous solution is much easier to spread on and also infiltrate into the hydrophilic glass/ceramic struts than other polymer solutions in which synthetic polymers (e.g. PHBV or PCL) are dissolved in organic solvent (e.g. dichloromethane or chloroform). Also, the interface between the hydrophilic polymer (i.e. gelatin) and hydrophilic glass/ceramic strut is likely to be stronger than that between the hydrophobic polymer (e.g. PHBV or PCL) and hydrophilic struts, given the evidence that GCG adheres well to the surface of scaffold strut (Figure 5-1(d)).

Publications

Antibacterial properties

PPXG exhibited high antibacterial activity as determined by MIC and MBC values. It showed MIC values of 7.81 $\mu\text{g/mL}$ and 32.25 $\mu\text{g/mL}$, and MBC values of 31.25 $\mu\text{g/mL}$ and 62.50 $\mu\text{g/mL}$ for *B. subtilis* and *E. coli*, respectively (Figures 5-S6 and 5-S7). PPXG was used for providing antibacterial property to GCG coated 45S5 BG scaffolds. The antibacterial property was tested using the Kirby-Bauer test and the samples were qualitatively checked for the zone of inhibition after incubation (Figure 5-8(a)–(b)). Both the uncoated and GCG coated 45S5 BG scaffolds (labelled 1 and 2) without PPXG did not show any zone of inhibition to the *B. subtilis* and *E. coli* (Figure 5-8(c)–(d)). GCG coated scaffolds loaded with PPXG showed an increasing zone of inhibition to the *B. subtilis* as the PPXG concentration, which is based on the used bacteria suspension in Time-dependent test, increased (Figure 5-8(c)). GCG coated scaffold loaded with 10 $\mu\text{g/mL}$ PPXG did not clearly exhibit a zone of inhibition to *E. coli* (Figure 5-8(d)). However, the zone of inhibition occurred and was further increased as the PPXG concentration increased. After checking the zone of inhibition, a swab from the area under the samples (Figure 5-8(c)–(d)) was further transferred to a new agar plate by sterile inoculation loop. After incubation, the colony formation was visually inspected. As shown in Figure 5-8(e)–(f), for the PPXG loaded samples, the only bacteria which obviously existed under the scaffolds were *E. coli* at the PPXG concentration of 10 $\mu\text{g/mL}$. In order to quantify the antibacterial properties, Time-dependent shaking flask test was further performed for up to 6 hours. A 6 hours post-implantation period has been identified during which prevention of bacterial adhesion is critical to the long-term success of an implant.²³ Since both of the uncoated and GCG coated scaffolds without PPXG did not clearly show antibacterial properties to both of the *B. subtilis* and *E. coli*, they were not further included in Time-dependent test. As shown in Figure 5-9, more than 95% of *B. subtilis* and *E. coli* were killed until 2 hours in the presence of GCG coated scaffolds loaded with 10–50 $\mu\text{g/mL}$ PPXG, and these antibacterial effects were kept until 6 hours with the only exception that the *E. coli* began to grow after 2 hours in the presence of GCG coated scaffolds only incorporated with 10 $\mu\text{g/mL}$ PPXG. In other words, the difference of sensitiveness of and *E. coli* to PPXG becomes evident at 10 $\mu\text{g/mL}$ after 2 hours. This would be explained by the different feature of the bacterial cell wall. Although all bacteria have an inner membrane in their walls, Gram-negative bacteria have a unique outer membrane which envelops a barrier function, i.e., prevents drugs from penetrating the cell wall. Therefore, *E. coli*, as one species of Gram-negative bacteria, is likely to be more resistant to PPXG than *B. subtilis* which belongs to Gram-positive bacteria.

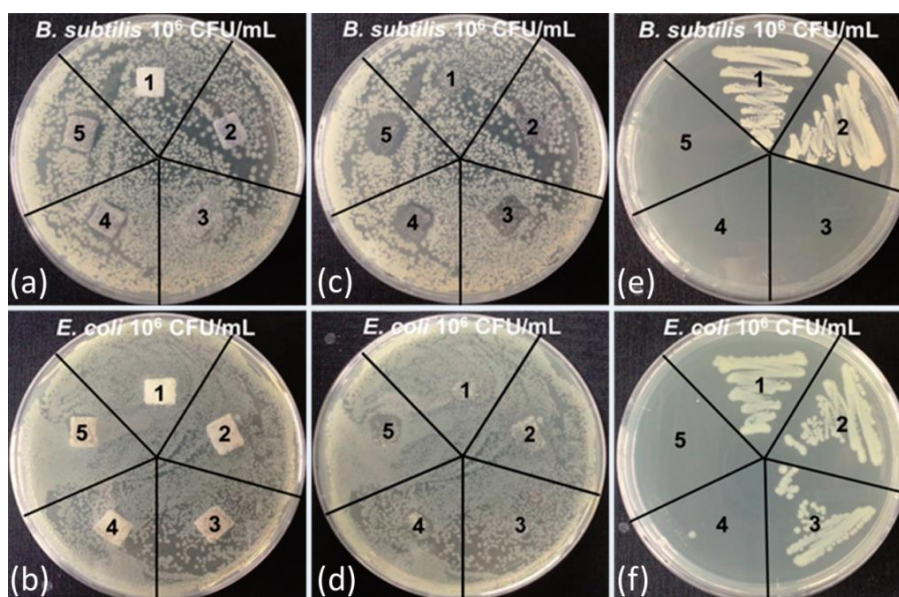


Figure 5-8. Kirby-Bauer test using *B. subtilis* and *E. coli* for samples 1: uncoated scaffold without PPXG, 2: GCG coated scaffold without PPXG, 3: GCG coated scaffold loaded with 10 $\mu\text{g/mL}$ PPXG, 4: GCG coated scaffold loaded with 30 $\mu\text{g/mL}$ PPXG, and 5: GCG coated scaffold loaded with 50 $\mu\text{g/mL}$ PPXG. (a) and (b): after incubation for 24 h, (c) and (d): area under the incubated samples, (e) and (f): smears on agar plate (bacterial growth after transferring swab from area under the samples to a new agar plate).

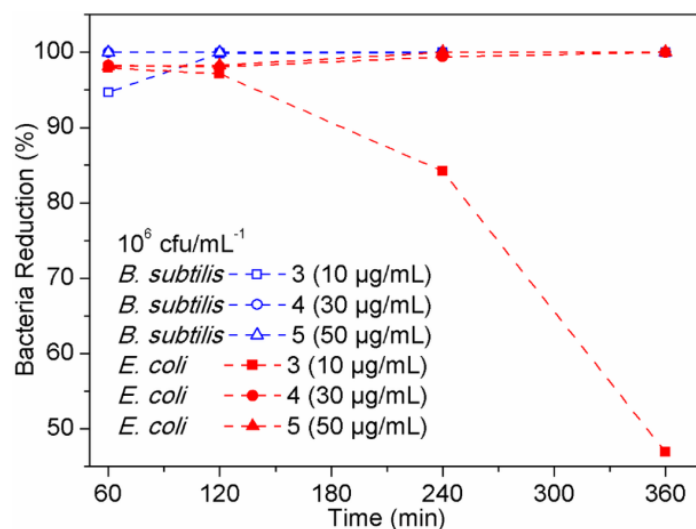


Figure 5-9. Time-dependent shaking flask test results of samples 3: GCG coated scaffold loaded with 10 $\mu\text{g/mL}$ PPXG, 4: GCG coated scaffold loaded with 30 $\mu\text{g/mL}$ PPXG, and 5: GCG coated scaffold loaded with 50 $\mu\text{g/mL}$ PPXG.

Incorporating antibacterial agent in scaffolds can allow the scaffolds themselves to fight bacterial infection. GCG coated 45S5 BG scaffolds incorporated with PPXG show effective antibacterial effects on both Gram-positive and Gram-negative bacteria, and the antibacterial effects increase with PPXG concentration, suggesting that PPXG and also other biocidal

Publications

cationic polymers belonging to polyguanidines are promising for the antibacterial purpose in bone tissue engineering scaffolds.

Biocompatibility of PPXG, genipin and GCG

The *in vitro* biocompatibility of PPXG, genipin and GCG was characterized by evaluating the cell proliferation and cell morphology. Cell proliferation was measured in terms of mitochondrial activity, and the cell morphology was observed using calcein AM that stains the cytoplasm of living cells. Apart from the calcein staining, cells were also stained with DAPI which gives information about the integrity of the nucleus. The concentration of the materials was calculated based on the volume of the used cell culture medium. The cell culture plate without any addition of material was used as a control. As shown in Figure 5-10, the mitochondrial activity of MG-63 cells grown in the presence of 10 $\mu\text{g/mL}$ PPXG is 79%, while it significantly decreases when PPXG concentration increases. This result is in accordance with the fluorescence staining results of MG-63 cells as presented in Figure 5-11(a)–(d), which also indicates a reduction in viable cell numbers as PPXG concentration increases. As shown in Figure 5-11(a)–(b), the cell shape, cell membrane integrity and nucleus integrity of MG-63 cells cultured in 10 $\mu\text{g/mL}$ PPXG solution are quite similar to that of the control group. Taking into consideration antibacterial test results in section 3.5, PPXG concentration between 10–30 $\mu\text{g/mL}$ would be a balanced concentration for both antibacterial properties and biocompatibility. As a natural crosslinking reagent, 50 $\mu\text{g/mL}$ genipin enabled MG-63 cells to show 51% mitochondrial activity (Figure 5-10), and the viable cells possessed intact nuclei and cell membrane (Figure 5-11(e)). In addition, compared to the control group, the cell shape was not obviously affected by the genipin. MG-63 cells exhibited 59% mitochondrial activity at a GCG amount of 1 mg/mL , and the mitochondrial activity decreased when the GCG amount increased to 5 mg/mL . The relatively low mitochondrial activity of MG-63 cells in the present study on one hand may be due to the existence of genipin, while on the other hand may mainly be due to the inhibition of MG-63 cell growth under overdose of gelatin.^{50, 51} As shown in Figure 5-11(f)–(g), compared to the control group, although an obvious reduction in viable cell numbers is observed, the cell shape is still similar to that of the control group. Interestingly, many of MG-63 cells formed clusters on the 1 mg/mL GCG films (Figure 5-11(f)) and were found to be considerably agglomerated on the 5 mg/mL GCG films as indicated by the large blue dot in Figure 5-11(g). This result indicates that on such concentration of GCG, cell-material interactions are weaker than cell-cell interactions, which becomes even more obvious when the GCG concentration increases.

Publications

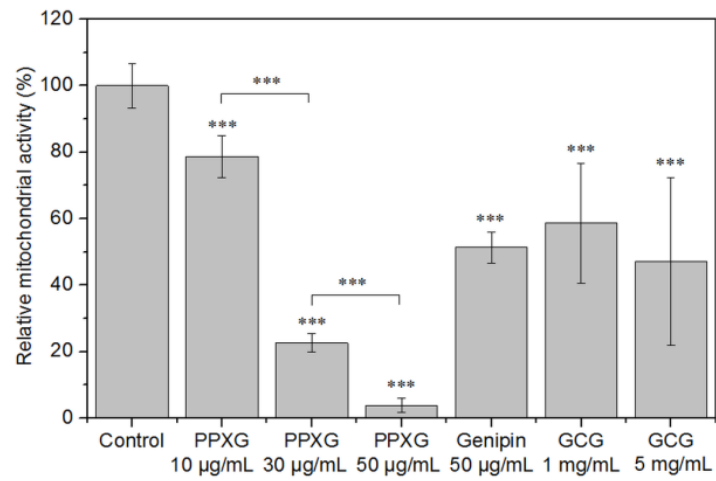


Figure 5-10. Mitochondrial activity measurement of MG-63 cells in the presence of PPXG, genipin and GCG at different concentrations after 2 days of cultivation. The values are mean \pm standard deviation. The asterisks indicate significant difference. *** $P < 0.001$.

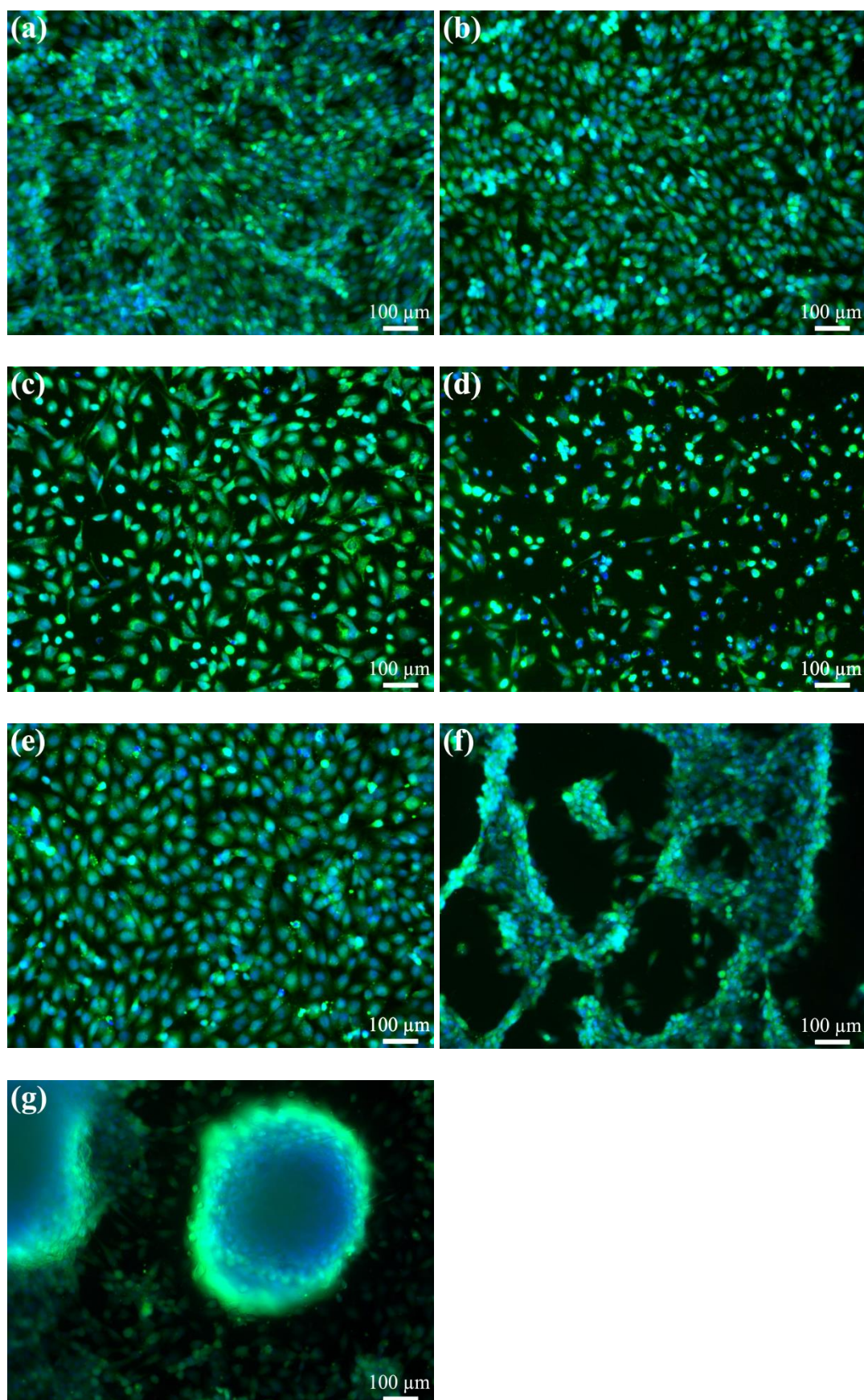


Figure 5-11. Fluorescence images of MG-63 cells after 2 days of cultivation in the presence of PPXG, genipin and GCG at different concentrations. (a) Control group (cell culture plate), (b) PPXG 10 $\mu\text{g/mL}$, (c) PPXG 30 $\mu\text{g/mL}$, (d) PPXG 50 $\mu\text{g/mL}$, (e) Genipin 50 $\mu\text{g/mL}$, (f) GCG 1 mg/mL and (g) GCG 5 mg/mL . Calcein/DAPI staining: living cells (green)/nuclei (blue).

Biocompatibility of scaffolds

Figure 12 shows that the mitochondrial activity of MG-63 cells on GCG coated 45S5 BG scaffolds is slightly higher than on uncoated 45S5 BG scaffolds after 2 weeks of cultivation. However, the difference between the mitochondrial activity of these two groups does not reach statistical significance ($P>0.05$).

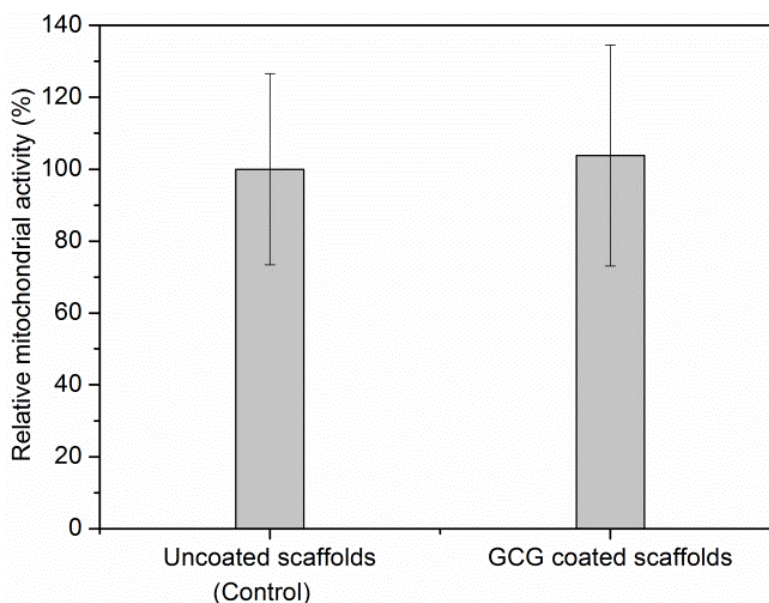


Figure 5-12. Mitochondrial activity measurement of MG-63 cells on GCG coated 45S5 BG scaffolds after 2 weeks of incubation, using uncoated 45S5 BG scaffolds as a control. The values are mean \pm standard deviation.

To visualize cell adhesion and cell distribution on the scaffolds, MG-63 cells were labelled with Vybrant™ cell-labelling solution. CLSM-images of uncoated and GCG coated scaffolds after 2 weeks of cell cultivation are shown in Figure 5-13. MG-63 cells were seen to have grown on the strut surfaces of both uncoated and GCG coated scaffolds. As judged by visual inspection of the images, the amount of cells on GCG coated scaffolds seems to be higher than on uncoated scaffolds, which is in agreement with the results of the cell proliferation assay (Figure 5-12). After cell cultivation for 2 weeks, the pores of uncoated scaffolds as well as GCG coated scaffolds were still open. This can be attributed to the highly porous and interconnected large pore structure of the scaffolds which facilitate oxygen and nutrient supply for the cells.

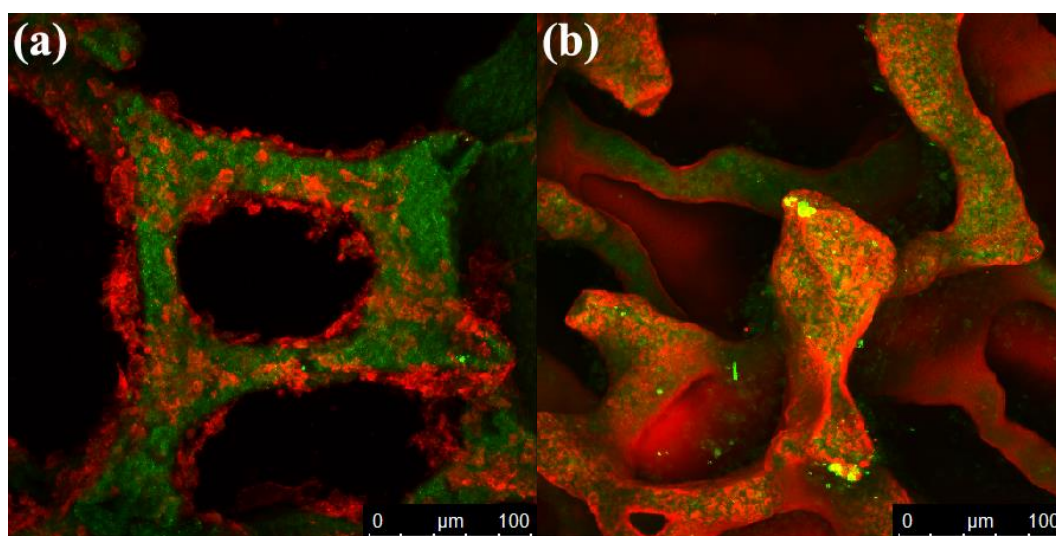


Figure 5-13. CLSM images of MG-63 osteoblast-like cells on the surfaces of (a) uncoated and (b) GCG coated 45S5 BG scaffolds after 2 weeks of cultivation. The cells were stained red and the 45S5 BG surface can be seen in green.

Furthermore, in order to reveal the cell-cell and cell-material interactions, the cell morphology, especially considering how cells attach and spread on both uncoated and GCG coated scaffolds, were observed by SEM. Representative images are presented in Figure 5-14. Figure 5-14 (a) and (d) show that the strut surfaces of both uncoated and GCG coated scaffolds are well covered by cells, and the well flattened cells covering the scaffold struts tend to form a monolayer in both scaffold types. A closer observation of the gap among the cells showed that the strut surface of GCG coated scaffold was smooth (Figure 5-14 (e)), while that of uncoated scaffold was rougher (Figure 5-14 (b)). The smooth strut surface of GCG coated scaffold is likely due to the remaining GCG coating on GCG coated scaffolds after 2 weeks of cell cultivation. Indeed, as shown in the FTIR results (Figure 5-3), GCG does exist on GCG coated scaffolds after immersion in SBF for 14 days. At higher magnifications (Figure 5-14 (c) and (f)), the cells on both scaffold types displayed a typical osteoblastic phenotype with mainly elongated polygonal and flat structures as well as expressed filopodias in contact with the scaffold surface.^{32, 52} Moreover, well developed microvilli were observed on the spread cells on both scaffold types, which indicates that the cells are highly active.

Publications

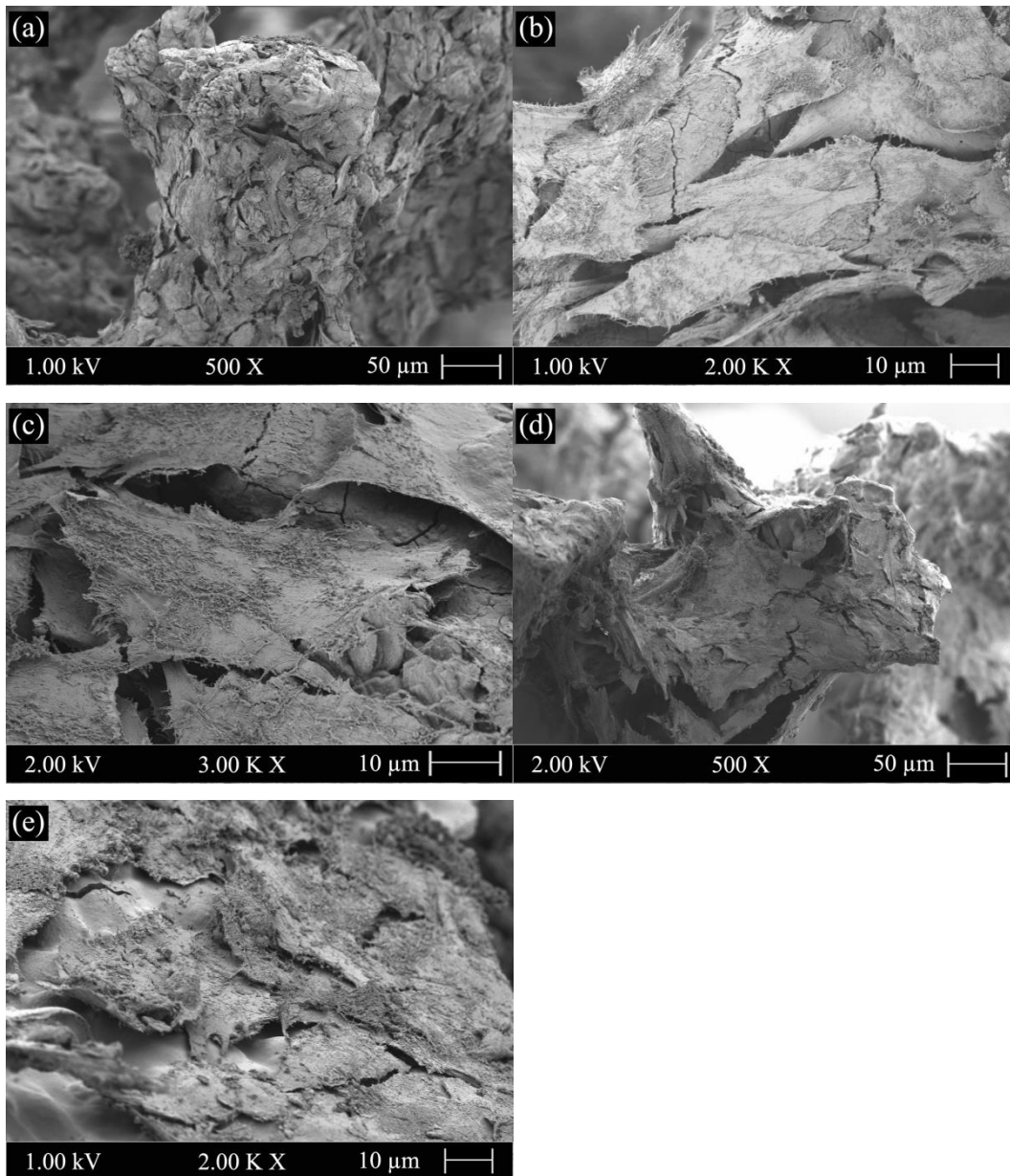


Figure 5-14. SEM images of MG-63 cells on the strut surfaces of (a)–(c) uncoated and (d)–(f) GCG coated 45S5 BG scaffolds after 2 weeks of cultivation. The inset in (f) indicates the typical morphology of the microvilli.

The quantitative result of WST assay indicates that GCG coating may have a slightly positive effect on the cell proliferation of MG-63 cells on 45S5 BG scaffolds. Indeed, GCG coating has been shown to be able to significantly increase the mitochondrial activity of human mesenchymal stem cells on porous PCL scaffolds, however, the realization of this significant improvement of cell response is due to the fact that pure PCL scaffolds were less satisfactory in supporting cell adhesion and growth because of their hydrophobic nature.⁵³ In contrast, uncoated 45S5 BG scaffolds (with their hydrophilic nature¹⁴) in the present study already could support suitable cell attachment and growth, as described above. The qualitative studies, i.e., CLSM and SEM images, confirmed that MG-63 cells could attach well and spread on uncoated

Publications

45S5 BG scaffolds, and the cell attachment, cell spreading and cell morphology were not significantly changed in the presence of GCG coating. All these results indicate that the GCG coating on the scaffolds seems to have no negative effects on the cell activity, which is different from the biocompatibility results of GCG films, as shown in section 3.6. The better biocompatibility of the GCG coating on scaffolds is due to the fact that part of the GCG is lost during the pH regulation of GCG coated scaffolds (pretreatment in DMEM) before starting the cell cultivation. The remained GCG on the scaffolds is in a reduced amount. As discussed in section 3.6, relatively lower concentration of gelatin is able to favor the growth of MG-63 cells.^{50, 51} Therefore, GCG coated 45S5 BG scaffolds, as well as GCG coating itself at a relatively low concentration, is biocompatible to MG-63 cells. The biocompatibility of GCG was also demonstrated in other studies.^{37, 54-56} Especially, MG-63 cells were shown to attach on genipin cross-linked gelatin porous scaffolds, and the cells exhibited a fibroblastic and a polygonal like morphology after 2 weeks of cell culture.⁵⁴

Conclusions

Significantly improved mechanical properties were provided to 45S5 BG scaffolds using GCG coating. The GCG coating slightly retarded but did not inhibit the cHA formation on 45S5 BG scaffolds upon immersion in SBF, confirming the bioactive character of the coated scaffolds. Additionally, the GCG coated 45S5 BG scaffolds were antibacterial against both Gram-positive and Gram-negative bacteria after the incorporation of polyguanidine, i.e. PPXG. *In vitro* biocompatible test indicated that PPXG was biocompatible to MG-63 cells at a low concentration, and the MG-63 cells could attach, spread and proliferate on the GCG coated scaffolds as on the uncoated scaffolds. The obtained bioactive, antibacterial and biocompatible composite scaffolds with improved mechanical properties represent promising candidates for bone tissue engineering applications. They belong to a growing family of functionalized, polymer coated BG-based scaffolds with expected superior *in-vivo* performance which, however, remains to be investigated in further studies.

Acknowledgements

Wei Li and Yaping Ding would like to acknowledge the China Scholarship Council (CSC) for financial support. Financial support provided by the German Science Foundation (DFG) to Hui Wang is acknowledged.

Publications

References

1. F. Baino and C. Vitale-Brovarone, *Journal of Biomedical Materials Research Part A*, 2011, **97A**, 514-535.
2. K. Rezwan, Q. Z. Chen, J. J. Blaker and A. R. Boccaccini, *Biomaterials*, 2006, **27**, 3413-3431.
3. D. W. Hutmacher, *Biomaterials*, 2000, **21**, 2529-2543.
4. A. J. Salgado, O. P. Coutinho and R. L. Reis, *Macromol. Biosci.*, 2004, **4**, 743-765.
5. S. Bose, M. Roy and A. Bandyopadhyay, *Trends Biotechnol.*, 2012, **30**, 546-554.
6. R. Detsch and A. R. Boccaccini, *Journal of Tissue Engineering and Regenerative Medicine*, 2014, n/a-n/a.
7. J. Yang, T. Long, N.-F. He, Y.-P. Guo, Z.-A. Zhu and Q.-F. Ke, *Journal of Materials Chemistry B*, 2014.
8. L. L. Hench, *Journal of Materials Science-Materials in Medicine*, 2006, **17**, 967-978.
9. J. R. Jones, *Acta Biomater.*, 2013, **9**, 4457-4486.
10. A. A. Gorustovich, J. A. Roether and A. R. Boccaccini, *Tissue Engineering Part B-Reviews*, 2010, **16**, 199-207.
11. Q. Z. Chen, I. D. Thompson and A. R. Boccaccini, *Biomaterials*, 2006, **27**, 2414-2425.
12. R. Detsch, S. Alles, J. Hum, P. Westenberger, F. Sieker, D. Heusinger, C. Kasper and A. R. Boccaccini, *Journal of Biomedical Materials Research Part A*, 2014, n/a-n/a.
13. V. Karageorgiou and D. Kaplan, *Biomaterials*, 2005, **26**, 5474-5491.
14. W. Li, P. Noeaid, J. A. Roether, D. W. Schubert and A. R. Boccaccini, *J. Eur. Ceram. Soc.*, 2014, **34**, 505-514.
15. Q. Yao, P. Noeaid, J. A. Roether, Y. Dong, Q. Zhang and A. R. Boccaccini, *Ceram. Int.*, 2013, **39**, 7517-7522.
16. K. A. Athanasiou, C. F. Zhu, D. R. Lanctot, C. M. Agrawal and X. Wang, *Tissue Eng.*, 2000, **6**, 361-381.
17. D. Desimone, W. Li, J. A. Roether, D. W. Schubert, M. C. Crovace, A. C. M. Rodrigues, E. D. Zanutto and A. R. Boccaccini, *Science and Technology of Advanced Materials*, 2013, **14**, 045008.
18. M. Erol, A. Ozyuguran, O. Ozarpat and S. Kucukbayrak, *J. Eur. Ceram. Soc.*, 2012, **32**, 2747-2755.
19. A. Bigi, G. Cojazzi, S. Panzavolta, N. Roveri and K. Rubini, *Biomaterials*, 2002, **23**, 4827-4832.
20. C.-H. Yao, B.-S. Liu, C.-J. Chang, S.-H. Hsu and Y.-S. Chen, *Mater. Chem. Phys.*, 2004, **83**, 204-208.

Publications

21. D. Bellucci, A. Sola, P. Gentile, G. Ciardelli and V. Cannillo, *Journal of Biomedical Materials Research Part A*, 2012, **100A**, 3259-3266.
22. H.-W. Sung, R.-N. Huang, L. L. H. Huang and C.-C. Tsai, *Journal of Biomaterials Science, Polymer Edition*, 1999, **10**, 63-78.
23. E. M. Hetrick and M. H. Schoenfish, *Chem. Soc. Rev.*, 2006, **35**, 780-789.
24. V. Mouriño, J. P. Cattalini, J. A. Roether, P. Dubey, I. Roy and A. R. Boccaccini, *Expert Opinion on Drug Delivery*, 2013, **10**, 1353-1365.
25. R. A. Smith, N. M. M'ikanatha and A. F. Read, *Health Commun.*, 2014, 1-6.
26. G. J. Gabriel, A. Som, A. E. Madkour, T. Eren and G. N. Tew, *Materials Science and Engineering: R: Reports*, 2007, **57**, 28-64.
27. D. Wei, Q. Ma, Y. Guan, F. Hu, A. Zheng, X. Zhang, Z. Teng and H. Jiang, *Materials Science and Engineering: C*, 2009, **29**, 1776-1780.
28. C. Mattheis, H. Wang, C. Meister and S. Agarwal, *Macromolecular Bioscience*, 2013, **13**, 242-255.
29. H. Wang, C. V. Synatschke, A. Raup, V. Jerome, R. Freitag and S. Agarwal, *Polymer Chemistry*, 2014, **5**, 2453-2460.
30. Z. X. Zhou, D. F. Wei, Y. Guan, A. N. Zheng and J. J. Zhong, *Journal of Applied Microbiology*, 2010, **108**, 898-907.
31. Z. Zhou, A. Zheng and J. Zhong, *Acta Biochimica et Biophysica Sinica*, 2011, **43**, 729-737.
32. W. Li, N. Garmendia, U. Perez de Larraya, Y. Ding, R. Detsch, A. Gruenewald, J. Roether, D. Schubert and A. R. Boccaccini, *RSC Advances*, 2014.
33. D. F. Wei, Y. Guan, Q. X. Ma, X. Zhang, Z. Teng, H. Jiang and A. N. Zheng, *E-Polymers*, 2012.
34. W. Li, M.-I. Pastrama, Y. Ding, K. Zheng, C. Hellmich and A. R. Boccaccini, *Journal of the Mechanical Behavior of Biomedical Materials*, 2014, **40**, 85-94.
35. T. Kokubo and H. Takadama, *Biomaterials*, 2006, **27**, 2907-2915.
36. D. M. Hashim, Y. B. C. Man, R. Norakasha, M. Shuhaimi, Y. Salmah and Z. A. Syahariza, *Food Chem.*, 2010, **118**, 856-860.
37. C. Tonda-Turo, P. Gentile, S. Saracino, V. Chiono, V. K. Nandagiri, G. Muzio, R. A. Canuto and G. Ciardelli, *Int. J. Biol. Macromol.*, 2011, **49**, 700-706.
38. M. N. Rahaman, D. E. Day, B. Sonny Bal, Q. Fu, S. B. Jung, L. F. Bonewald and A. P. Tomsia, *Acta Biomater.*, 2011, **7**, 2355-2373.
39. Y. Zhu and S. Kaskel, *Microporous Mesoporous Mater.*, 2009, **118**, 176-182.
40. X. Liu, M. Rahaman and D. Day, *J. Mater. Sci. Mater. Med.*, 2013, **24**, 583-595.
41. S. Sanchez-Salcedo, S. Shruti, A. J. Salinas, G. Malavasi, L. Menabue and M. Vallet-Regi, *Journal of Materials Chemistry B*, 2014, **2**, 4836-4847.

Publications

42. D. Groh, F. Döhler and D. S. Brauer, *Acta Biomater.*, 2014, **10**, 4465-4473.
43. W. Tang, Y. Yuan, D. Lin, H. Niu and C. Liu, *Journal of Materials Chemistry B*, 2014, **2**, 3782-3790.
44. J. M. Qian, Y. H. Kang, Z. L. Wei and W. Zhang, *Materials Science & Engineering C-Biomimetic and Supramolecular Systems*, 2009, **29**, 1361-1364.
45. M. Dressler, F. Dombrowski, U. Simon, J. Börnstein, V. D. Hodoroaba, M. Feigl, S. Grunow, R. Gildenhaar and M. Neumann, *J. Eur. Ceram. Soc.*, 2011, **31**, 523-529.
46. M. Peroglio, L. Gremillard, J. Chevalier, L. Chazeau, C. Gauthier and T. Hamaide, *J. Eur. Ceram. Soc.*, 2007, **27**, 2679-2685.
47. G. Pezzotti and S. M. F. Asmus, *Materials Science and Engineering a-Structural Materials Properties Microstructure and Processing*, 2001, **316**, 231-237.
48. A. Philippart, A. R. Boccaccini, C. Fleck, D. W. Schubert and J. A. Roether, *Expert Review of Medical Devices*, 2015, **12**, 93-111.
49. Q. Yao, P. Noeaid, R. Detsch, J. A. Roether, Y. Dong, O.-M. Goudouri, D. W. Schubert and A. R. Boccaccini, *Journal of Biomedical Materials Research Part A*, 2014, **102**, 4510-4518.
50. B.-S. Liu, C.-H. Yao, Y.-S. Chen and S.-H. Hsu, *Journal of Biomedical Materials Research Part A*, 2003, **67A**, 1163-1169.
51. K.-Y. Chen, P.-C. Shyu, Y.-S. Chen and C.-H. Yao, *Macromolecular Bioscience*, 2008, **8**, 942-950.
52. Q. Z. Chen, A. Efthymiou, V. Salih and A. R. Boccaccini, *Journal of Biomedical Materials Research Part A*, 2008, **84A**, 1049-1060.
53. Q. Zhang, K. Tan, Y. Zhang, Z. Ye, W.-S. Tan and M. Lang, *Biomacromolecules*, 2013, **15**, 84-94.
54. G. Teti, A. Bigi, M. Mattioli-Belmonte, R. Giardino, M. Fini, A. Mazzotti and M. Falconi, *Journal of Life Sciences*, 2013, **7**, 965-970.
55. M. Giofrè, P. Torricelli, S. Panzavolta, K. Rubini and A. Bigi, *J. Bioact. Compatible Polym.*, 2012, **27**, 67-77.
56. S. Baiguera, C. Del Gaudio, E. Lucatelli, E. Kuevda, M. Boieri, B. Mazzanti, A. Bianco and P. Macchiarini, *Biomaterials*, 2014, **35**, 1205-1214.

Supplementary information

Antibacterial 45S5 Bioglass[®]-based scaffolds reinforced with genipin cross-linked gelatin for bone tissue engineering

Wei Li^{a,1}, Hui Wang^{b,1}, Yaping Ding^c, Ellen C. Scheithauer^a, Ourania-Menti Goudouri^a, Alina Grünewald^a, Rainer Detsch^a, Seema Agarwal^b, Aldo R. Boccaccini^{a,*}

^a Institute of Biomaterials, Department of Materials Science and Engineering, University of Erlangen-Nuremberg, Cauerstrasse 6, 91058 Erlangen, Germany

^b University of Bayreuth, Macromolecular Chemistry II and Bayreuth Center for Colloids and Interfaces, Universitaetsstrasse 30, 95440 Bayreuth, Germany

^c Institute of Polymer Materials, Department of Materials Science and Engineering, University of Erlangen-Nuremberg, Martensstrasse 7, 91058 Erlangen, Germany

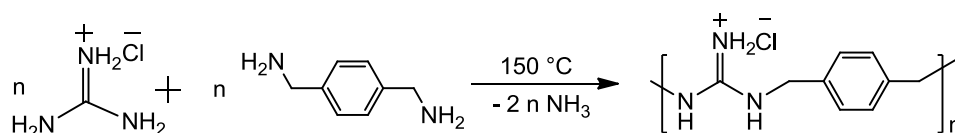
* Corresponding author at: Institute of Biomaterials, Department of Materials Science and Engineering, University of Erlangen-Nuremberg, Cauerstrasse 6, 91058 Erlangen, Germany. Tel.: +49 9131 85 28601; fax: +49 9131 85 28602. E-mail address: aldo.boccaccini@ww.uni-erlangen.de (A.R. Boccaccini).

¹ These two authors contributed equally to the experimental part.

Poly(*p*-xylyleneguanidine) hydrochloride (PPXG) synthesis and structural characterization

Synthesis and NMR characterization

Poly(*p*-xylyleneguanidine) hydrochloride (PPXG) was made by condensation polymerization according to the Scheme 5-S1.



guanidine hydrochloride	[95.54]	0.050 mol	6.18 g	1 eq
<i>p</i> -xylylenediamine	[136.19]	0.050 mol	4.78 g	1 eq

Scheme 5-S1. Synthetic scheme for the formation of PPXG.

Publications

The polymer was structurally characterized using NMR. ^1H - (300 MHz) and ^{13}C - (75 MHz) NMR spectra were recorded on a Bruker Ultrashield-300 spectrometer in MeOD. The peaks were assigned as follows:

^1H -NMR: 300 MHz, MeOD; δ (ppm) = 3.81(s, 2H, $(\text{CH}_2)\text{NH}_2$) 4.45 (m, 2H, $\text{NHCH}_2\text{C}_6\text{H}_5$); 7.02 (m, Ar-H); 7.35 (m, Ar-H).

^{13}C -NMR: 75 MHz, MeOD; δ (ppm) = 45.56 (s, $\text{NHCH}_2\text{C}_6\text{H}_5$); 46.13 (s, $(\text{CH}_2)\text{NH}_2$); 128.81, 137.55 (m, Ar-C); 157.64, 158.64 (s, $\text{C}=\text{NH}$).

^1H - ^{13}C correlation experiments were conducted on a Bruker Avance 600 spectrometer with a 5 mm multinuclear gradient probe at 25 °C using MeOD as solvent. 2D NMR spectrum heteronuclear single quantum coherence (HSQC) was used to assign peak positions in ^{13}C -NMR as shown in Figure 5-S1.

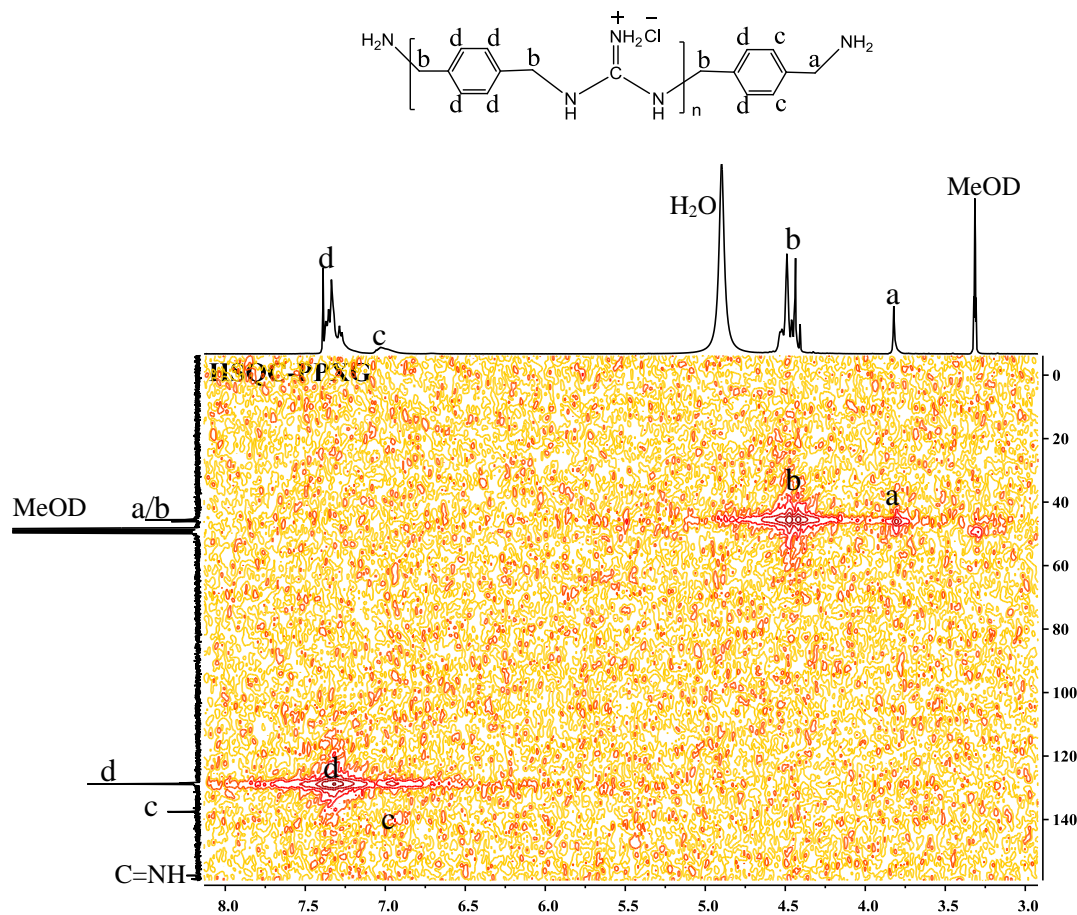


Figure 5-S1. 2D ^1H - ^{13}C HSQC NMR spectrum of PPXG in MeOD.

Publications

APCI analysis

APCI-mass spectrum was recorded on a Thermo Fisher Scientific Finnigan LTQ-FT spectrometer. The sample was dissolved in methanol. APCI-mass spectra were used to confirm the chain ends of PPXG (Figure 5-S2). Four different types of chain structures were found i.e. PPXG chains with one guanidine and one amino group (structure A), guanidine and amino groups at both chain-ends (structures B and C) and ring structure without any chain-ends (structure D). No attempts were made to separate different structures and the sample was used as such for antibacterial tests and coating of scaffolds.

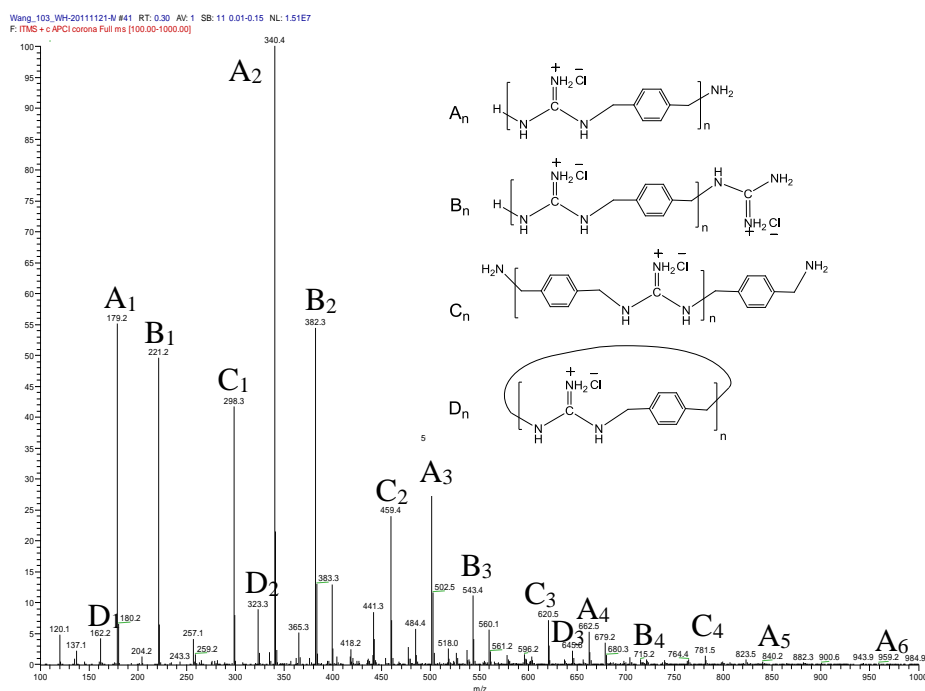


Figure 5-S2. APCI-Spectrum of PPXG.

Matrix-assisted laser desorption/ionization time-of-flight mass spectrometry (MALDI-ToF-MS) analysis

MALDI-TOF MS was used for determination of molecular weight of PPXG. Bruker Reflex III apparatus equipped with a N₂ laser ($\lambda = 337$ nm) in linear mode at an acceleration voltage of 20 kV was used. Indole-3-acetic acid (IAA, Fluka, 99.0%) was used as a matrix material. Samples were prepared with the dried droplet method from Methanol solution by mixing matrix and polymer in a ratio of 20: 5 (v/v) and applying approximately 1 μ L to the target spot.

The molecular weight of the PPXG determined by MALDI-TOF MS was M_n : 2200, M_w : 2500 and PDI: 1.12.

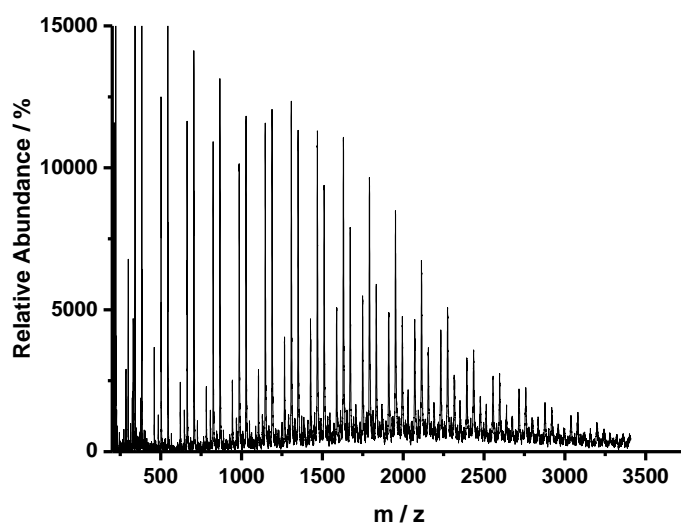


Figure 5-S3. MALDI-ToF-MS-Spectrum of PPXG.

Thermal characterization

Thermal Analysis was performed on Mettler Toledo thermal analyzers comprising 821 DSC and 851 TG modules. By recording thermogravimetric (TG) traces in nitrogen atmosphere with a flow rate of $60 \text{ mL} \cdot \text{min}^{-1}$, the thermal stability was determined; a sample size of $12 \pm 2 \text{ mg}$ and a heating rate of $10 \text{ K} \cdot \text{min}^{-1}$ was used for each measurement. The temperature of thermal decay (T_d) was taken as the inflection point of the TG curve. Differential scanning calorimetry (DSC) was performed in nitrogen atmosphere (flow rate $80 \text{ mL} \cdot \text{min}^{-1}$) with a heating rate of $20 \text{ K} \cdot \text{min}^{-1}$; the inflection point of the baseline in the second heating cycle was taken as glass transition temperature (T_g).

PPXG showed high glass transition temperature ($T_g = 150 \text{ }^\circ\text{C}$; Figure 5-S4). Thermogravimetric analysis (Figure 5-S5) showed, that the significant mass loss (85%) took only after 350°C thereby showing high thermal stability.

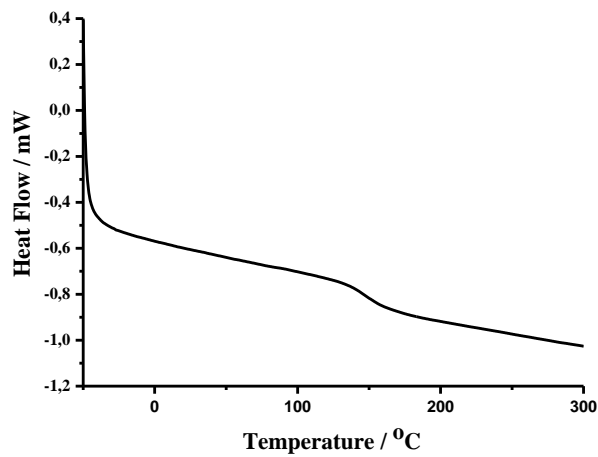


Figure 5-S4. Differential scanning calorimetric analysis of PPXG showing glass transition temperature at 150°C.

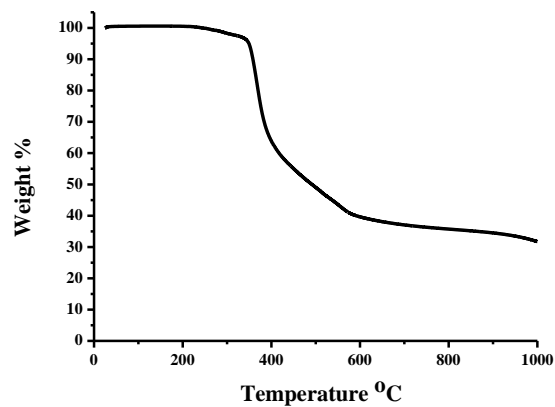


Figure 5-S5. Weight loss vs. temperature curve for PPXG.

Antibacterial Test (MIC and MBC Test)

E.coli (Gram-negative)

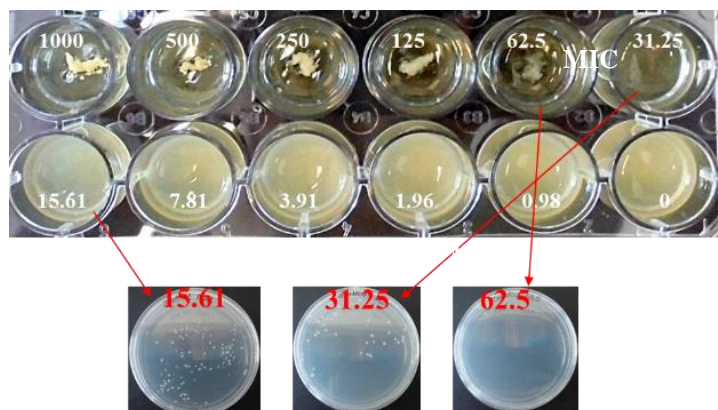


Figure 5-S6. Photographs of MIC and MBC test with *E.coli* as test organism.

Publications

B.subtilis (Gram-positive)

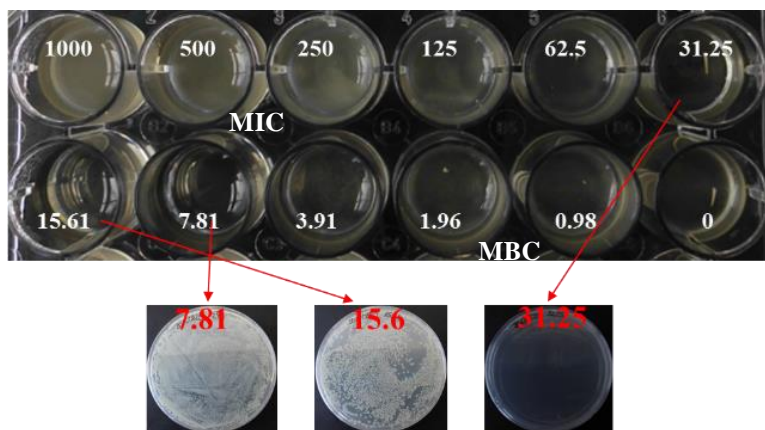


Figure 5-S7. Photographs of MIC and MBC test with *B.subtilis* as test organism.

List of Publications

Publications included in the thesis:

[1] Biodegradable aliphatic-aromatic polyester with antibacterial property

H. Wang, M. Langner, S. Agarwal, *Polymer Engineering & Science*, **2016**, DOI: 10.1002/pen.24347.

[2] Antibacterial 45S5 Bioglass[®]-based scaffolds reinforced with genipin cross-linked gelatin for bone tissue engineering

W. Li, H. Wang, Y. Ding, E. C. Scheithauer, O. Goudouri, A. Grünewald, R. Detsch, S. Agarwal and A. R. Boccaccini, *J. Mater. Chem. B*, **2015**, *3*, 3367-3378.

[3] Oligomeric dual functional antibacterial polycaprolactone

H. Wang, C. V. Synatschke, A. Raup, V. Jérôme, R. Freitag, S. Agarwal, *Polym. Chem.* **2014**, *5*, 2453-2460.

Publications not included in the thesis:

[4] Structural exploration of phantom oligoguanidine from asymmetric diamine and guanidine hydrochloride

H. Wang, C. Benke, M. Hermann, G. Frenking, S. Agarwal, *Macromol. Chem. Phys.* 2016 DOI: 10.1002/macp.201600154.

[5] Protection of vine plants against Esca disease by breathable electrospun antifungal nonwovens

V. Buchholz, M. Molnar, H. Wang, S. Reich, S. Agarwal, M. Fischer, A. Greiner, *Macromol. Biosci.* 2016 doi: 10.1002/mabi.201600118.

[6] Exploring suitable oligoamines for phantom ring-closing condensation polymerization with guanidine hydrochloride

C. Mattheis, H. Wang, M. C Schwarzer, G. Frenking, S. Agarwal, *Polym. Chem.*, **2013**, *4*, 707-716.

[7] Effect of Guanidinylation on the Properties of Poly(2-aminoethylmethacrylate)-Based Antibacterial Materials

C. Mattheis, H. Wang, C. Meister, S. Agarwal, *Macromol. Biosci.*, **2013**, *13*, 242-255.

Acknowledgements

Acknowledgements

First and foremost, I would like to express my great appreciation to Prof. Dr. Seema Agarwal for her guidance and constant support. Prof. Agarwal enabled me to join many conferences and meetings during my thesis, where I could present my work. There, I have had many chances to meet other researchers and discuss science. Her kindness towards me and confidence in me has been the greatest motivation. I thank her for all those opportunities she created and the responsibilities she trusted me with.

Moreover, I want to express my sincere appreciation to Prof. Dr. Andreas Greiner. His way of leading the group, – the group–spirit, made working in his chair special. I want to thank him for all the involvement he had in my work. He has been a trusted advisor for any questions of scientific research.

I thank Deutsche Forschungsgemeinschaft (DFG) and the University of Bayreuth Graduate School for financial support.

I would also like to thank Prof. Dr. Aldo R. Boccaccini, Wei Li, Prof. Dr. Ruth Freitag, Dr. Valérie Jérôme, Alexander Raup, for the good cooperation, especially for the publications of my thesis. I thank those people who did influence my work, or discuss ideas, Claudia Mattheis, Yi Zhang, Ilka E. Paulus, Holger Pletsch, Peter Ohlendorf, Christopher V. Synatschke, Dr. Roland Dersch, Dr. Reiner Giesa.

Many people including the Marburg colleagues came and went during my time here in MC 2. For collaboration I thank those people, who made my time there an exceptional experience and created a remarkable atmosphere: Tobis Moss, Arne Lerch, Paul Pineda, Amanda Pineda, Viola Buchholz, Amir Reza Bagheri, Judith Schöbel, Markus Langner and Pin Hu. The technicians kept the lab in good condition. I want to thank Annette Krökel, Rika Schneider, Bianca Uch, Melanie Förtsch and Annika Pfeppenberger.

Acknowledgements

The time-consuming burden of proof-reading of the present thesis was kindly carried by Oliver Hauenstein, Paul Pineda, Amanda Pineda, Judith Schöbel, Markus Langner.

Most importantly, I would like to thank Oliver Hauenstein and my family. They always listened to my adventures, successes and in some rare cases my frustrations. In particular my parents 郑捷 and 王学仁, for their endless support and encouragements.

(EIDESSTATTLICHE) VERSICHERUNGEN UND ERKLÄRUNGEN

(§ 8 S. 2 Nr. 6 PromO)

Hiermit erkläre ich mich damit einverstanden, dass die elektronische Fassung meiner Dissertation unter Wahrung meiner Urheberrechte und des Datenschutzes einer gesonderten Überprüfung hinsichtlich der eigenständigen Anfertigung der Dissertation unterzogen werden kann.

(§ 8 S. 2 Nr. 8 PromO)

Hiermit erkläre ich eidesstattlich, dass ich die Dissertation selbstständig verfasst und keine anderen als die von mir angegebenen Quellen und Hilfsmittel benutzt habe.

(§ 8 S. 2 Nr. 9 PromO)

Ich habe die Dissertation nicht bereits zur Erlangung eines akademischen Grades anderweitig eingereicht und habe auch nicht bereits diese oder eine gleichartige Doktorprüfung endgültig nicht bestanden.

(§ 8 S. 2 Nr. 10 PromO)

Hiermit erkläre ich, dass ich keine Hilfe von gewerblichen Promotionsberatern bzw. -vermittlern in Anspruch genommen habe und auch künftig nicht nehmen werde.

Ort, Datum, Unterschrift